Residual Ground Fault Detector for Bipolar LVDC Grids

A Novel approach towards selective protection

Balaji Subramanian

Technische Universiteit Delft

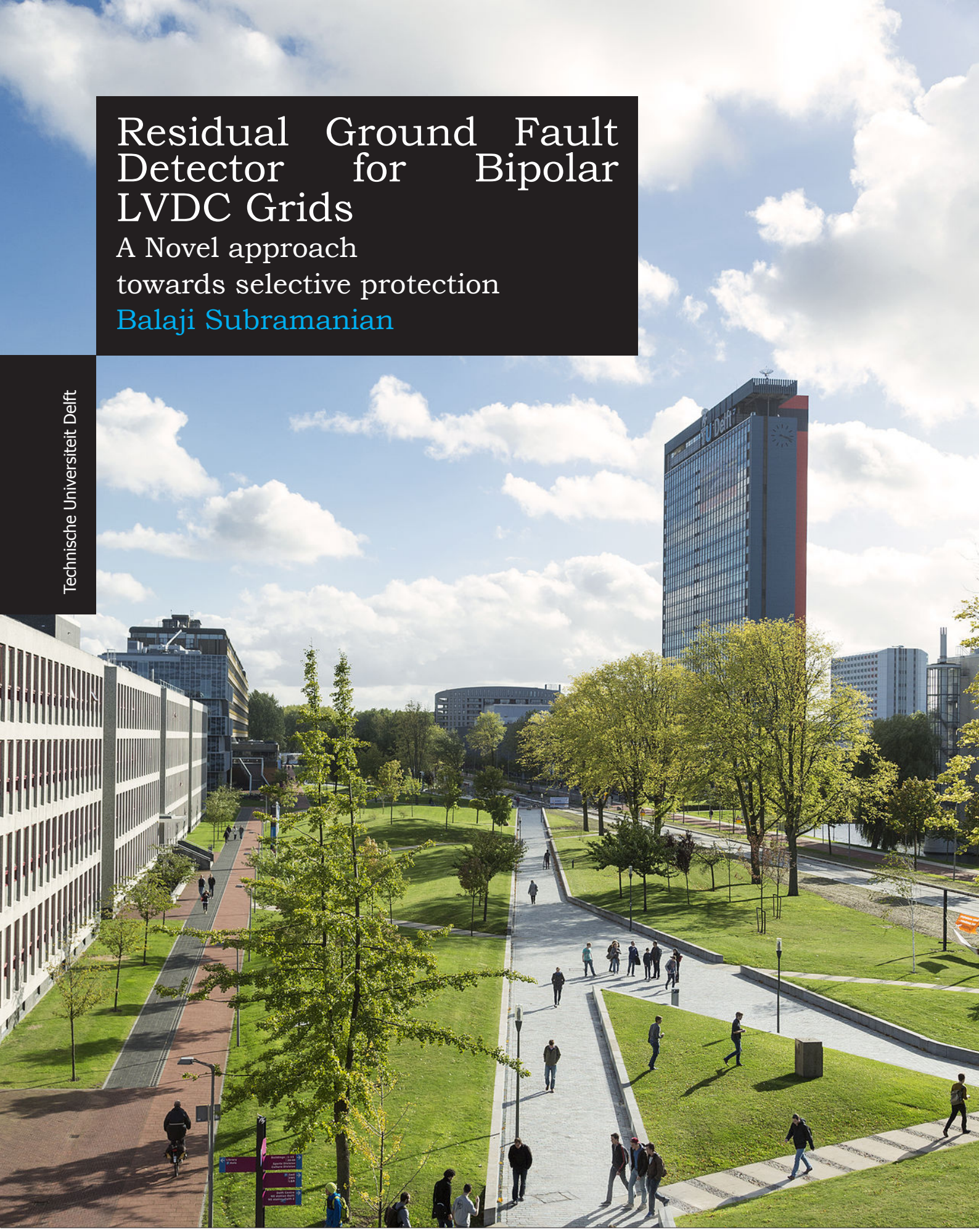

TU Delft Delft University of Technology

Challenge the future

Residual Ground Fault Detector for Bipolar LVDC Grids

A Novel approach towards selective protection

by

Balaji Subramanian

in partial fulfillment of the requirements for the degree of

Master of Science
in Electrical Power Engineering

at the Delft University of Technology,
to be defended publicly on Tuesday Sep 26, 2023 at 11:00 AM.

Supervisor:	Prof. Dr. Ir. Marjan Popov,	TU Delft
Advisors:	Dr. Ir. Laurens Mackay,	DC Opportunities R&D BV
	Ir. Samad Shah Khawaja,	DC Opportunities R&D BV
Thesis committee:	Prof. Dr. Ir. Marjan Popov,	TU Delft
	Asst. Prof. Dr. Zian Qin,	TU Delft
	Prof. Dr. Peter Palensky,	TU Delft

This thesis is confidential and cannot be made public until September 18, 2025.

TU Delft Delft University of Technology

DC pportunities

Acknowledgement

In this section I would like to thank everyone involved in making this project a successful one. First and foremost I owe the accomplishment to my parents without whose unconditional support I would not have reached this far in my academic career.

My greatest gratitude to my Supervisor Dr. Ir. Laurens Mackay for having given me an invaluable opportunity to work at the frontier of future electrical power distribution grids which are predicted to be predominantly DC based. At DC Opportunities R & D B.V , I not only gained the technical skills and professional exposure to fuel my ambition and zeal to continue working in the Electrical sector but it provided a special platform to combine brains and work alongside people coming from different nations and cultures to solve unique problems in an area harbouring immense research potential.

I thank my company Supervisor and mentor Ir. Samad Shah Khawaja for his active and continuous support and guidance over the period of development of the project. I also wish to convey my special thanks to my friend and colleague Ir. Jesse Echeverry, whose clarity of ideas, open communication and ability to simplify complicated problems helped me tide through the toughest parts of the project.

I take this opportunity to thank my Supervisors Prof. Dr. ir. Marjan Popov, Prof. Dr. Peter Palensky and Asst. Prof. Dr. Zian Qin who were my inspiration to taking this project.

My humble gratitude to all my colleagues at DC Opportunities R & D B.V and Professors from the EEMCS Dept., administration and staff members for providing me an opportunity to be a student of one of the most demanded courses, the knowledge gained from which could be used to push the agenda of sustainability forward and brighten the future of millions of lives globally.

Balaji Subramanian
Delft, September 2023

Abstract

Residual current detectors have been used widely as protective devices against shocks and to monitor insulation failure in electrical grid systems, especially at the load centres and sub stations where chances of electrocution due to leakage currents is high. Modern day implementation of RCD are mostly at the load end and deal with both alternating current and smooth direct current. However there is less research in the area of pure DC RCD that detect DC residual currents and standardization of these devices for bipolar LVDC distribution grids.

Meshed DC Grids with multiple grounding points in a TN-S configuration, present a unique problem where difference in voltage between two or more grounding points may create current loops increasing the current level measured by traditional residual current detectors (RCD). Additionally other current rise phenomenon in meshed DC grids which could lead to false tripping such as the Circulating Net Currents (CNC) in a bipolar DC grid configuration caused due to asymmetrical line resistance or opening of a faulty pole which would cause increased loading on the other poles creating a current imbalance. Temporary discharge of grounding capacitors in capacitively grounded systems such as EV charging networks, instantaneous load changes and PE switching could also add to the causes for false tripping of residual current detectors in Meshed LVDC grids.

This false tripping often occur because traditional residual current detectors (RCD) are designed specifically to detect certain current levels or with specific delays in their rise time. In meshed DC distribution grids, there is a certainty of detection of high differential currents which maybe due to isolation of a pole for maintenance or repair or due to other phenomenon as mentioned above. There are equally high chances of residual ground fault current flowing during this period thereby blinding the RCD from detecting the actual residual current, causing false tripping. Moreover it is highly probable that due to such high currents, the primary circuit element used in these sensors such as magnetic cores get permanently magnetized thus requiring active Degauss or maintenance after such an event which is both, expensive and time consuming.

Due to the above mentioned challenges, the requirement for a new type of DC RCD with standardization becomes evident. Thus a need arises to design and develop a residual current detector (RCD) which is both, sensitive to residual currents during high current phenomenon and also resilient to them while at the same time being accurate and maintaining a decent level of precision. In this thesis, the design of a residual current detector based on fluxgate current sensing technology is presented along with development of a working model for the same. The response of the built model of the sensor is tested for different residual current levels at extra low voltage (<120 V_{DC}) and low voltage (120 - 350 V_{DC}) settings for Unipolar and Bipolar DC distribution Grid configurations.

keywords: Low Voltage Direct Current (LVDC), Electric Grids, Residual Current Detector (RCD), Residual Ground Fault Detection, Indirect current measurement, Fluxgate Sensors, Differential current sensing, Printed Circuit Board (PCB)

Contents

Nomenclature

μ_0	Permeability of free space
μ_r	Relative Permeability
μ_e	Effective Permeability
B	Magnetic flux density (in mT)
N_s	No. of turns of compensation coil
N_p	No. of Primary turns
L	Inductance provided by the magnetic core for a specific no. of turns of compensation coil (in mH)
V_{Out}	Output voltage of current sensor (in V)
V_{shunt}	Voltage drop across Shunt Resistor R_{Shunt}
R_{shunt}	Shunt resistance (in Ω)
I_p	Primary current - Residual Current (in mA)
I_s	Compensation current (in mA)
A_c	Effective Cross Sectional Area of Magnetic Core in mm^2
DG	Distributed Generation
DC	Direct current
AC	Alternating current
LVDC	Low Voltage Direct Current
LVAC	Low Voltage Alternating Current
RES	Renewable Energy Sources
MCB	Main circuit Board
RCD	Residual Current Detector
GHG	Greenhouse Gas
IEC	International Energy Council

1

Introduction

1.1. Motivation

1.1.1. Climate Change and Integration of Renewable Energy Sources (RES)

Climate change is a huge factor affecting the quality of life on Earth, including everything from agriculture to economics [1–4] and has been of the highest concern since the previous decade. This change in climate is influenced largely by Greenhouse Gases (GHG), prominent of which being Carbon Dioxide (CO_2), are byproducts of human activities ranging from smog released from factories till generation of electrical power by burning fossil fuel like coal,petroleum and natural gas. With increase in population, the need for electrification has grown phenomenally over the decades with most of the power generated using conventional (or fossil) fuels. Many developed and most developing nations are dependent majorly on fossil fuels to ensure continuous and uninterrupted electricity supply to it's citizens and for their various economic activities. Recent report by the International Energy Agency (IEA) in 2020 [5], shows the electric power generation as the highest contributor of Carbon Dioxide (CO_2) at 40 % of the net 0contribution per sector worldwide. Net electric power consumed in 2018 was around 23,398 TWh. Total electric power demand is predicted to rise by 4.5% in 2021 i.e. over 1000 TWh [6]. The domination of fossil fuels in the power generation sector till the year of 2020 can be observed from the graph published by the BP Statistical Review, Figure 1.1 which shows the gross energy in terawatt hours (TWh) consumed worldwide from different sources.

Following the 2015 United Nations General Assembly, 17 Sustainable Development Goals (SDG) were drafted under an **Agenda 2030** as a blueprint to achieve sustainable development [8]. Goal 7 of the Sustainable Development Goals (SDG) named "Affordable and Clean Energy" focuses on ensuring sustainable, reliable, affordable and modern energy to all people. The year 2020 saw a rise in total share of renewable energy generation to global electricity generation to 28% from 26% in 2019 and is predicted by IEA to increase in the coming years [6].

Increased dependence on dwindling fossil fuel reserves in developing nations and higher costs involved in changing the already prevalent infrastructure for power generation in developed nations, have resulted in very high costs of electrical energy per kilo-Watt hour (kWh), consumed by both residential and industrial customers worldwide. This has further encouraged adoption of renewable energy sources favouring self generation. This being specifically applicable to rural and isolated village communities to whom electricity access cannot be provided chiefly due to difficulties posed by the terrain or distance from the main power distribution grid.

Self - generation of electricity through renewable energy sources has thus highly encouraged and promoted by Governments especially in middle and low income economies, through donations for installation of Rooftop PV for individual homes, PV Farms for residential communities and public facilities like airports etc. along with increased subsidies for the power supplied from these sources to the main electrical grid.

Unlike in developed nations like Germany where electricity per kWh per household increases with increasing penetration of renewable energy to incentivize self-generation [10], in developing economies the

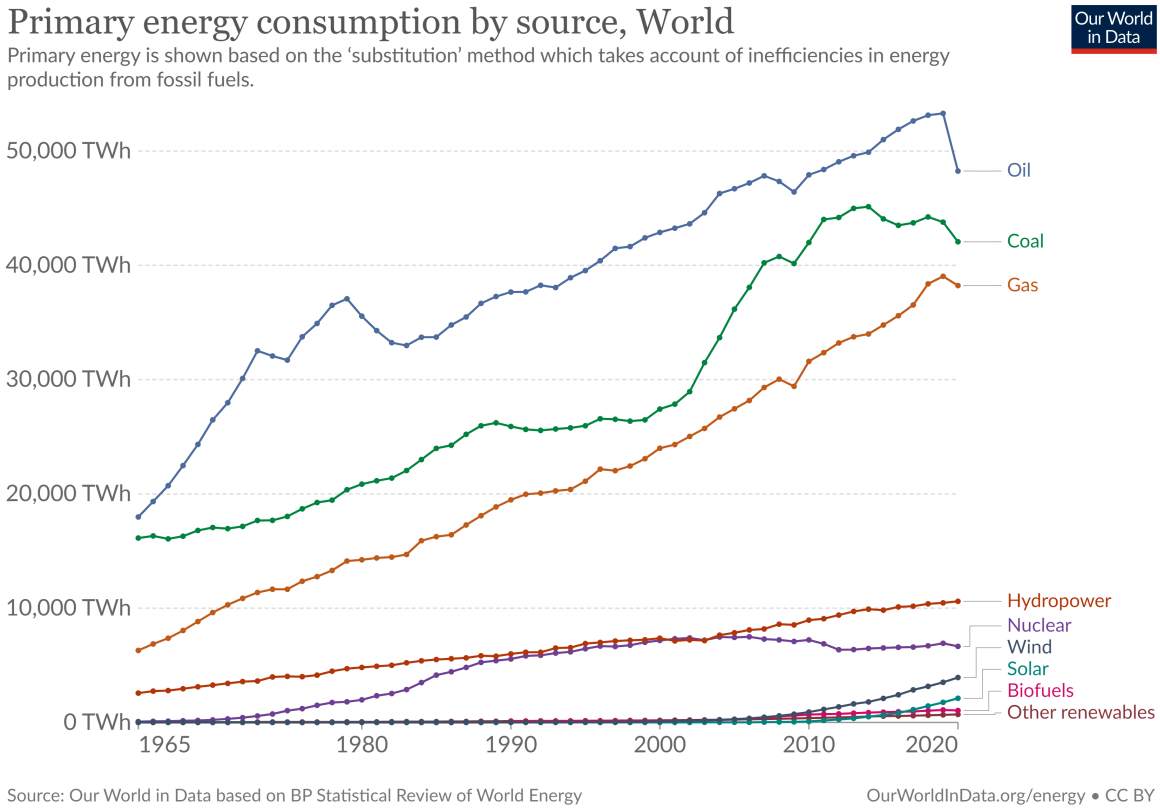

Figure 1.1: Primary Energy consumption by source worldwide from data published by BP Statistical Review of World Energy [7].

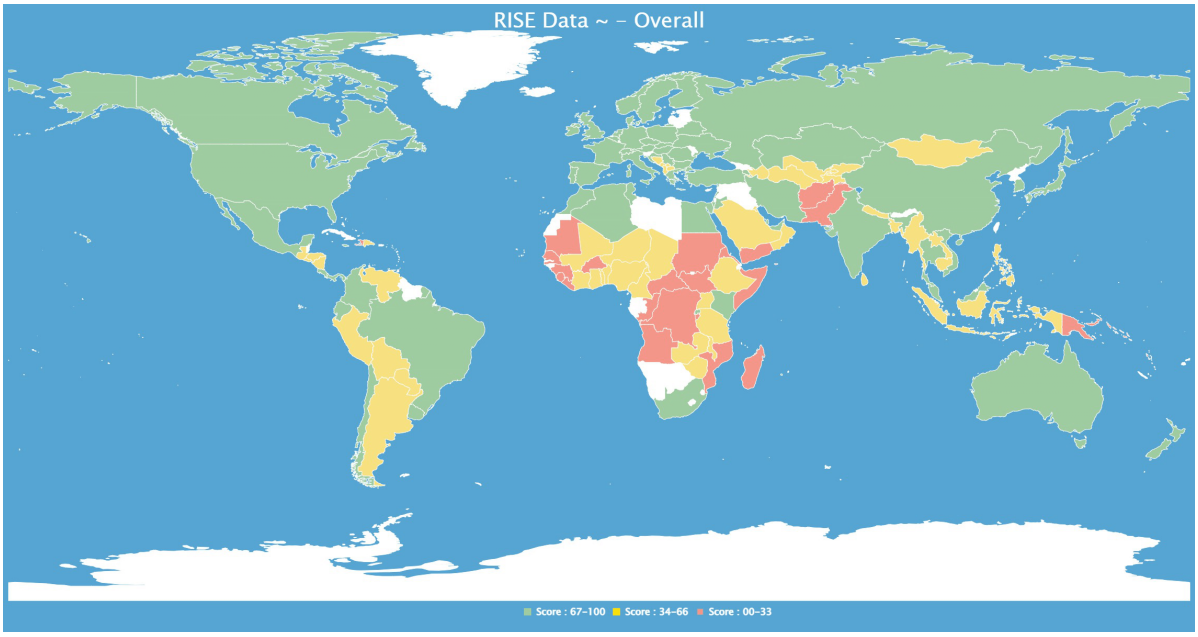

Figure 1.2: The map by RISE Global scores each country by colour Green: 80 - 100 ; Yellow: 60 - 79 ; Red: <60 points based on availability of suitable laws and policy regulation to enable RES integration and potential to increase capacity [9].

increase in price is related more to increased demand, depleting fossil fuel reserves in contrast to increased individual power usage along with other physical and financial factors like distance from the energy reserves, installation, maintenance and operating costs of the power stations and transmission system as a whole [11]. This has motivated residents in many developing nations to invest in and install rooftop PV panels or sizeable solar farms for entire residential societies or communities which provide not only free electricity but provide income in the form of subsidies by supplying excess power generated to the main grid. The Fig 1.2 shows the increasing flexibility in policies and regulation shown by many developed and developing countries across the globe to enable successful adoption of and accessibility to clean energy sources for the residents of each nation. This points to a global effort in increasing the share of power generation from renewable energy sources worldwide.

Increase in distributed generation (DG) mostly from renewable energy sources such as Solar and Wind along with them being inherently DC in nature, calls for a new distribution grid infrastructure based on DC for efficient integration of such sources with the mainline electricity supply. Implementation of Smart Grids to effectively integrate Renewable Energy sources with a direct current (DC) distribution grid architecture and development of independent (or islanded) microgrids with the support of intelligent and self monitored systems has been highly recommended to facilitate better utilization of electric power generated by these sources and cited as one of the best method to combat climate change [12][13].

1.1.2. Low Voltage Direct Current (LVDC) Distribution Grids

To achieve the sustainability goals, an increase in renewable energy sources in the near future is evident. With most of the loads used at homes and offices functioning on DC supply by rectifying AC to DC, it is found more practical for the entire supply grid to run on DC which has many advantages such as better power utilization, since most DC operated devices can run directly on DC which increases power utilization with less losses owing to lesser no. of power conversion stages compared to AC grids [14]. The implementation of LVDC grids however, has a significant set of challenges including control and safety to ensure reliable and uninterrupted power supply to the customers and consumers which opens a large scope for research. Following points delineate some of the advantages of implementing LVDC Distribution Grids :

- **Better utilization of Electric Power**: Consumer electronics and loads at homes, factories and offices or certain public areas are increasingly incorporating DC components. They are either run entirely on direct current (DC) by converting ac to dc via use of converters such as most consumer electronics or vice versa such as variable speed control for motors using dc - ac and ac - dc conversions. LED Street Lights which are now popular for having higher lumens per watt and lower maintenance compared to the older street lights are run on DC. Since more and more electrical appliances and electronics are run on DC, it becomes practical to consider a larger DC Distribution Grid and allow these devices or appliances to run directly on DC power eliminating requirement for ac/dc or dc/ac conversions. Higher the power conversion stages higher the power loss. Hence implementation of LVDC Distribution Grids provides better power utilization.

- **Better power transfer**: Power transferred by DC is higher than AC. This increases the effectiveness of power delivery.

- **Easier Control**: It is easier to control the power output using programmable converters to satisfy the load requirements compared to controlling the output of generators or transformers. Smart Grid infrastructure enabled demand side management allow regulation of the power usage of intelligent loads and power output of storage such as E.Vs and Battery Energy Storage Systems (BESS) to satisfy local demands.

- **Increased safety in DC grids**: The danger threshold for current is higher in DC compared to AC. For AC, the magnitude of threshold for safe isolation is 40 - 50 mA while for DC the value is around 150 - 200 mA. This allows for more relaxation to the constraints in protection with respect to the magnitude of currents found to be hazardous when flowing through a body for a certain period of time.

- **Easier integration of RES :** Renewable Energy Sources like Solar Farms being inherently DC, it is found practical to connect these sources directly to a larger DC Distribution Grid at the same bus voltage level which can remove need for conversion and reduce power loss.

- **Reduced cost of implementation and maintenance of Distribution Grids :** DC enabled loads can directly run on DC power commissioned on the basis of power usage and nature of function. Direct connection to DC reduces and often removes excessive power conversion stages and conductors used for the same thereby leading to a reduction in costs for installation and maintenance compared to LVAC distribution grids which employ step down and step up transformers and thus increase the complexity.

Smart LVDC grids provide more than the above mentioned advantages such as effective islanding at load centres during disconnections with local or regional distribution systems along with reducing the complexity of black-starts for stations and load centers after an interruption in power delivery for maintenance, repairs, accidents or due to contingencies. However despite LVDC distribution grids having so many advantages over traditional LVAC distribution systems, there are challenges in their implementation. Most predominant challenge are availability of dc enabled loads which can directly run on dc power and the replacement of the traditional system itself which will require high initial investments. Primarily there needs to be more research into the area and functional realistic models to gain insights as to their functioning in real time. Additionally, there must be a clear planning to shift to LVDC distribution systems from the traditional system taking into consideration the costs of implementation and risks involved. For cities and advanced locations where distribution grids already running at peak loading, it has been suggested that LVDC distribution grids could be considered for newer upcoming localities and bottom - up approach for rural areas and villages without access to electricity allowing residents of these places to purchase different segments of the Solar Home Systems (SHS) within their individual capabilities [15][16].

1.1.3. Rural and Urban Electrification :

Rural Electrification

Due to the challenges faced in implementation of LVDC Distribution Grids, the bottom - up approach has been found to be feasible especially in rural areas around the world and developing countries. This approach involves individual customers or consumers adopting DC enabled loads and self - generation through Distributed Energy Sources (DERs) such that there is a possibility to connect the residencies into a larger bipolar LVDC mini-grid that can supply at ± 350 - 700 V_{dc}.

Figure 1.3: Installation of Rooftop PV as part of Solar Home Systems(SHS) in a rural area in Africa [17]

Figure 1.4: Thatched roof houses aligned with PV panels as part of Solar Home Systems(SHS) in African rural areas [18]

Rural areas around the world would benefit from electrification from Distributed Energy Sources (DER) which enables them to draw energy without having to pay too much. As per World Bank records 3.4 Billion people still stay in rural areas around the world as of July 2021 [19] which is around 32 % of the total world population. Out of the total population residing in rural areas, the continent of Africa has the highest percentage of population living in rural areas which is around 58 % of the total population of Africa as per World Bank estimates [20]. Modern Solar Home Systems implemented in these rural areas do not entirely meet the needs of the people. With standard installed capacities such as 10 W_p that generally run on 12 - 24 V dc power, the duration of continued supply is only said to last for four to five hours [21]. Most of power produced by Solar Home Systems for the rural areas goes into lighting and phone charging. Solar Home Systems (SHS) in rural areas have not climbed the energy ladder to generate the necessary amount of energy to satisfy all the requirements of the people including energy for cooking, water heating etc. Although there being policies issued by local governments or non - profit organizations to assist the people living in rural localities financially to set

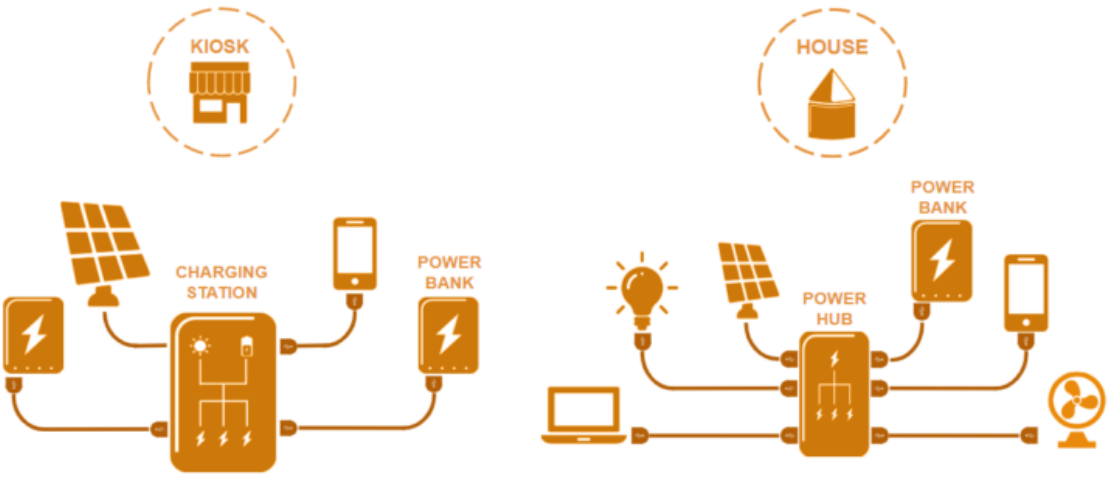

Figure 1.5: The figures represent different ways PV systems can be connected to the loads and storage systems for rural electrification.**Image on Left** : DC loads and power banks connected to central PV source through a fast charging station using USB - C housed in a solar kiosk. **Image on Right** : Common DC loads in a house and power banks connected to Central PV system through a power hub for charging and usage. [23].

up these Solar Home Systems, the initial down-payment are often too high to be affordable with their daily income. For example, in Bangladesh the cost of setting up a single SHS comes around €300 - 1000 depending on the size, quality and the country of sales [21][22]. Despite the prevalence of payment methods such as PAYG (Pay As You Go) which initially demand a 20 - 35 % of the total price for the SHS as down-payment then allowing the consumer/customer to continue paying in installments for the next few months or years, the end costs for the SHS are driven up owing to high interests in addition to financing costs.

A solution to this issue has come about by considering USB - C for power transfer application which allows power flow of 100 W thus increasing the power delivery capabilities of the system. USB - C is considered to be the next generation standard for power distribution and data transfer [24]. Larger centrally installed PV systems in contrast to individual Solar Home Systems complemented with USB - C for power delivery can be considered as a solution to lessening the costs of rural electrification.

Re-designing of AC loads to make them compatible to run on dc power and utilization of USB - C for power delivery and communication would increase the power output and efficiency of Solar Home Systems with the capability of growth to a mini - grid which runs on ± 350 - 700 V. An example for rural households connected to a central PV System through USB - C based fast charging station and power distribution hub is shown in Fig1.5.

Meshing each rural households with a SHS to other DER would provide more reliability and resiliency to a rural electrification system. In Fig1.6 it can be observed how individual households are connected to several DERs apart from the centrally installed PV source or farm while being interconnected among themselves. This improves redundancy and increases the reliability of the distribution system on the scale of a village. Diversification of energy sources ensures most requirements of a household is met while bringing down the cost of power generated compared to traditional SHS. Furthermore, linking the local micro-grids of each village to form a larger LVDC distribution grid which opens more research scope including energy markets for rural areas. Up-scaling in this manner could completely alter the face of rural electrification from independent solar home systems which provide limited power for specific applications, to large grids that are capable of fully supporting the rural ecosystem removing the dependency on traditional centralized grids.

Urban Electrification

Increased penetration of RES such as Solar Energy can be seen now also in urban areas. An 8% increase in share of Distributed PV amongst the total installed power capacity worldwide from 2021 has been observed by IEA in it's reports and predicted rise to 76 GW in 2023 from 71.1 GW in 2022 [25]. This increase is related to the incentivization of distributed power generation through renewable energy sources by local municipal and metropolitan authorities to foster adoption of clean energy sources in urban areas to meet SDG goals set

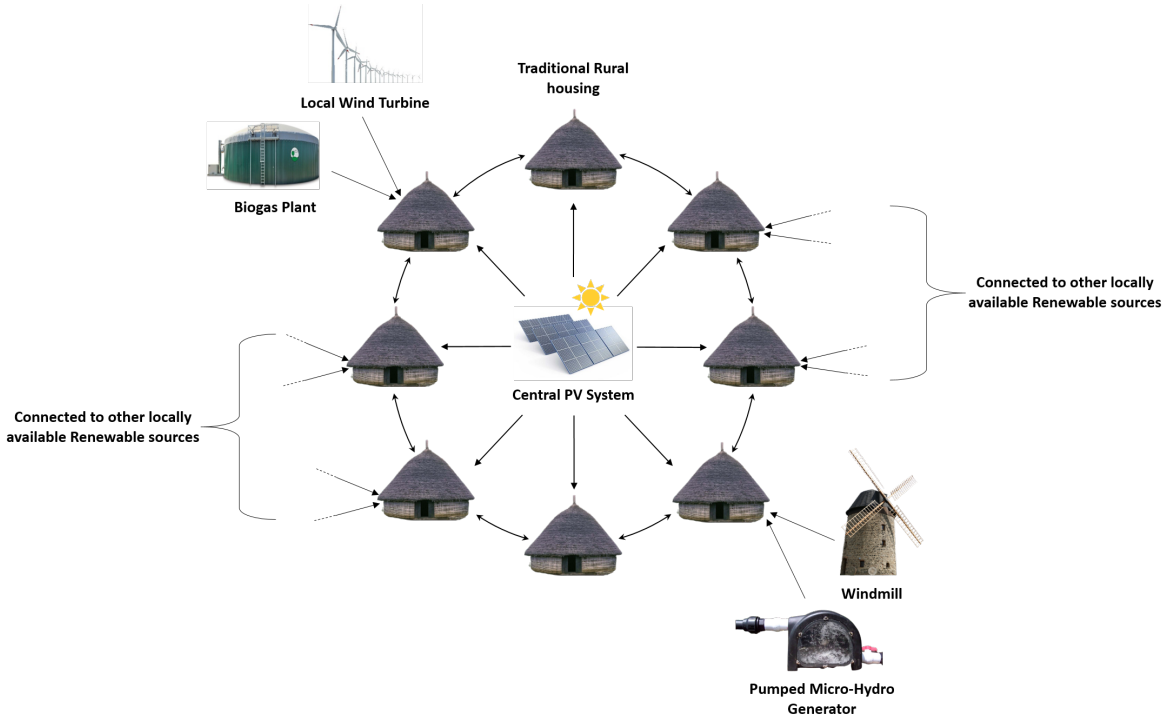

Figure 1.6: Rural households with each house connected to distributed energy sources and with each other to allow sharing of excess power produced. Example for a meshed DC distribution grid system.

in Agenda 2030. Annual installed capacity of solar power in the Netherlands in 2021 was 3.6 **GW** off which 1.3 **GW** is total installed capacity by independent homes. This is a very large penetration of renewable energy in the main power distribution system in the Netherlands which is predicted to increase in the years to follow thereby making implementation of LVDC grids feasible and advantageous in urban areas.

Transition from AC to DC power supply infrastructure, both in rural and urban areas calls for research and development for expansion of DC based power distribution and transmission systems world over. This gives rise to new scope for research in various areas of study. Protection in LVDC distribution grids is one such critical area that lacks in research.

1.2. Residual Ground Fault Protection in DC Grids

Residual ground faults are a critical area of study in relation to touch protection in any power distribution system, the components of which are exposed to the environment. Effective touch protection implemented in an electric distribution system ensures safety of living beings and property from electric shocks or leakage related hazards like fire. This is very relevant to the scenario in rural electrification where often the Mains from the renewable energy source (DC power source) are connected directly to the respective residences or rural homes or shelters via cables that are laid on the ground. The exposed mains supply pose a threat to the humans and any other living being including livestock , wild animals, birds etc. that dwell in the area especially because the probability of insulation failure due to wear and tear and exposure to high temperatures and humidity (in tropical, arid or coastal regions) is high. Residual ground faults occur when the current from a live wire (pole) of the mains supply finds an alternate route to ground (GND). This can be due to wetness in the cable insulation or the surface in contact with an ageing or broken insulation of any pole owing to humidity, rains and other climatic conditions. The surface in contact can be the exterior shell or insulation of an equipment, machine or a living being directly in contact with the poles that have aged, weakened or broken insulation.

Residual ground fault detectors or residual current detectors (RCD) are generally used to detect residual ground faults or leakage currents within homes, residential complexes, offices or commercial areas. They are usually integrated with the Main Circuit Breaker (MCB) unit that form the interface between the power

supply and the load. In short, RCD are implemented at the load side to prevent shock and other hazards like insulation failure and fires due to leakage currents. The installed RCD have a specified trip level in milli-amperes for e.g 20 mA, 30 mA, 100 mA etc. that mention the magnitude of current at which they trip the circuit breaker to isolate the fault. These detectors are also used at substations, construction yards etc. to protect workers, operators and employees from electric shocks and other hazards.

RCD are not employed directly along the AC distribution lines. This is because in large AC grids (between substation and loads and between two substations) have a high stray capacitive current with respect to ground. These high currents are enough to cause the traditional RCD to falsely trip the circuit breakers. However in LVDC distribution grids, this problem of stray capacitive currents do not occur. Even if the grid is capacitively grounded, the capacitive current will not linger for long owing to the DC Voltage and current. This comes as a great advantage because it allows to implement RCD along low voltage distribution lines.

What is to be noted is that the magnitude of residual current for a given DC voltage is higher than that for an equivalent AC voltage [26]. The minimum dc supply voltage recommended for Bipolar LVDC grids as per the master thesis by E.M vandeventer [27] is ± 350 V. For 350 V and a minimum human body resistance of a wet person i.e. 1 kΩ, the value of residual current comes out to be 350 mA. As per IEC 60479-1 standard [26], the recommended tripping time of the RCD should be within 10 ms. This calls for design of a RCD with fast reaction time and high accuracy.

1.3. Problem Statement

RCD in Bipolar LVDC grids as discussed in previous section, needs quick response to trip the circuit breaker especially due to high magnitude of DC residual currents for low voltages. Added to this is the requirement for high accuracy and sensitivity to detect lower magnitude currents.

For the purpose of rural electrification, there is requirement for a RCD which has simple design, is compact and cost effective. Such a RCD could be implemented widely across interconnections in the low voltage domain.

1.4. Research Questions

1. **How to design a Residual Current Detector (RCD) for Bipolar LVDC Distribution Grids.**

   In this thesis, a design approach using a Texas Instruments IC DRV 421 is used alongside a planar magnetic compensation coil to create a RCD to detect residual currents. The RCD is non invasive so that the issue of voltage drop does not arise.

2. **What is the suitable technique for measuring residual currents in Bipolar LVDC grids.**

   The two major types of detecting residual currents are resistive and non - invasive techniques. In the former technique a resistor is used in series of the main line where the residual current is to be detected and in the latter the difference in magnetic flux caused by the fault current is used to detect the same.

   The main techniques of non - invasive detection of residual current are :

   - Hall Effect Sensing
   - Fluxgate Sensing

   In Chapter 2 Literature Review, both the types of techniques are discussed and the selection of one technique over the other is substantiated with critical points that led to the selection.

3. **What will be the design of the magnetic core for the proposed RCD with planar compensation winding ?**

   Magnetic Core is a central component for any non - intrusive residual current detector be the configuration of the secondary winding (compensation winding), coil wound or planar. The differential current that appears across the three polarities of a bipolar power supply during a residual ground fault is converted to an equivalent secondary current across the compensation coil for detection and measurement of the residual ground current using a magnetic core.

In this thesis project, the design of the magnetic core from selection of the core material, the shape till the calculation of air gaps for effective detection by a sensor IC for the proposed RCD prototype to be implemented in Bipolar LVDC Distribution Grids is explored.

4. **What will be the reaction time of the proposed RCD ? What will be the accuracy of the RCD ?**

   The recommended time constraint for detection and isolation of a faulty pole or portion of the grid for DC as per IEC 60479-1 standard is ideally within 10 ms [26]. This is taking into consideration the net time taken for detection of the residual current and subsequent operation of the DC circuit breaker to disconnect the circuit. Therefore the reaction time for the proposed RCD prototype for use in a bipolar DC distribution grid is necessitated to be very fast within the time recommended in the standard. A good accuracy and precision with robustness of the sensor output is critical to provide reliable protection from residual ground faults.

1.5. Report Structure

This chapter gives a background and motivation for undertaking the research study. Chapter 2 provides detailed insight into Residual Ground Faults, Types of Residual Current Detectors and the technologies used for non - intrusive detection. It also reviews the literature that was used as a foundation and referred to for this thesis. Chapter 3 covers the design aspects and components used for the residual current detector for Bipolar LVDC Distribution Grids with special focus on the current detector IC used. The functioning, working principle, features and requirements of the fluxgate sensor DRV 421 IC from Texas Instruments which is used as the primary component is presented in detail in this chapter. Following this, Chapter 4 expounds on the Magnetic Core that was found compatible to be used with the selected fluxgate sensor IC DRV 421. The design, development and assembly of the PCBs for the RCD are discussed in detail in Chapter 5 while Chapter 6 presents the conducted tests on the developed RCD across various voltages and the results obtained from those tests are discussed in detail. Finally Chapter 7 concludes the report by summarizing the project and outlines the future scope for research.

2

Literature Review

2.1. Residual Ground Current Detectors for LVDC Grids

Residual ground fault protection has been an integral part of electric distribution grids especially at critical locations such as sub stations and load centres where the chances of leakage currents to cause hazards such as fires or pose a threat of electrocution to humans or any living being in contact with a grid element. Power grids having been predominantly AC, the residual current detectors (RCD) were and still are only installed at specific locations, generally nearby the loads such as water heaters, air conditioners, room heaters and other electrical or electronic equipment located at independent houses, residential complexes, factories, offices etc. Mostly they form part of the main circuit board (MCB) of each apartment in a building or to the entrance to an independent house, factory, offices or supermarkets . Main reason for this is to enable the RCD to trip a single phase or pole on which a fault is detected. Common reasons for tripping mostly being consumption of excess current by the load, stray current due to faulty insulation or a temporary short between a faulty insulation to ground through a human body, which is the main reason behind an electric shock.

2.2. Classification of Residual Current Detectors

Residual current detectors are classified based on the characteristics of the residual current waveform to be detected, area of application, programmed time delay and magnitude of residual currents for which they are designed to trip. Based on these attributes, there are many different types of residual current devices like RCBO (residual current breaker with overcurrent protection), RCCB (residual current circuit breaker), SRCD (Socket residual current device) etc. with each having their own area of use.

Based on the characteristic of residual current waveform the RCD detects, it is classified into Type A, B, F, AC etc. The Fig. 2.2 from the BEAMA RCD Handbook [28], a document created by the electrotechnical sector trade commission called BEAMA under it's Building Electrical Systems Portfolio prepared in collaboration with companies like ABB, Schneider Electric, Legrand, Western Automation (WA), Eaton etc. shows the different types of Residual current detectors and their respective areas of application.

Below the different types of RCD devices namely RCD types AC, A, F and B that are mentioned in the Fig. 2.2 are explained in detail :

1. **Type AC :** This type of RCD is used to detect AC residual currents that have sinusoidal waveform. These are implemented mainly across electrical equipment and components that run on pure AC such as fans, certain motors in industries especially in automated work processes such as bottle capping in beverage industries. The RCD can detect and trip during an abrupt rise in current or along plane and smooth AC waveform. In addition to these applications, Type AC RCD have wide range of uses and can be used in almost every electric circuit.

2. **Type A :** This type of RCD has the ability to detect both pulsating DC residual currents along with alternating sinusoidal residual currents. Type A RCD detect residual currents and trip along the rising and

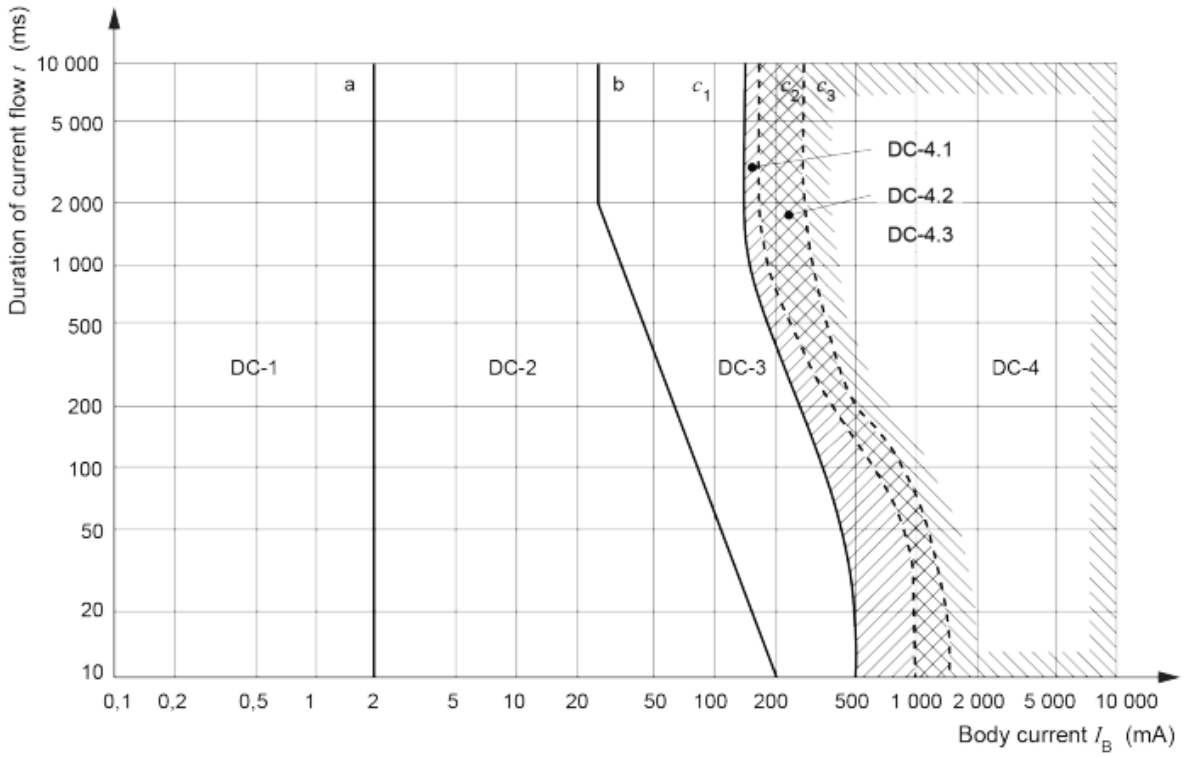

Figure 2.1: The Graph represents Touch Voltage vs. Trip Levels for DC taken from IEC 60479 - 1 Standard [26].

falling edges of pulsating DC residual currents and sinusoidal AC residual currents. This type of RCD also has the capability to detect and trip pulsating DC residual currents that are superimposed on pure DC current that has magnitude upto 6 mA as per standard IEC 62955 [29] for preventing incorrect operation of Type A RCD during current rise and BEAMA RCD Handbook [28]. Type A RCD are implemented specifically in electronic circuits containing DC-DC converters, DC/AC inverters etc. where pulsating DC residual currents have a high probability of occurrence.

3. **Type F :** The type F RCD allows detection of composite residual currents (residual currents with multiple frequencies overlapped) along with the features offered by type A RCD i.e. pulsating DC residual currents and alternating sinusoidal residual currents. It also is capable of detecting pulsating DC residual currents superimposed on pure DC upto a value of 10 mA as per the given standards for Type - F and Type - B RCD in IEC 62423 [30]. Type F RCD are specifically developed and implemented in application with variable speed motors (drives) where the residual current could be composed of multiple frequencies including the line, motor and converter switching frequency.

4. **Type B :** All the features of Type AC, A and F RCD are available in the Type B RCD. This type of RCD can detect pulsating DC residual currents, AC sinusoidal residual currents upto 1 kHz [30], alternating residual currents superimposed on constant direct current, pulsating residual direct currents superimposed on constant direct current, multi-frequency residual currents (composite residual currents), rectified DC pulsating residual currents originating from two phases or poles and smooth residual direct currents. The RCD can detect abrupt changes or rise in smooth residual direct current or with a pre - existing smooth direct current.

As discussed above, type B RCD devices are capable of detecting AC and DC residual currents hence are found to be applicable in DC residual ground fault detection where sudden increase or decrease in current is a common feature. In addition to this the type B RCD allows detection of residual currents of different frequencies which is useful to detect residual ground fault currents with any added frequency from the supply mains. The main goal of this thesis project is to design and develop RCD with the capability of detecting pure DC residual currents which match with the features of type B RCD.

RCD	Examples of type of equipment / load
Type AC	Resistive, Capacitive, Inductive loads generally without any electronic components, typically: • Immersion heater • Oven/Hob with resistive heating elements • Electric shower • Tungsten & halogen lighting
Type A	Single phase with electronic components, typically: • USB socket outlets (unless specifically advised by the USB socket outlet manufacturer that Type AC RCDs are suitable). • Single phase invertors • Class 1 IT and Multimedia equipment • Power supplies for Class 2 equipment • Appliances such as a washing machine that is not frequency controlled e.g. d.c. or universal motor • Lighting controls such as a dimmer switch and home and building electronic systems LED drivers • Induction hobs • Electric Vehicle charging where any smooth DC fault current is less than 6 mA **Type A is also suitable for Type AC applications.**
Type F	Frequency controlled equipment / appliances, typically: • Some washing machines, dishwashers and driers e.g. containing synchronous motors* • Some air conditioning controllers using variable frequency speed drives **Type F is also suitable for Type AC and Type A applications.**
Type B	Three phase electronic equipment typically: • Inverters for speed control • UPS • Electric Vehicle charging where any smooth DC fault current is greater than 6mA • Photo voltaic Power Electronic Converter Systems (PECS) typically: • industrial machines • cranes **Type B is also suitable for Type AC, Type A and Type F applications.**
Type B+	Type B+ RCDs are not recognised in BS 7671 and do not have an international or harmonised (BS EN) standard.

Figure 2.2: Tabular Overview of Load/Equipment handled by different types of RCD from Beama RCD Guide Handbook [28].

2.3. Major Residual Current Sensing Technologies

There are many methods of detecting and measuring magnitude of electric currents in power grids. The methods are mainly classified as Invasive and Non - Invasive detection techniques.

Many laboratory equipment like strain gauge among other electronic component including consumer electronics use resistive detection method in which the voltage drop across a suitable resistance connected in series to any of the phases or poles of the main power supply line is used to calculate the true value of the current flowing in the respective phase or pole. The analog value is converted to digital to trigger the protection systems during faults or for general purpose of measurement or storage. This technique is generally used where the voltage drop is insignificant compared to the current magnitude being measured. For currents of very low magnitudes, voltage drops can lead to loss of accuracy in detection. Hence Non - Invasive detection technique is preferred over Invasive for detection of residual ground fault currents. Below the two predominant residual current sensing techniques are explained in detail :

I. Flux Gate Technology

The type B residual current detectors (RCD) are the most commonly used for pure DC residual current detection. Generally all RCD utilize flux gate detection technique for low magnitude current detection. This is because using flux gate technique extremely low magnitude magnetic fields in the range of nano teslas (nT) can be detected. This is also the reason why flux gate magnetometers are used in compasses to detect direction since earth's magnetic flux which is very small in the range between 25 - 65 μT [31] due to their high sensitivity to extremely low magnetic field intensities.

RCD using flux gate current detection technique are found almost in every electrified residence or offices. They either come integrated with Main Circuit Board (MCB), Lighting Systems, Water Boilers and Kitchen equipment like ovens. Tripping threshold in RCD vary from as low as 20 or 30 mA to 300 or 500 mA as every RCD is designed to trip at a specific current magnitude and each of them have different uses. AC residual currents cause irreversible damage to the human body at just 20 - 40 mA magnitudes while it takes a 200 mA direct current to have the same effect. However, for DC mains voltages in LVDC distribution grids a low voltage range of 200 V is enough to cause irreversible damage in the human body as per the Tripping time vs. touch voltage given in IEC 60479 - 1 standard graph 2.1.

Residual current detectors in general utilize toroidal cores across which the differential flux due to a residual ground fault is detected. Installations with 10 mA threshold is also not uncommon for extra protection near water boilers and other current leakage vulnerable places.

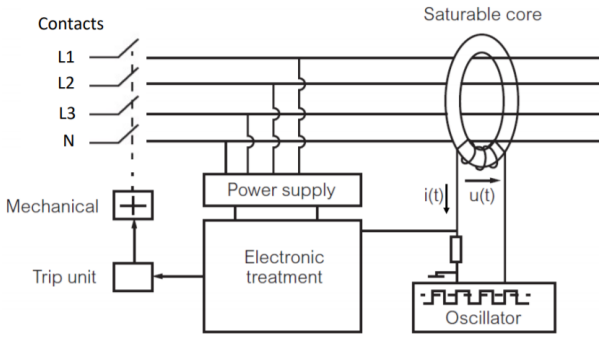

Figure 2.3: Type - B Residual Current Detector using Flux Gate Technology [32].

Basically in flux-gate type of sensing the primary conductors (or poles) in which the residual current to be sensed is passed through a magnetic core with high permeability (Figure 2.3). High frequency Square wave pulses are passed through the secondary winding to saturate the core via an oscillator. When fault is absent in the system, the combined magnetic flux density in the core is zero. The current in the secondary winding symmetrically matches the high peak value of current in secondary winding.

Residual ground fault in one of the poles causes waveform modification of the secondary current signal. The extra DC value, when filtered and measured is equivalent to the DC residual current that has occurred in the network. Since most signal comparisons and computations are digitally carried out, this type of detection is highly precise and accurate. Most advantageous part of flux gate technology is the ability to detect very

small current magnitudes in milliamps of both AC and DC. Additionally it is also bi-directional.

In addition to all the advantages, flux-gate current sensing technique allows flexibility in design that can aid in making the RCD cost effective. This makes wide scale implementation in residential complexes, malls and other large scale installations where these residual current detectors (RCD) are brought in bulk possible. Especially for rural electrification that require a highly sensitive and fast reacting RCD, the flux-gate technique is found useful.

II. Hall - Effect Technology

Hall Effect technology, compared to other indirect sensing methods, proves highly advantageous in the sensing of direct current with lesser power consumption. This is because a constant magnetic field is sensed across a constant applied voltage which when crosses a particular threshold triggers the hall effect phenomenon. The voltage created across the hall element's alternate terminals are then passed through signal conditioning and amplification to get the true value of the residual current being sensed.

Hall effect sensing technique consists of a hall element with four terminals which forms the front - end sensor. A constant voltage is applied across a single pair of terminals. When an external magnetic field intensity or flux perpendicular to a hall element cross a particular threshold, owing to the doping within the hall element, a voltage appears across it's other terminal pair. The higher the constant voltage and magnetic flux density, the higher the voltage across these terminals. The voltage is then equivalent to the generated residual current which can then be calculated. The power consumed in the process is lesser compared to the flux-gate detection technique as alternating pulses are not involved in constantly magnetising and demagnetising the magnetic core.

A Hall element's output linearly varies with the applied magnetic field. The main challenge in sensing low magnitude current is the small magnitude and range of the differential flux generated during a residual ground fault. If the hall effect is manufactured with a higher magnetic flux threshold that needs to be crossed to initiate the hall effect, this would mean lower magnitude currents cannot be detected. Hence the detection and accuracy of the sensor depends entirely upon the properties of the hall element.

Bipolarity of the current in DC mains adds the requirement of sensing **bidirectional current flow**. Hall Voltage Output ($\mathbf{V_H}$) driven through a differential amplifier with fixed bias, satisfies the requirement. This ensures detection of residual currents in both power supply polarities and the Neutral.

In Hall-effect current sensing, the magnetic core is basically left unsaturated. During normal operation as there is no net magnetic flux in the magnetic core. During a residual ground fault, a magnetic flux density equivalent to the residual current appears in the magnetic core. This flux is sensed by a hall effect sensor placed in an air gap in the core.

The signal measured can either be directly measured (in case of higher frequencies using transformer effect) or used to drive a compensation current in the secondary winding (for low frequency direct currents). The second method ensures that the flux in the core is always zero, to prevent saturation of the magnetic core.

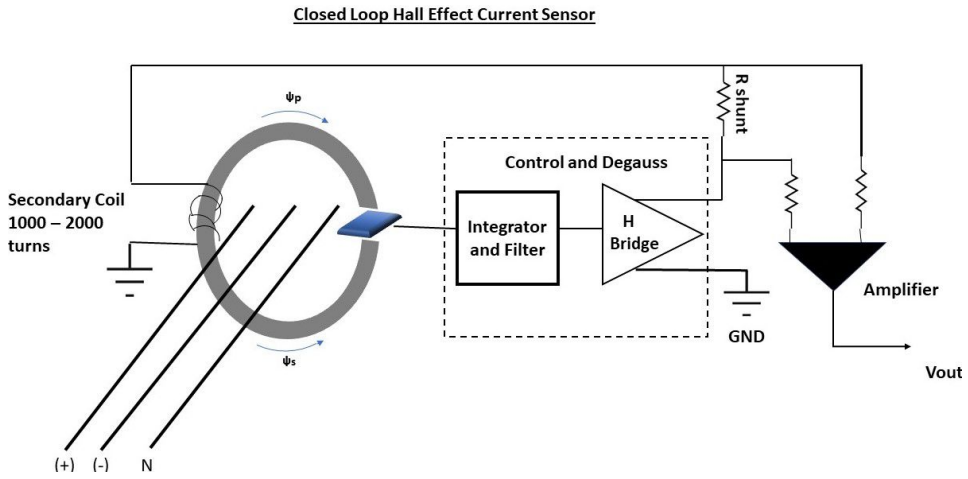

Figure 2.4: Closed Loop Hall effect Current Sensor

First method is called **Open-Loop sensing** and latter is called **Closed-Loop sensing**. Closed - Loop sensor allows for high accuracy and precise measurements. This is possible as core saturation is prevented by flow of an equal but opposing current to induced current in the secondary winding. In effect the magnetic flux in the core is nullified.

The signal generated by the hall element is used to drive the secondary current in the secondary winding which drives the net magnetic flux to zero. In essence the Hall Effect sensor just functions as a gate switch, which switches closes secondary circuit during fault and remains open when no fault. This operation also remove necessity of temperature compensation in hall sensor it is used a null detector and flux in core is always kept at zero. This is a very essential feature for sensing extremely small currents in tens of milli- amperes.

2.4. Conclusion

The different non - invasive or galvanic sensing techniques of Hall Effect and Flux-gate have their own respective advantages and disadvantages. While Hall Effect consumes less power and is easier to implement,the Flux-gate is more precise and accurate especially while sensing fault currents of very small magnitudes like Residual Ground Fault currents which often have magnitudes in range of several milli amps. Also using the flux - gate technique allows for detection of extremely low magnitude magnetic flux densities which in a hall effect sensor will depend on the sensitivity of the hall element that is defined by it's size and dimensions. For increased sensitivity the size of the hall element needs to be proportionally larger which is not feasible when designing a compact and cost effective RCD especially for implementation in rural electrification.

It also forms one of the major reasons why flux-gate technology has been primarily used in RCD over decades. The Hall effect though used widely for various other applications like speed detector in vehicles, position detection etc. the technology is being improved to make Hall sensors more sensitive to smaller currents through use of select doping materials and combinations. Available hall effect technologies that are highly sensitive however are at nascent stage with respect detection of currents at very low magnitudes. Hence for this study , flux-gate sensing technique was found to be more effective both cost wise and accuracy wise.

3

Design of RCD for Bipolar LVDC Grids using Fluxgate Detector IC

3.1. DC Detection : An Overview

Design approach for the RCD is discussed in this chapter along with deatiled explanation on the critical components needed for the sensor operation. Based on the discussion from the previous chapter 2, a requirement analysis is done to draw up.

3.2. Requirement Analysis

Following the discussions in Chapter 2, it is decided that a Type B RCD with Fluxgate technology would match the description for the proposed DC RCD to be designed and developed for use in Bipolar LVDC Distribution Grids. As per IEC 60479 - 1 standard it is well defined that a DC RCD at higher voltage levels should have a tripping time within 10 ms owing to the high contact currents that could pass through the human body in contact with high voltage lines.

This is especially true for the case of rural electrification where there is a higher probability of any living being coming to contact with the main lines with the mains being exposed at various locations. To ensure fast and effective protection from high currents being the main aim of the project, the RCD sensor is required to be both accurate and precise.

3.3. DRV 421 IC

The DRV 421 IC is a closed loop fluxgate sensor which operates on the principle of fluxgate sensing. The Fig. 3.1 shows the DRV 421 fluxgate sensor IC which is a Surface on Contact (SoC) package selected for use in this thesis project. The features provided by the DRV 421 IC are presented in the datasheet [33].

3.3.1. Functionality:

The DRV 421 sensor IC works on the fluxgate sensing principle. The front end sensor is an iron piece housed Voltage in the form of square wave signal is used to continuously saturate the magnetic

Based on the functional requirements of the DRV 421 IC, the critical elements necessary for the development of a RCD using the IC is explored in this subsection.

$$I_{Res} = \frac{(V_{out} - V_{ref}) * N_s}{Gain * R_{shunt}} \tag{3.1}$$

where,

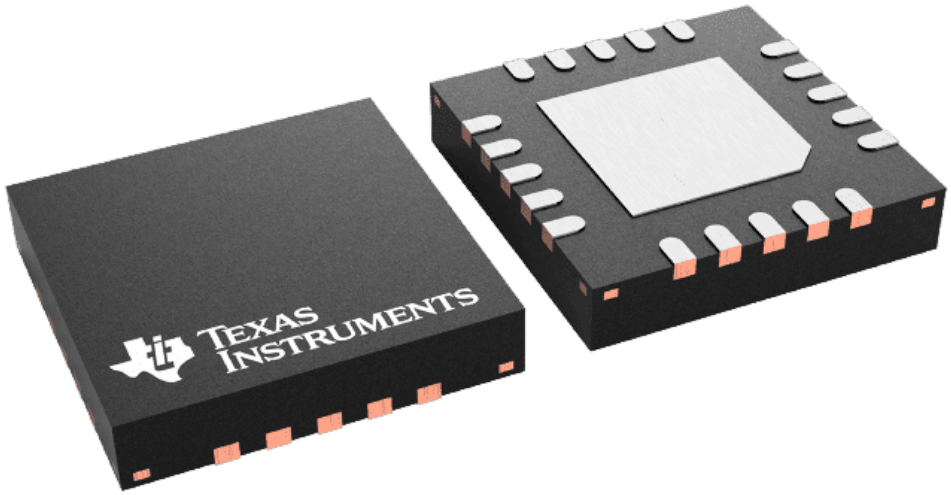

Figure 3.1: DRV 421 IC by Texas Instruments. Surface on Contact (SoC) model.

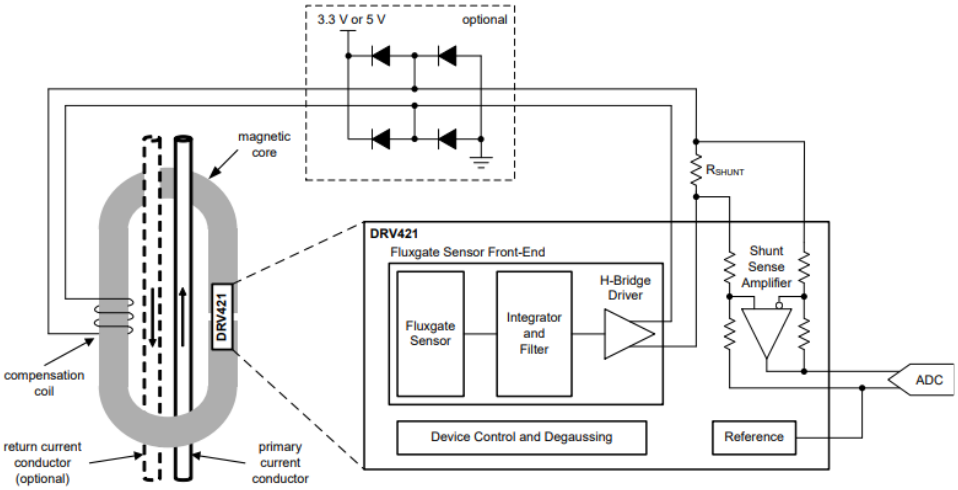

Figure 3.2: Closed loop flowchart for DRV 421 Fluxgate IC

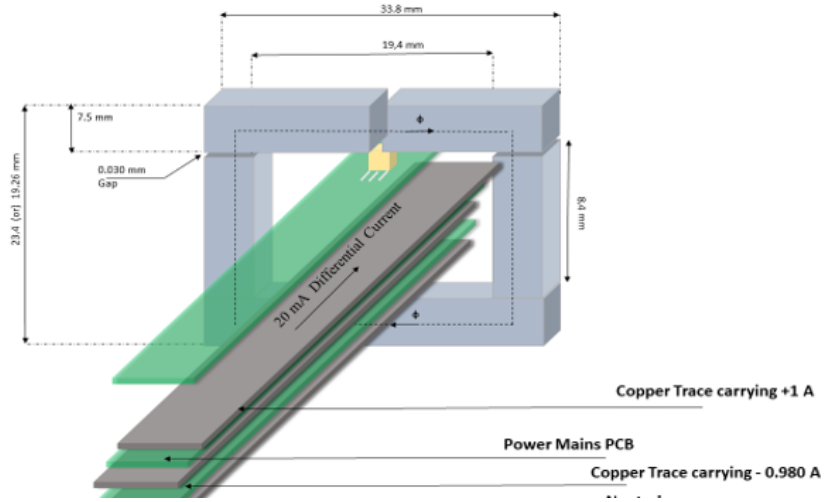

Figure 3.3: Construction of PCB for DRV 421

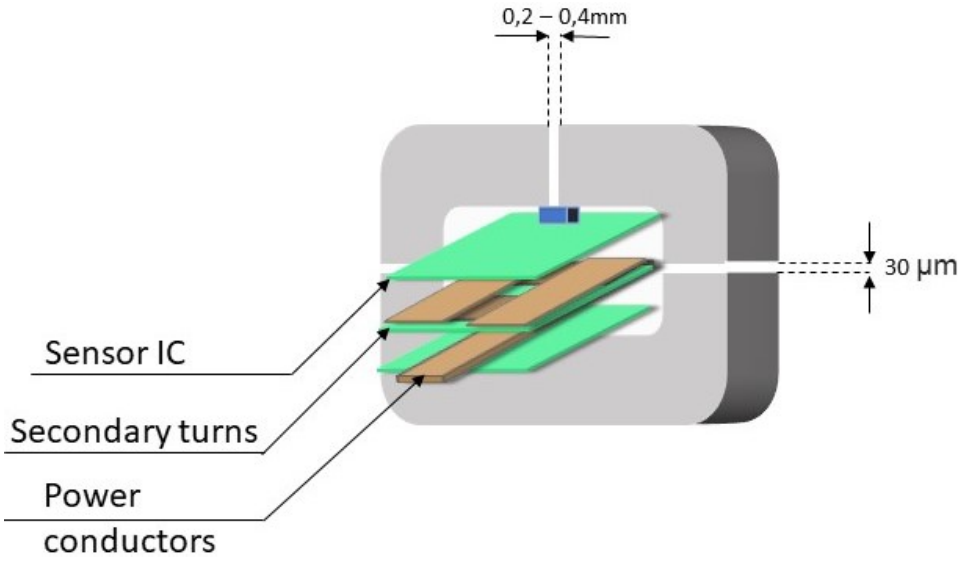

Figure 3.4: PCB Stack alignment for DC RCD. The figure is for representation purpose only.

V_{out} - Output Voltage of the DRV 421 IC.

V_{ref} - Set reference voltage of DRV 421 IC (1.65 or 2.5 V for 3.3 V and 5 V rail voltages respectively)

N_s - No. of turns on Secondary winding Gain - Shunt Sense Amplifier Gain of DRV 421 IC i.e. 4

R_{shunt} - Shunt Resistance.

3.3.2. Magnetic Core

Magnetic core forms a major part of the residual current detector to be designed using the DRV 421 IC. The main functionality of the magnetic core is to guide and concentrate the magnetic flux generated due to a differential current onto the surface of a DRV 421 IC for detection. A magnetic flux density of 13 μT is set as the polarity detection threshold or the minimum flux density required for the DRV 421 detector to operate. Due to residual current sensing being a high sensitivity application, a magnetic core with material of very high initial relative magnetic permeability (μ_r) is desired.

Generally, soft magnetic cores with high magnetic permeability values are used for residual current sensing applications. Toroidal cores are a preferred choice when it comes to any current sensing application owing to their simplicity in design, lower reluctance and for direct wound winding configurations. In this project planar compensation coil has been selected for the winding configuration and requirement of an air gap with compactness of the RCD module to be designed necessitated the use of racetrack shaped magnetic cores, a variant of rectangular cores with smooth edge curves allowing smooth guidance of magnetic flux lines to the sensor location. The magnetic core design has been discussed in detail in Chapter 4.

3.3.3. Planar Compensation Coil

Generally magnetic cores for residual current sensing applications use Direct Wound coil that are directly wound on the surface of the core for compensation purposes. They are simpler to implement, symmetric and uniformly cover the surface of the core. However there come two disadvantages with this type of winding. At higher currents, direct wound application can quickly lead to saturation of magnetic core being directly wound on the surface of the core. Secondly, the no. of windings using direct wound method is limited by the total surface area available on the magnetic core and the thickness of the coil itself. The direct wound coil can also lead to increased heating of the core owing to formation of eddy currents along the contact surfaces can lower the magnetic field strength provided by the core on the surface of the DRV 421 fluxgate sensor. This will cause errors in the output reading, a risk to be avoided especially for residual current sensing where sensitivity and accuracy are critical.

In contrast, a planar compensation coil is implemented using Copper traces on the PCB layers surround-

ing the magnetic core. In this configuration a relative isolation between the surface of the magnetic core and the Copper windings is present which prevents rapid heating of the magnetic core. A great advantage of planar compensation coil is that, many no. of turns can be implemented on every single layer of a PCB thereby increasing the total no. of turns that can be used for compensation. Each PCB layer with a certain no. of windings can be stacked one on top of the other to achiever a certain value of inductance required for the application. The minimum recommended inductance for residual current sensing application using the DRV 421 is 100 mH for the control loop stability and overload current robustness. The minimum no. of turns required for the same is calculated by the following equation :

$$L_{ind,PCB} = \frac{\mu_0 \mu_e N^2 A}{L_m} \tag{3.2}$$

$$\mu_e = \frac{\mu_i}{1 + \frac{L_g * \mu_i}{L_m}} \tag{3.3}$$

where,

N - No. of turns required on the compensation winding

μ_i - Initial Magnetic Permeability of the magnetic core material (H/m)

μ_0 - Magnetic Permeability of Free Space (H/m)

A - Cross sectional area of the magnetic core (in sq. mm)

L_g - Net Air Gap length (in mm)

L_m - Magnetic path length of the Magnetic Core (in mm)

$L_{ind,PCB}$ - Net inductance offered by the Magnetic core and no. of secondary windings (in mH)

3.4. Conclusion

The design of the RCD to be implemented in Bipolar LVDC Distribution Grids for rural electrification has been discussed in this chapter. The design approach is presented with reference to the requirements of DC RCD for Bipolar LVDC grids delineated in the previous Chapter 2. The DRV 421 IC is selected as the primary sensor due to it's closed loop sensing technology using fluxgate sensing technique and compensation that aid in zero flux detection which has increased accuracy and sensitivity for detection of low magnitude currents in the range of milliamps. Other Features such as gain amplification, automatic de - magnetization (DEMAG) operation, availability of three reference voltage levels, and Gain selection to adapt to the type and magnitude of current being sensed (AC or DC) influenced the choice of selection of the sensor. The functionality and features of the DRV 421 is discussed in detail along with brief explanations of the components needed for the sensor operation such as magnetic core and secondary winding. The chapter basically sets the base for the design approach to be adopted for the RCD using the DRV 421 IC.

4

Magnetic Core

4.1. Magnetic Core and Applications : Overview

Magnetic cores are used for applications ranging from power transfer in transformers till sensing devices as tools for causing motion or detection. As such magnetic cores vary by their application and area of use.

4.2. Magnetic Core for residual ground fault detection

Magnetic Cores for detection of residual ground fault currents are characterized by high initial magnetic permeability denoting high magnetic storage capacity to suit requirement to be sensitive enough to detect differential magnetic flux caused due to extremely small magnitude currents (in the range of mA). Another reason for this characteristic is for accurate and precise measurement of small magnitude currents. The higher the initial permeability of the magnetic core the higher the sensitivity of the sensing device. Additionally only higher permeability of the core lowers the possibility of introduction of errors in large magnitudes to the sensitive measurement operation.

4.3. Shapes of Magnetic Cores

There are various shapes of magnetic cores utilized for various purposes. A combination of E and I Cores for e.g. are used in center tapped multi-winding transformers requiring effective magnetic coupling between the primary and secondary windings and Isolation while a combination of U and I cores are used for simple two winding transformer solutions with a set reluctance for use in consumer electronics and gadgets like toys and model robots.

Residual current detectors traditionally use Toroidal cores to ensure effective magnetic coupling between primary and secondary circuits in galvanically isolated non - invasive current sensing techniques. The DRV 421 IC requires an air gap to detect fringing flux caused due to a differential current in the mains owing to a residual ground fault. In this case a traditional toroidal core would find difficulty in application as the IC is to be kept beneath an air gap for detection of the fringing flux caused due to a differential current. Further, the circular shape of the Toroidal core makes it difficult to be placed across a stacked PCB in a compact manner.

Rectangular cores have sharp edges that can cause localized eddy currents and concentrate magnetic flux at particular points which carries potential to heat and corrode the edges at high magentic flux densities caused by higher differential currents around 1 A for example. It also has an adverse impact in detection of low magnitude currents as the magnetic path would deviate causing stray fluxes around the core instead of concentrating them at the sensor itself. These issues call for selection of a different type of core called the 'Racetrack Core'.

A Racetrack core is rectangular in shape but with curved edges and laminated to prevent eddy currents and stray flux. The magnetic path of a racetrack core ensures that the maximum flux is redirected to the correct location which is on the DRV 421 sensor IC in this project. The net reluctance provided by a racetrack

core is lesser compared to the previously mentioned cores owing to the shape. Additionally the core has a good geometry to be placed across a stacked PCB unit to detect residual ground faults. Hence a Racetrack shaped core is selected for use in this project.

4.4. Core Material Selection: Fe-Amorphous based Nanocrystalline Magnetic Core

Material selection for a magnetic core to be used to detect low magnitude currents is affected by the above mentioned requirements mainly a high initial permeability. Further accounting for the use in rural electrification, the core material must be easily available and affordable.

Nanocrystalline Fe material for magnetic cores are the ones commonly being used for residual current sensing applications owing to their high initial permeability - high magnetic storage capacity. The higher initial permeability also takes into account, losses in the net magnetic permeability of the core with alterations in it's geometry and air gaps constituted to fit the sensor requirements.

For this project Fe - Amorphous Nanocrystalline core from Wurth Elektronics has been selected owing to it's characteristics matching the above mentioned requirements. Further due to a large availability of the product renders it cost effective for use in residual current sensing application using the DRV 421 IC.

4.4.1. Geometric Shape of the Core

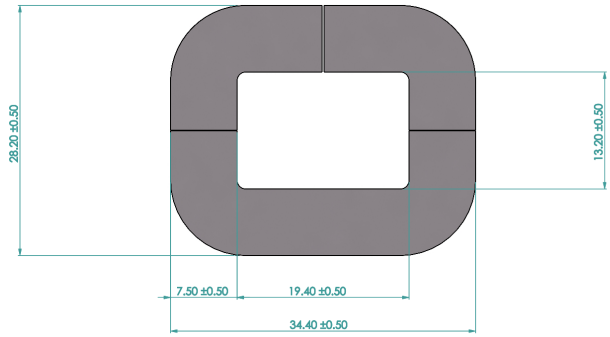

Figure 4.1: Front view of designed Magnetic Core with the design dimensions

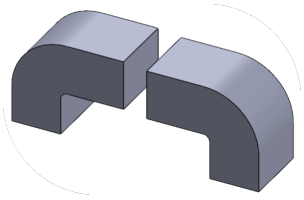

Figure 4.2: L-Shaped upper halves of the designed Magnetic Core.

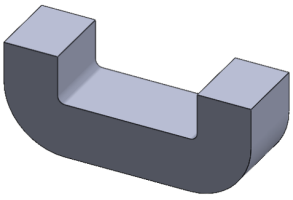

Figure 4.3: U-Shaped Bottom half of the designed Magnetic Core.

A racetrack shaped magnetic core was selected for this project owing to it's ability to guide the magnetic flux lines smoothly onto the surface of the DRV 421 IC placed directly under the air gap. The construction and design of the magnetic core with it's dimensions are presented in Fig. 4.1. The selected core is of 34.4 mm length, 28.2 mm width and 10 mm thick. The girth of the front facing surface is 7.5 mm. The dimensions in detail are presented in Appendix A. The data-sheet of the custom designed core is shown in Fig. A.2.

The Figure 4.4 shows the 3D image of the fully assembled magnetic core rendered in Solidworks CAD software version 2023. The two air gaps at the sides are 30 μm each with the air gap at the top being 1 mm wide if assembled with the L-Shaped upper halves sit exactly on the U-shaped base. A maximum of 0.8 mm

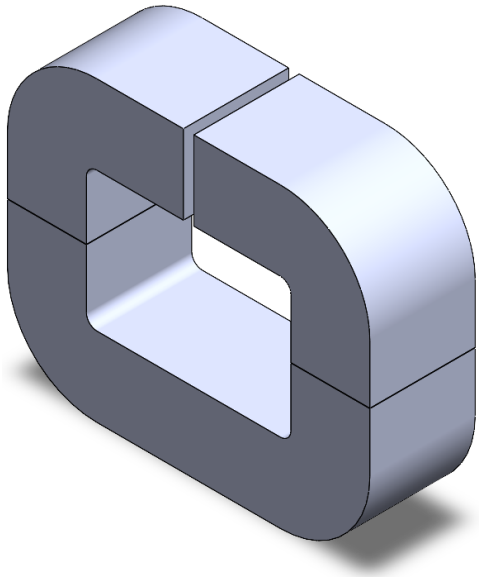

Figure 4.4: Fully assembled Magnetic Core designed for RCD with DRV421 IC and planar compensation winding

needs to reduced by moving the two L-shaped pieces closer by 0.4 mm each to make the 0.2 mm air gap underneath which the flux-gate residual current detector DRV 421 will sit.

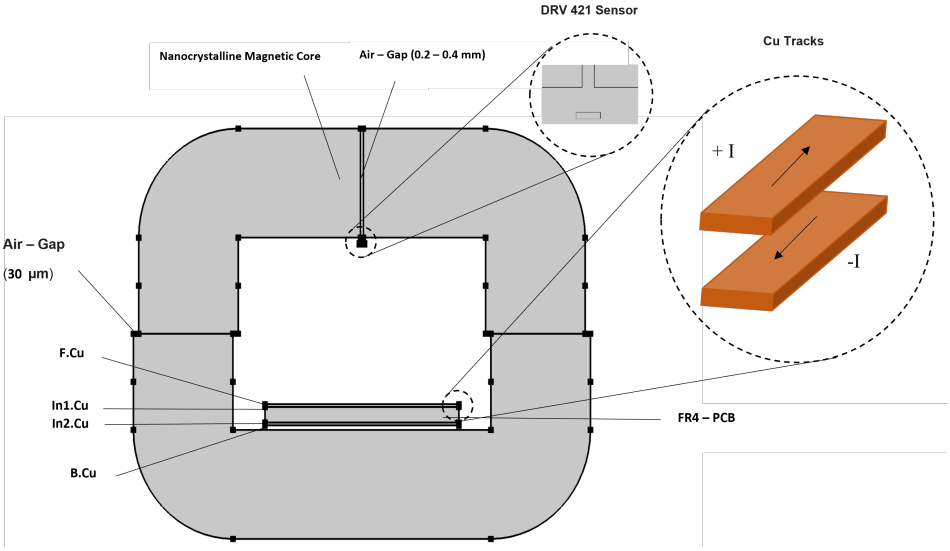

Figure 4.5: Arrangement of the Residual Current Sensor with the designed Magnetic Core

4.5. Determination of Air - Gap for Core

The Air Gap between the top two halves of the magnetic core beneath which the DRV 421 IC is to be placed for detection of magnetic flux produced by differential current in the mains is decided by the amount of magnetic flux strength that the gap can produce onto the fluxgate IC. Increase in air gap leads to reduced net initial magnetic permeability across the magnetic core due to increase in magnetic path length while increasing the fringing flux across the IC making detection of differential flux easier. Decrease in the air gap leads to decreased area of fringing flux across the IC but increases the total initial permeability of the magnetic core owing to reduced magnetic path length.

Hence a balance between the magnetic flux density on the DRV 421 IC and the net initial permeability (μ_0) of magnetic core needs to be kept in mind while deciding the air gap of the magnetic core. The actual mag-

netic permeability of the magnetic core during operation would definitely be lesser than the initial magnetic permeability as per the BH curve. Numerically, an air gap of **0.2 - 0.3 mm** was found apt for the application and the calculation has been provided in Appendix A.

4.6. Comsol Simulation of Magnetic Core

This section contains simulation results of the magnetic core used for developing the residual current detector (RCD) for use in LVDC Grids in COMSOL 5.3 FEM software.

For simulation, the Magnetostatic domain is considered neglecting the effects of external influences and other factors that impact the result.

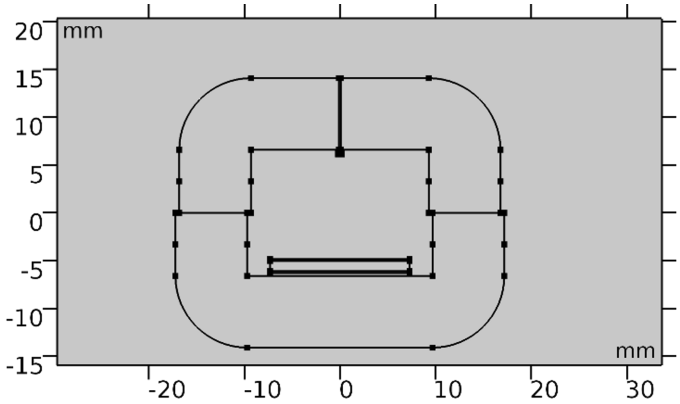

Figure 4.6: Simulation model of designed Magnetic Core in COMSOL 5.3 FEM software

The Fig. 4.6 is an overview of the 2D representation used for the magnetic simulations. Proceeding sections will explain the simulation in detail.

Main objective is to observe the Magnetic Flux density B at the sensor just sitting below the air gap at the top. The resulting simulation due to magnetic flux created by a differential current of 1A passing through the core can be observed in Fig. 4.7

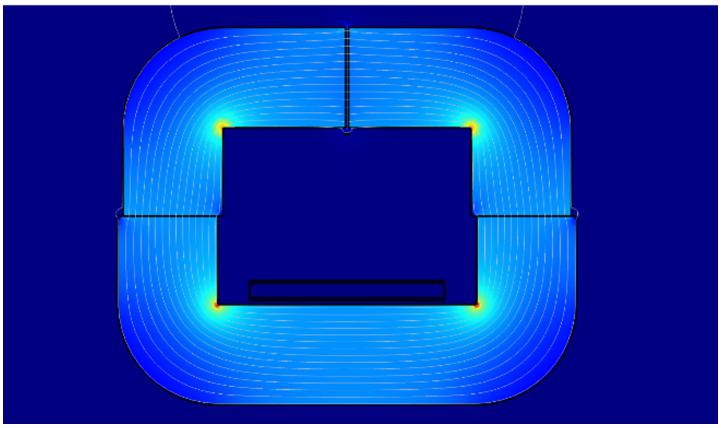

Figure 4.7: Magnetostatic Simulation of built model of the designed Magnetic Core in COMSOL 5.3 FEM Graphical interface with Magnetic Flux created by 1A differential current passing through the core.

Simulations for various magnetic flux strengths caused due to different differential current magnitudes across the magnetic core as detected by the DRV 421 IC are given below.

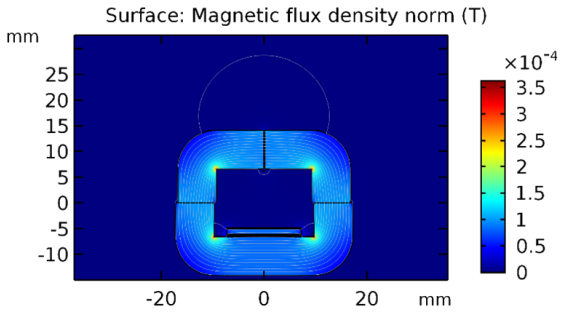

Figure 4.8

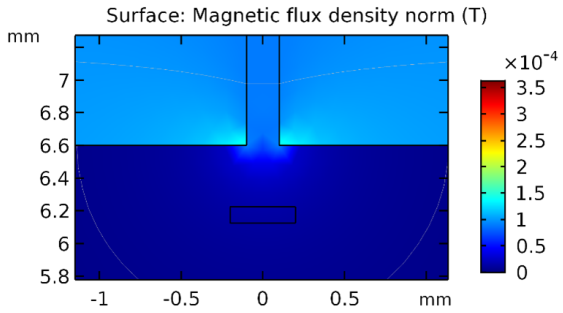

Figure 4.9

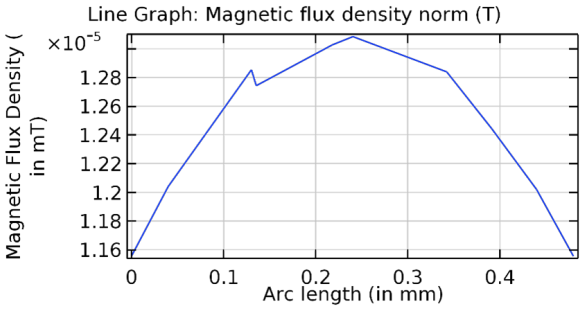

Figure 4.10

Figure 4.11: FEM Simulation for 20 mA residual current.**B = ~ 13 μT**

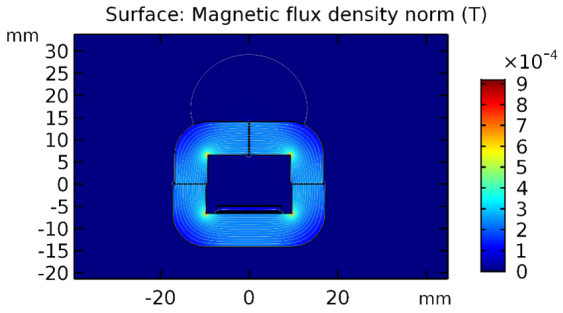

Figure 4.12

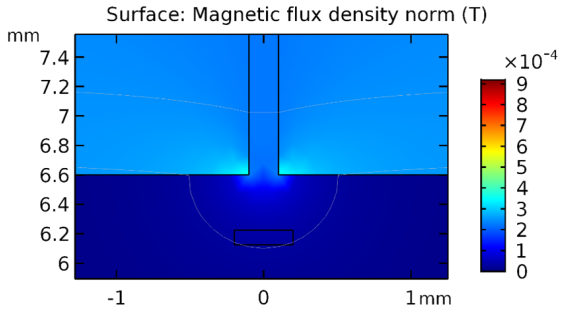

Figure 4.13

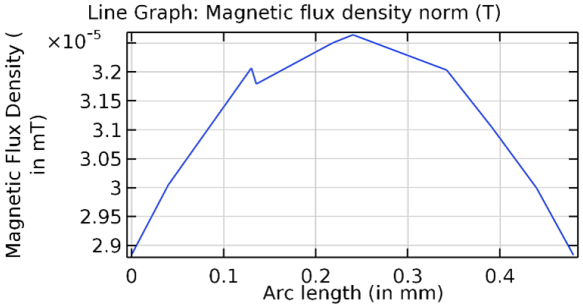

Figure 4.14

Figure 4.15: FEM Simulation for 50 mA residual current.**B = ~ 33 μT**

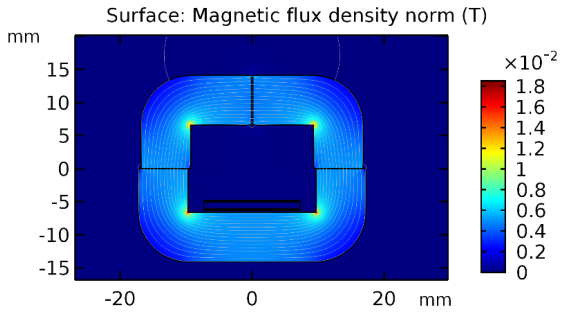

Figure 4.16

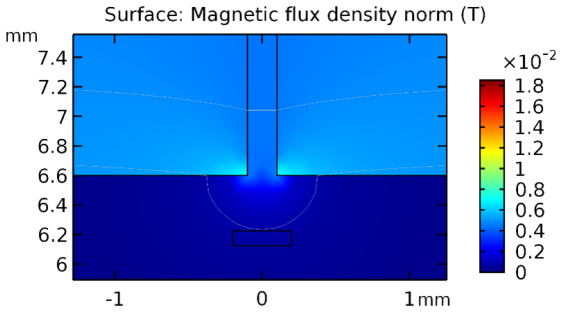

Figure 4.17

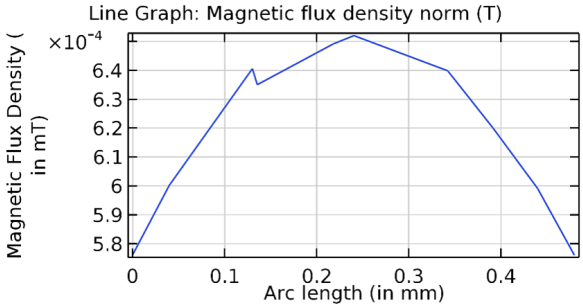

Figure 4.18

Figure 4.19: FEM Simulation for 1 A residual current.**B = ~ 0.65 mT**

4.7. Conclusion

In this Chapter, we discussed the design of the magnetic core to be used in the development of the Residual Current Detector (RCD) using DRV 421 IC. The Chapter began with an overview of the requirement of magnetic cores in residual current sensing applications and proceeded to discriminate the various shapes and material of cores available in order to determine the best core configuration that would suit the residual current sensing application.

Fe - Amorphous Nanocrystalline is the material selected for the application owing to it's high initial magnetic permeability (μ_i) and layered design to prevent eddy currents. This allows the material for use in applications requiring high sensitivity like residual current sensing.

The curved edges of a racetrack shaped core allows smooth guidance of magnetic flux lines to the surface of the DRV 421 IC placed beneath the air gap for detection. The rectangular shape allows it to be placed like an inductor core on the PCB reducing the total space required for the residual current sensing operation. Moreover, the planar winding configuration can be easily implemented around the core owing to the shape and necessary air gaps introduced for install it on a PCB. This lead to the selection of the racetrack shaped core was selected for the development of the RCD PCB.

The selected shape and material are created in Finite Element Modeling (FEM) software of COMSOL version 5.3 and simulated for various magnitudes of differential currents. The simulation is performed with the main objective to determine the net magnitude of magnetic flux density that can be provided by the selected magnetic core configuration on the surface of the DRV 421 IC. It is determined that magnetic flux density greater than the required minimum threshold of 13 μA is generated for differential currents ranging from 5 mA - 1 A magnitudes. Therefore, the proposed racetrack Nanocrystalline core configuration is selected for the RCD application.

5

PCB Development and Assembly

5.1. Chapter Overview

This Chapter discusses the design and construction of the PCBs that constitute parts of the proposed RCD and the process of integration of all units to form it. The design details of the constituent PCB and their respective functions are presented followed by brief description of the configuration of the integrated unit and its development process. The chapter ends with a discussion of the capabilities of the developed RCD device and outlines the special features of the design. Following sections describe in detail the design of the PCB types and their development process.

5.2. RCD PCB : DRV 421 PCB

In this section we explore the design of the primary PCB of the proposed RCD that contains the circuit layout of the DRV 421 IC and the STM 32 bit microcontroller used to program the IC. The PCB is designed based on the requirements of the DRV 421 IC to detect fringing flux from the air gap of the magnetic core while maintaining zero flux at the core via compensation current. This is considered the primary PCB due to the rest of the RCD PCB setup being dependent on the configuration of the DRV 421 IC which is the main component of the RCD. This PCB is placed at the top of all PCB since the DRV 421 IC is to be positioned exactly below the air gap of the magnetic core to detect fringing flux generated by a differential current flowing in the main line PCB which is discussed in detail in the subsection 5.4.

The primary or RCD PCB contains the schematic split into three parts. The DRV 421 IC and STM 32 bit 48 pin Micro-controller sub layers connected together by the main layout to form the primary RCD PCB. The main layout is discussed first to provide an overview and top layer understanding of the operation and control of the RCD PCB followed by the respective sub layers of the DRV 421 IC and the STM Micro-controller in detail.

5.2.1. Main Layout

The main layout of the primary PCB shows the date exchange between the DRV 421 IC and the STM 32 bit Microcontroller for programming and ADC along with the provision for the external demagnetisation discussed in Chapter 3 via a switch that can be controlled via the STM micro-controller. The Fig. 5.1 shows the schematic of the top level design built in KiCad software. The entire PCB is powered at 3.3 V supply via a linear dropout regulator (LDO).

The DRV421 IC is connected to the STM 32-bit microprocessor with 48 pin provision to be programmed and used for sensing fringing flux across the air gap created in the designed racetrack shaped magnetic core as discussed in Chapter 4 Section4.5. The reference voltage (V_{ref}) and the corner frequency for the integrator of the DRV421 are set using the reference selector pins (RSEL0,RSEL1) and the gain selector pins (GSEL0 and GSEL1) respectively. The STM32 micro-controller is used to set these values in the DRV 421 IC. The values of RSEL0,RSEL1,GSEL0 and GSEL1 are therefore connected as output from the STM32 micro-controller and

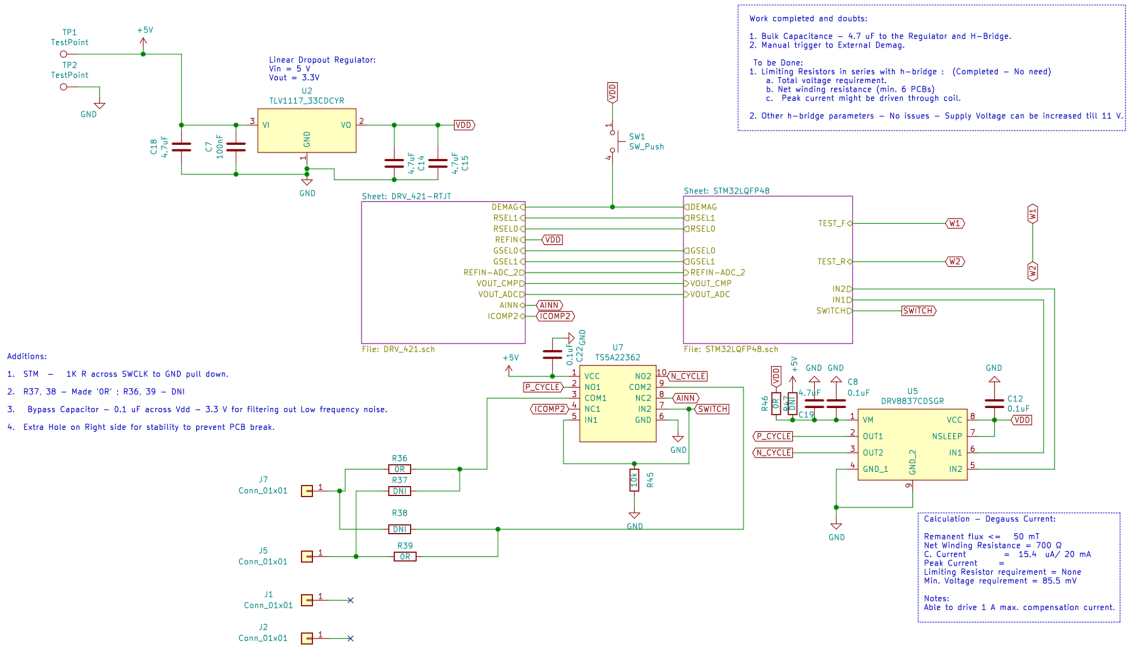

Figure 5.1: Schematic overview of RCD PCB in KiCAD.

input to the DRV 421 IC.

The DRV 421 provides the option for demagnetising the magnetic core when the core gets saturated due to high magnetic fields produced from high currents. This option can be initiated by pulling the DRV421 IC pin to a higher voltage level i.e. DEMAG is set to 1 from 0 for at least 25 μs. A manual option via a push button switch (SW1) is provided for this along with the ability to do the same via the STM32 micro-controller. Hence the DEMAG pin is connected as input to the DRV 421 IC from the STM32 micro-controller as shown in Fig. 5.2. Although the DRV 421 flux-gate IC already has an inbuilt search function to detect saturation and automatically initiate a demagnetisation cycle, this option can be used to manually initiate the same. This is useful in case the built-in search function of the IC is unable to determine whether or not the magnetic core is saturated within the stipulated amount of time programmed for the function to run post which it gives an error signal. By externally monitoring the stable value of the output voltage (V_{out}) of the residual current detector and continuously checking whether the value equals the reference voltage value (V_{ref}), the manual option can be used therefore to initiate the demagnetisation function when required.

5.2.2. DRV 421 IC Sub-Layer

The DRV 421 IC sub-layer details the circuit for DRV 421 IC. The Fig. 5.2 shows the circuit schematic of the DRV 421 IC sub layer. To determine the residual current magnitude, the Output Voltage (V_{out}) and the Reference Voltage (V_{ref}), from the DRV 421 (REFIN-ADC_2 and VOUT_ADC) are subtracted and Equation 3.1 is used to compute the true value of the residual current. The output and reference voltages are fed as inputs to the STM32 micro-controller.

The shunt resistors (R_shunt) R33 and R9, the voltage drop across which are measured to calculate the residual current are connected in-between the AINP, ICOMP1 and ICOMP2 terminals. The voltage drop across these resistors is amplified by a gain of 4 by the internal op amp of the DRV 421 which appears as output voltage (V_{out}) at the VOUT terminal (pin 6).

DRV 421 IC sub layer. The terminals of the IC are connected to the

An over-range comparator is used to detect whether the output signal (V_{out}) crosses the thresholds of 2.2 V or 1.1 V - set as higher and lower threshold respectively corresponding to residual current values of ± 18 mA. The Comparator TLV3202 is used to send a high signal if the output voltage has gone above +18 mA or if it has gone below -18 mA. The Output of the Comparator via the terminal VOUT_COMP is fed as input to the MCU as an input signal. This signal is used to determine if the residual current trespasses the threshold and

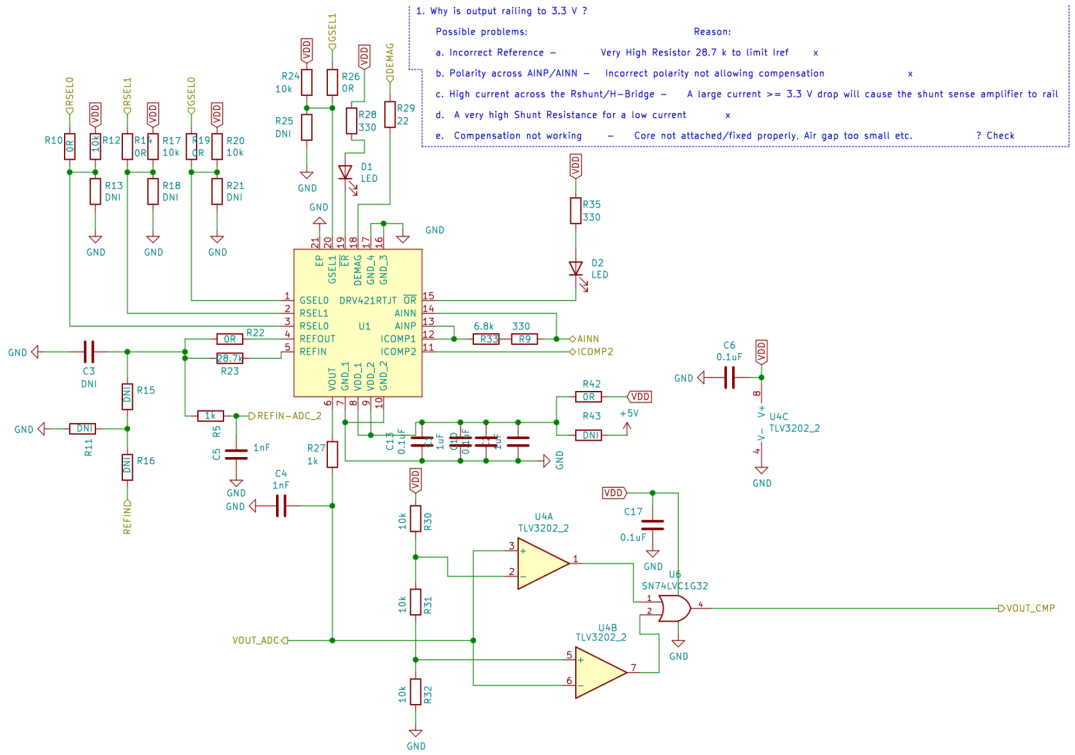

Figure 5.2: Circuit Schematics of DRV 421 IC in KiCad.

this signal can be used to trigger the Circuit Breaker via the MCU.

The DRV 421 provides an option for demagnetisation that is initiated through pulling the DEMAG terminal (pin) high.

5.2.3. STM32 Microcontroller Sub-Layer

The Fig.5.3 shows the circuit schematic for the STM32LQFP48 micro-controller used for programming and controlling the DRV 421 IC. The Microcontroller is powered with 5V supply via ferrite bead 'BF1' to reduce EMI.

The analog values of output and reference voltages (V_{out} and V_{ref}) are provided as input to the STM32 micro-controller at the analog to digital (ADC) pins of 22 and 24 (PB10 and PB12) respectively. The residual current can be determined through programming using the equation 3.1. This can be used to trigger the quickly initiate the circuit breaker operation on detection of a residual ground fault. It can also be used to store the values of residual currents and for display to the operator for keeping a registry of the residual fault currents for later reference.

The pin nos. 30 and 31 of the Micro-controller are used for setting the Integrator corner frequency as discussed in A below the Equation A.4. The pins are named as GSEL0 and GSEL1 corresponding to the similar terminals on the DRV 421 IC so that the Gain mode can be set using the micro-controller. The GSEL0 and GSEL1 are output of the micro-controller and sent as input to DRV 421 IC. Two pins, Pin 26 and 27 of the Micro-controller are also used to set the RSEL0 and RSEL1 on the DRV 421 IC that are Reference Selector terminals. The selected reference voltage for the DRV 421 is 1.65 V with a supply voltage of 3.3 V. The (RSEL1,RSEL0) are set to (0,1) to select 1.65 V as the reference voltage.

A provision for manual or automatic RESET has been provided to Reset the STM 32 micro-controller. This is initiated through pulling the Pin 10 (PFR-NRST) pin to high. Two options have been provided for this : A push button reset using SW2 and RESET command through the JTAG programmer that is used to program the STM 32 micro-controller. The STM MCU is also used to provide a signal across it's Test_F and Test_R (Pins 37 and 38) to generate an artificial residual current of 5 mA for testing purposes.

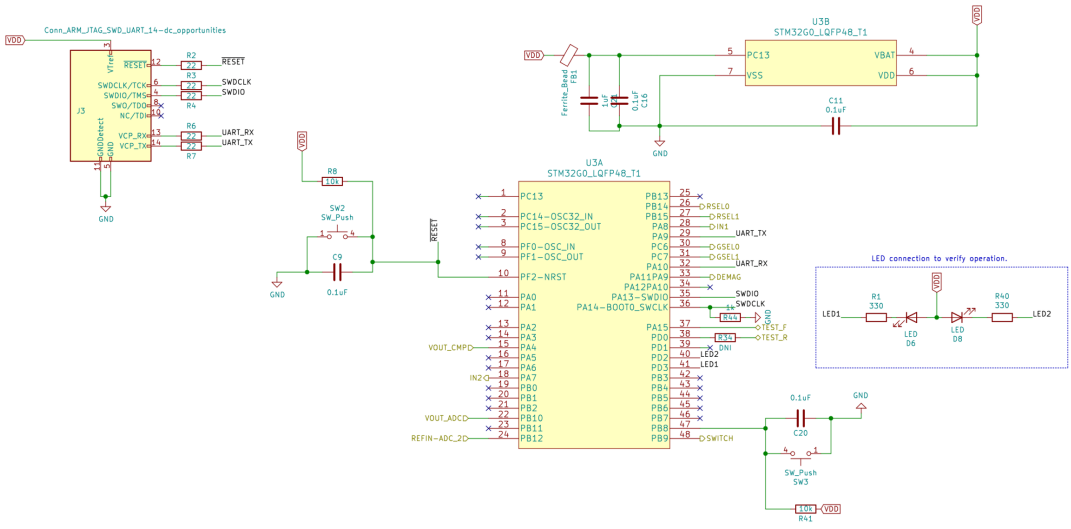

Figure 5.3: Circuit Schematic of STM32 Microcontroller with 48 pins in KiCad.

5.3. Planar Compensation Coil PCB

The design of the planar compensation coil PCB are discussed in this section beginning with detailed description of the schematics and PCB layout built in KiCAD. Then the design and operation of the compensation winding PCB are described briefly followed by presentation of 3D rendered images from KiCad PCB layout editor and the actual images post the PCB fabrication stacked on top of the PCB carrying the main LVDC Bipolar power supply line.

The Fig. 5.4 shows the schematics of the compensation coil PCB built in KiCad. The compensation winding PCB uses planar winding configuration wherein Cu tracks on the PCB are laid in an oval shape around each leg of the racetrack shaped magnetic core. The no. of winding turns are split into equal halves on each PCB layer and laid around each leg of the magnetic core. Further the winding turns are distributed evenly across the four PCB layers to ensure balanced compensation due to the presence of air gaps in the core. There are 26 turns per layer split into two halves : 13 around each leg of the magnetic core. The same no. of turns are repeated on each layer to make in total 104 turns in split winding configuration on each compensation winding PCB. The PCB Layout of the same is presented in the Fig. 5.5 comprising the Type 1 and Type 2 compensation winding PCB.

The Compensation winding PCB as can be seen in Fig.5.5 is divided into two types Type - 1 and Type - 2 PCB depending on the positioning of the terminals. The position of the Via and Cu pad are interchanged in Type - 2 PCB. That forms the only major difference between the two types of PCB. This allows for the Compensation winding PCB to be stacked on top of each other and finally on the Mains PCB. The Fig. shows the layout of the planar Cu winding on each layer of the compensation winding PCB.

According to the calculations shown earlier approximately 9 PCBs are required to get 936 that correspond to 312 mH. Compared to physically winding Cu coil on top of a core such as in coil wound configurations, the planar winding configuration simplifies the task of increasing or decreasing the no. of turns as PCB containing hundreds of turns can just be stacked on top of each other to achieve the minimum inductance rating required for the operation. In this case the minimum recommended inductance as per DRV 421 datasheet by Texas Instruments is 300 mH for assured closed loop stability for the DRV 421 operation despite a minimum of 100 mH is recommended in case 300 mH is not possible to be obtained.

5.4. Mains PCB

The Mains PCB carries the main power lines in bipolar configuration. The polarities of Positive (+), Neutral (N) and Negative (-) are split across the four layers of the PCB namely Front Cu. , In1, In2 and Bottom Cu. layers respectively. The Figure 5.9 shows the schematic of the Mains PCB that carries the power line conductors across which the differential current is to be sensed.

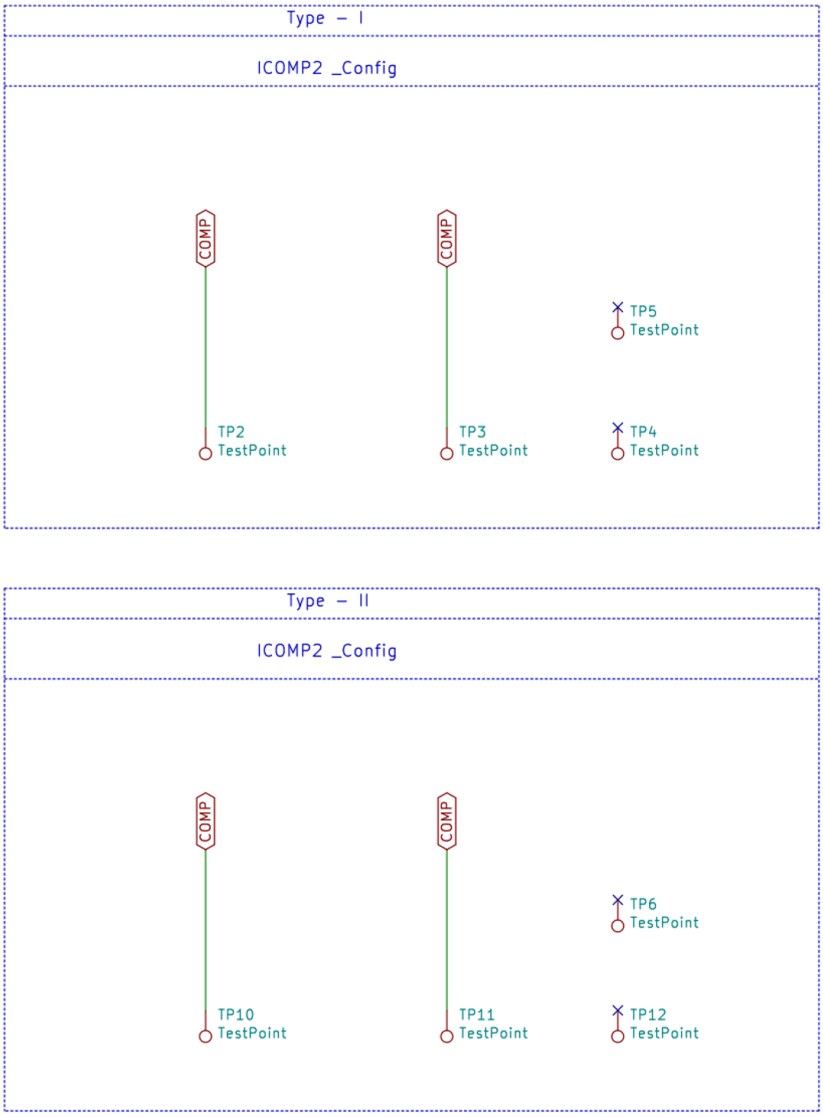

Figure 5.4: Schematics of Planar Compensation Coil.

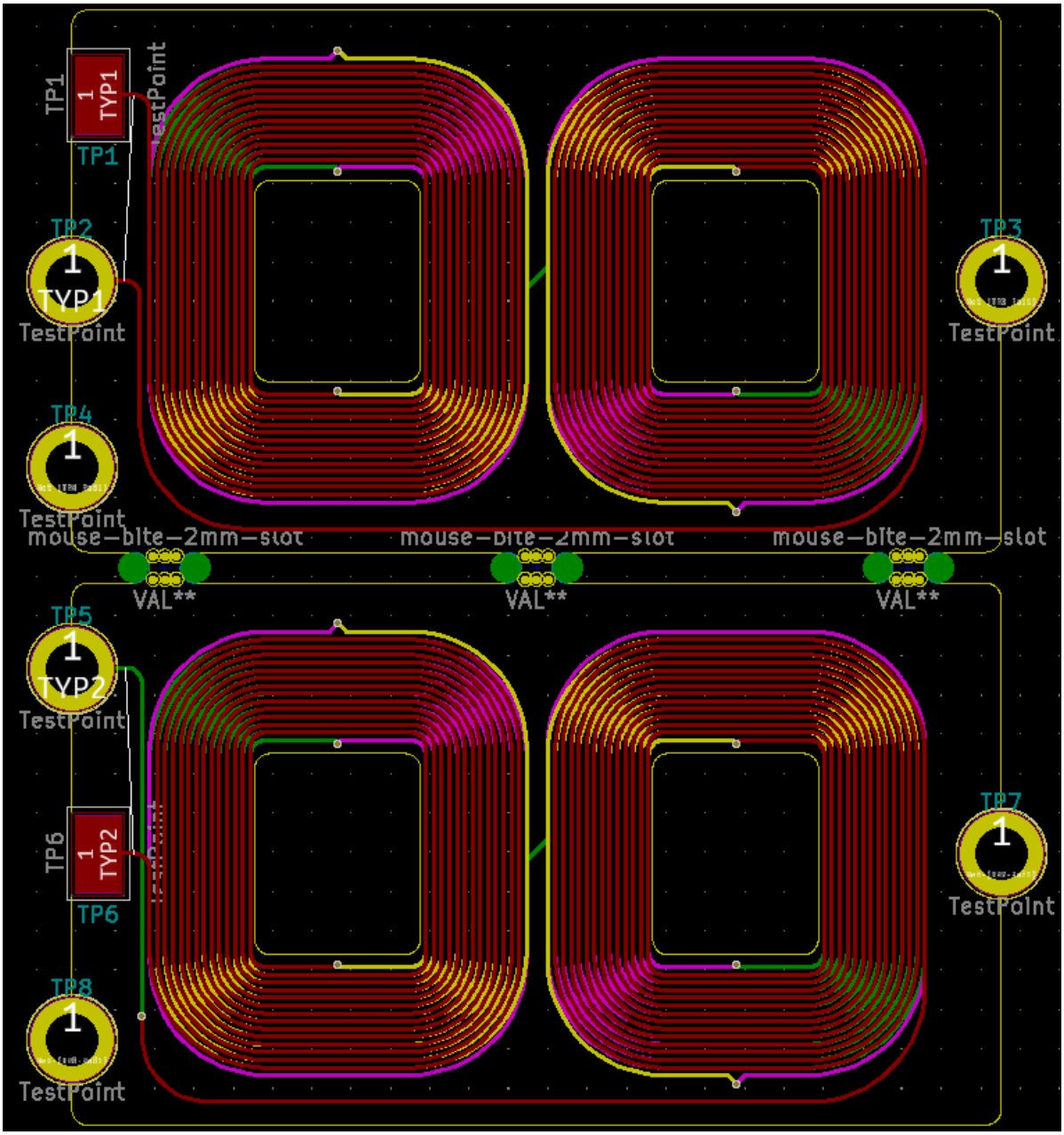

Figure 5.5: PCB Layout of Type 1 and Type 2 compensation windings on 4 layer PCB designed in KiCAD PCB Layout Editor.

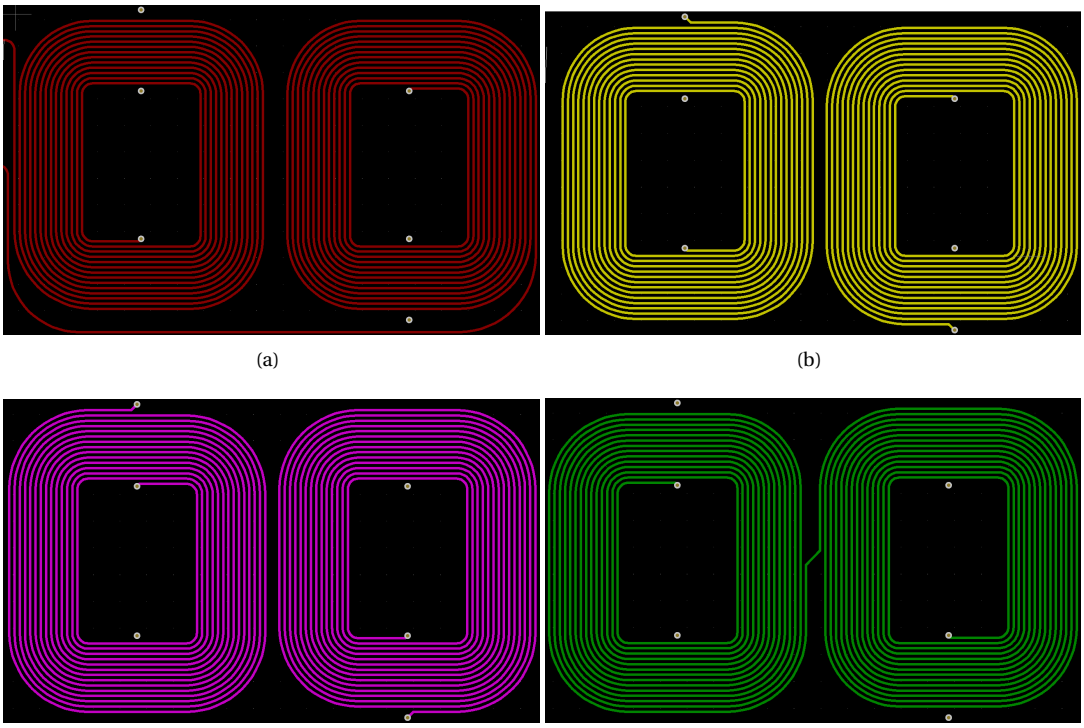

(a) (b)

(c) (d)

Figure 5.6: (a) Winding on Front Cu (F.Cu) (b) Winding on In1.Cu (c) Winding on In2.Cu (d) Winding on Back Cu (B.Cu)

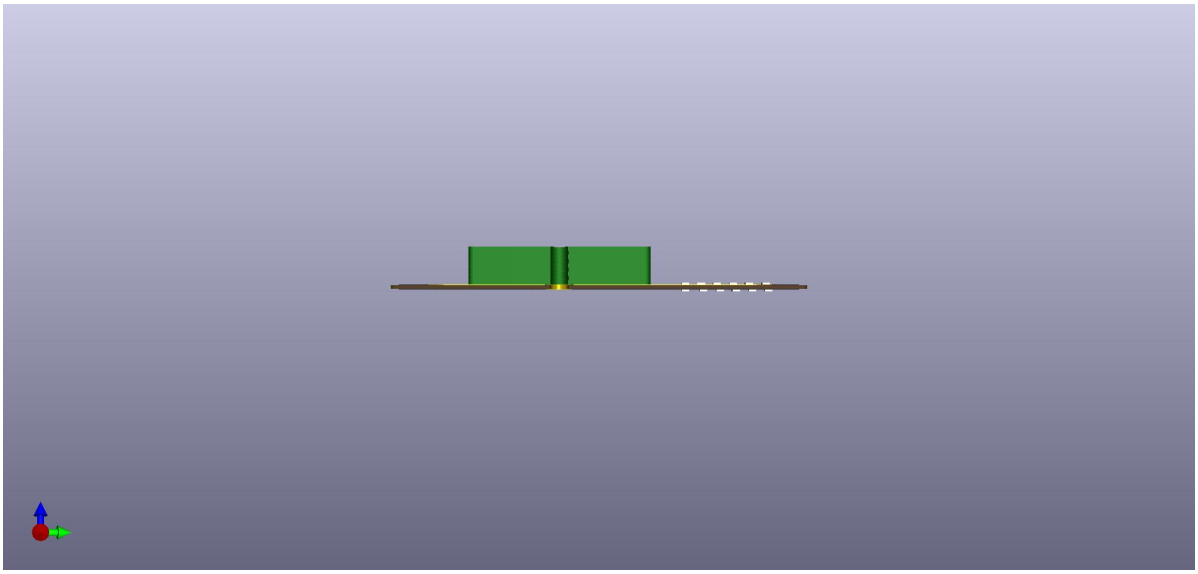

Figure 5.7: Right Side - View of Stacked Compensation Winding PCBs consisting of Type - 1 and Type -2 Winding PCBs.

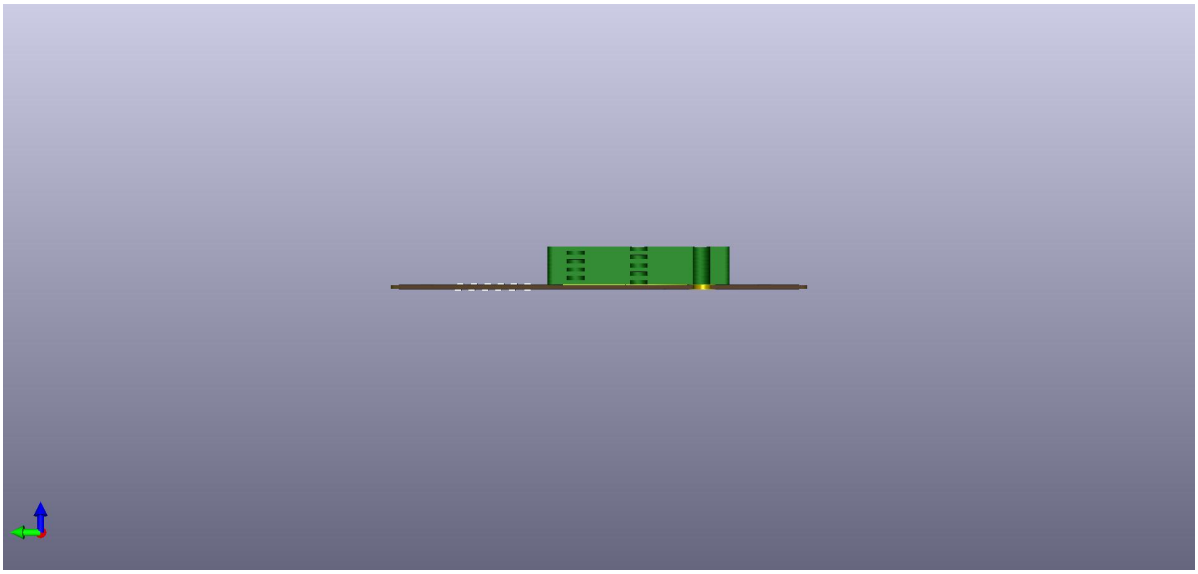

Figure 5.8: Left Side View of 3D image rendered on KiCad displaying the of the stacked Planar Compensation Coil PCBs.

The Fig. 5.10 and Fig. 5.11 show the Top and Bottom view of the Mains or Power Conductor PCB. There are two Cu pads as provision for connection to the Type 1 or Type 2 of the Compensation Winding PCBs. The Via TP7 is used to connect the Bottom PCB to the RCD PCB in order to complete the circuit for the compensation coil. The TP2 via on the Right side is used to solder all the PCB layers together and hold as a single unit.

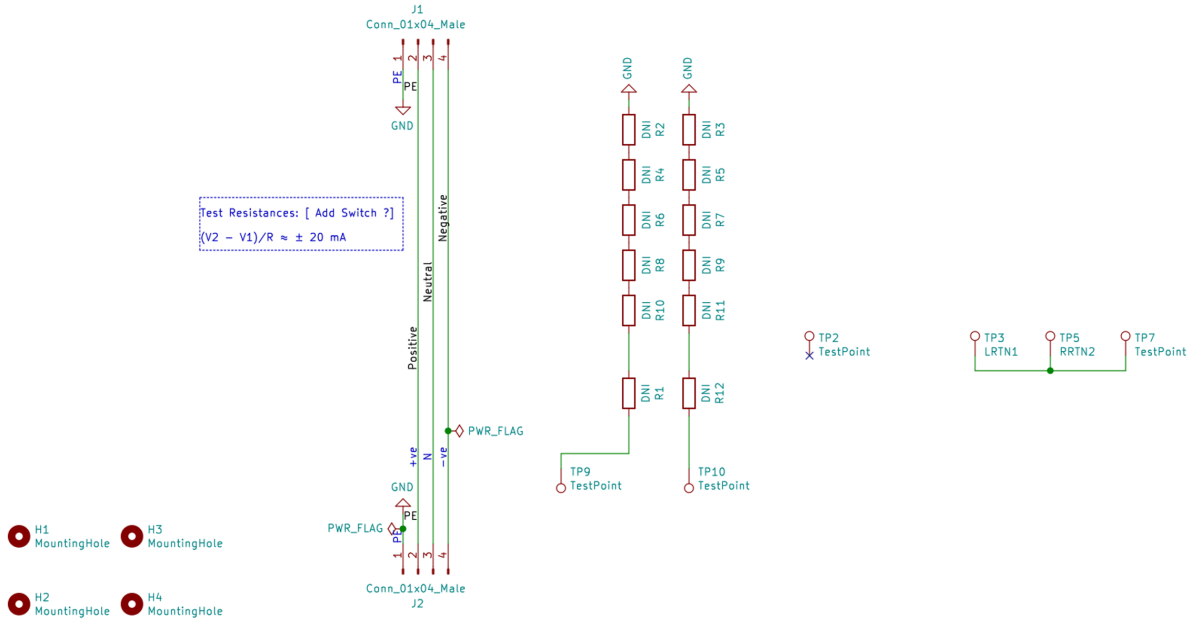

Figure 5.9: Schematics of Mains PCB constituting the Power Carrying Conductors of the main line in bipolar configuration.

5.5. PCB Development

The RCD is composed of three different PCB types namely : RCD PCB, Compensation Winding PCB and Mains PCB. The design and development of these three PCB types that constitute the proposed RCD prototype using DRV 421 IC has been discussed in the previous sections. In this section, the integration of these three PCB types to build the end product are discussed.

In this section, the PCB configuration/arrangement (RCD PCB on top, Comp Wind in between and Mains

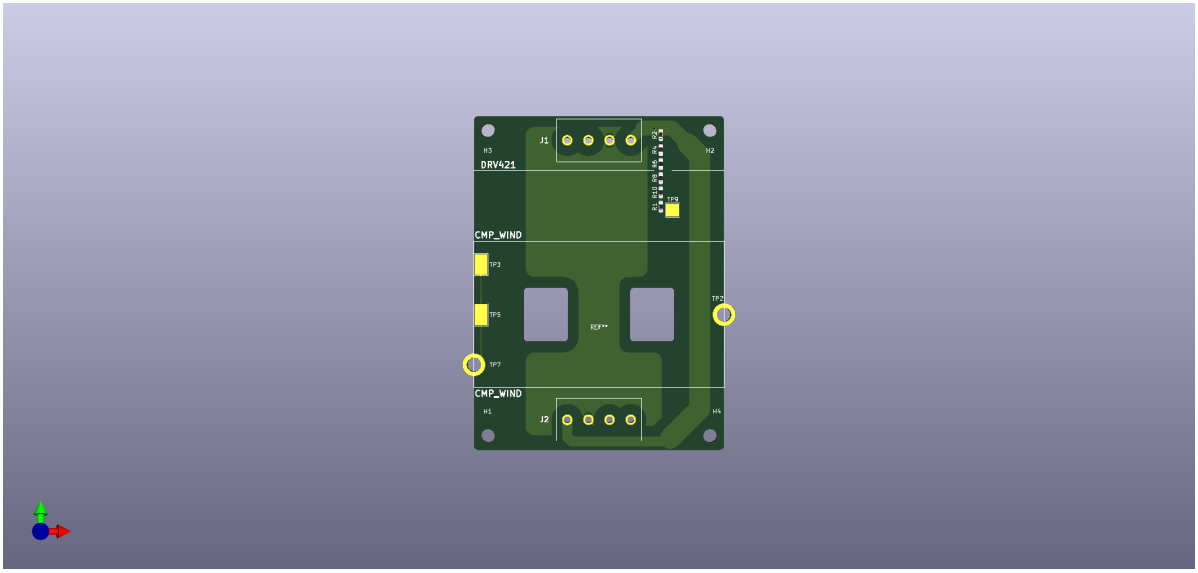

Figure 5.10: Top view 3D image of the Mains PCB rendered in KiCad.

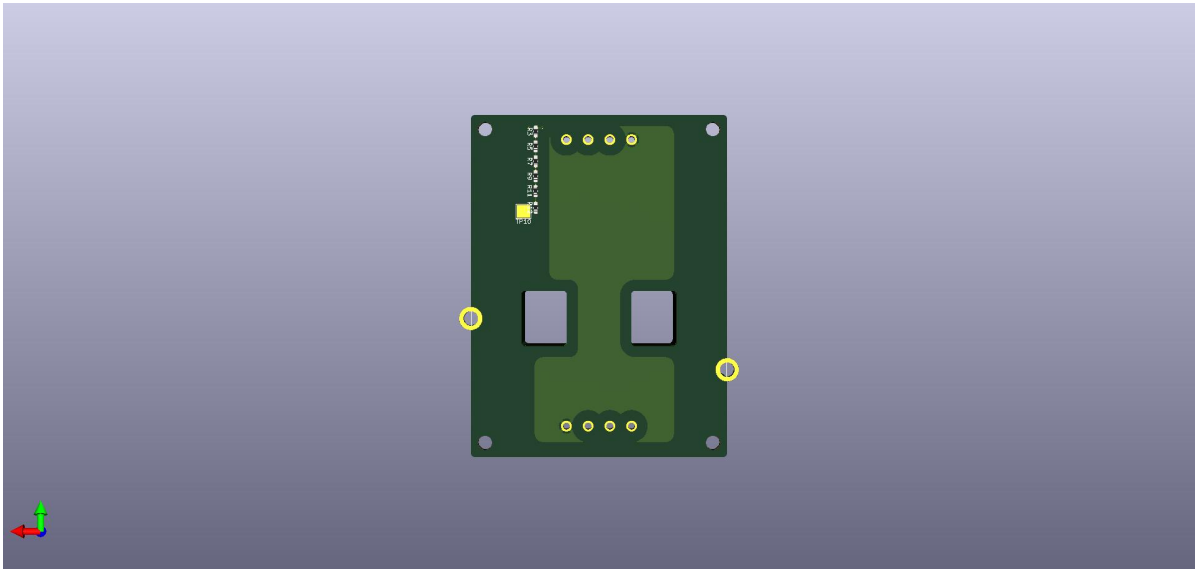

Figure 5.11: 3D Bottom view of the Mains PCB rendered in KiCad.

PCB at the bottom) is explained followed by the process of PCB preparation from applying solder paste, heating in oven, component placement, soldering of the different PCB together till placement of core and attachment of probes for testing. Then the PCB capabilities specific to the RCD design of how much inductance it can deliver via removing or placing of compensation winding PCB is presented.

The arrangement of the designed RCD prototype is such that the PCB containing the RCD is placed at the top due to the requirement of the DRV421 IC to be positioned exactly below the air gap of the magnetic core. The compensation winding PCB are stacked placed below the RCD PCB and the PCB carrying the Supply Mains are placed at the bottom. This allows for the other PCB types to be soldered on top of the Mains PCB.

The 3D rendered images of the fully designed PCB with all the PCB types stacked are displayed in this section.

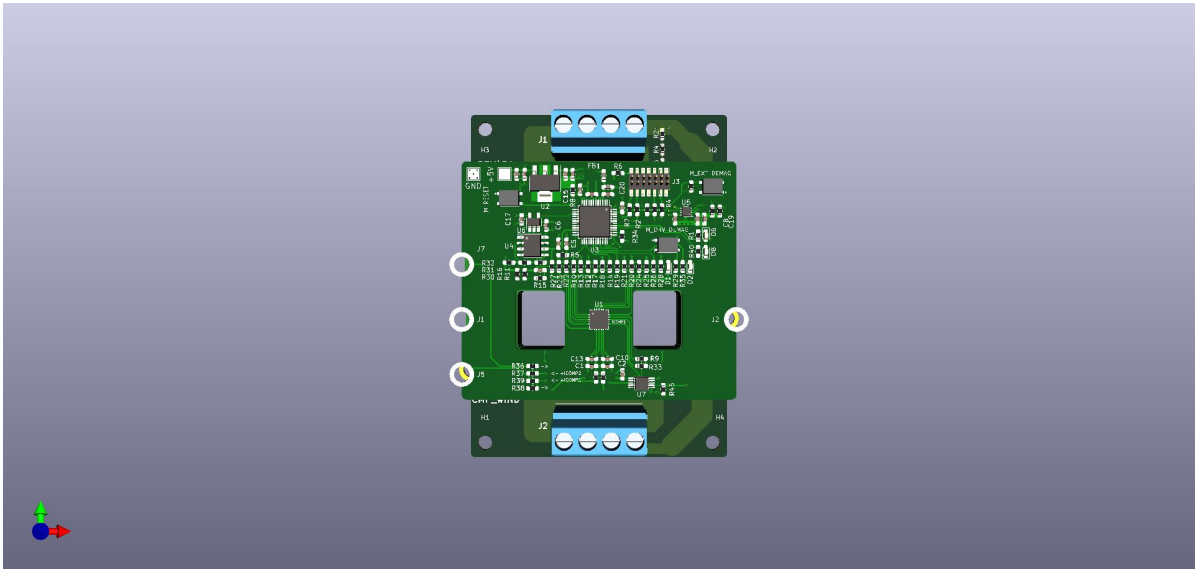

Figure 5.12: A 3D image rendered on KiCad displaying the Top view of the designed PCB.

The Assembled RCD PCB is presented in the Fig.5.13

The developed PCB has many capabilities specific to it's design that are advantageous for successful implementation in Bipolar LVDC grids for rural electrification. The small and compact design ensures that the net cost for the PCB is reduced. This is also because of the non - dependence on external copper wires for passing through the magnetic core. The integrated RCD unit detects differential current directly from the Cu tracks which is beneficial as the RCD can directly be installed on the Circuit Breaker PCB in line with the supply mains. This reduces the no. of components and saves space on the Circuit Breaker PCB providing a modular and robust design for residual current protection. The provision for increasing or decreasing the no. of turns on the compensation winding by increasing or decreasing the no. of compensation winding PCB with planar winding configuration also enables likewise to increase or decrease the net inductance by adding or removing PCB. This comes as a huge advantage removing the necessity to physically increase or decrease the no. of turns around the magnetic core and thereby the net inductance provided by the core and winding combination. The relative isolation between the magnetic core and the compensation winding remove the possibility of heating and burning up of copper wires due to heating up of the magnetic core due to higher magnitude differential currents. The increased reluctance due to air gaps in the core prevent saturation due to sudden current peaks in the main supply line.

5.6. Conclusion

In this Chapter the design and development of the proposed prototype of RCD was presented and discussed. The RCD comprises of three different types of PCB named as : RCD PCB, Compensation Winding PCB and Mains PCB. The RCD PCB consists of the DRV421 flux-gate sensor IC and the required components and power supply and programmer for the IC. Secondary compensation windings in split winding configuration for achieving zero flux closed loop detection form the next PCB type which is further split into Type 1 and Type 2

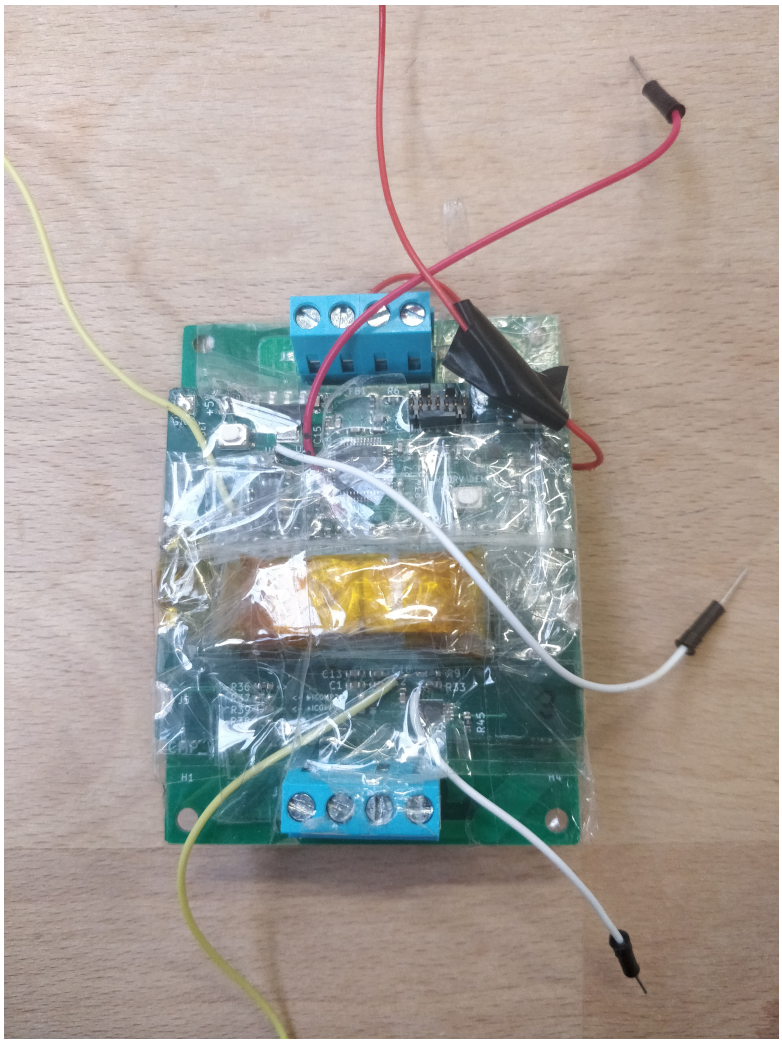

Figure 5.13: Top View of RCD PCB.

PCB based on the terminal connections of the compensation winding respectively. The compensation windings in split configuration along the two legs of the racetrack shaped magnetic core ensure proper balanced compensation especially due to presence of air gaps along the core. One of the main advantages of planar compensation winding PCB is the provision to increase or decrease the no. of turns of the compensation winding and thereby the inductance offered by the magnetic core and winding combination. Further the relative isolation between the core and the turns of the compensation winding prevent quick saturation of the magnetic core in case of sudden current spikes on the main power supply line. Additionally the built sensor configuration is more compact and robust in design compared to core wound type RCD models commonly in use today. The smaller the size of the magnetic core the lesser the price and simpler the built model cheaper the sensor. Therefore the chapter can be concluded by safely saying that a compact, cheap and robust design of a RCD for Bipolar LVDC grids for rural electrification could be developed.

6

Experimentation and Results

The RCD assembled as discussed in Chapter 5, is tested for different residual currents under different mains voltage levels. In the current chapter, the results obtained through these tests are presented and discussed. This chapter is divided into two sub-sections which present the results obtained from the tests in two different voltage ranges namely : **Extra Low Voltage** and **Low Voltage**. These two subsections are further divided into four sections dedicated to the tests conducted in **Unipolar** and **Bipolar** circuit configurations respectively.

Initially the RCD PCB is tested in the ELV range (< 120 V_{DC}) in Unipolar grid configuration to test it's response to a residual current in differential current sensing mode and to determine the reaction time, sensitivity and linearity.Then the same device is tested in Bipolar grid configuration to determine the same three parameters for the same voltage range. Similarly the device is then tested in the Low Voltage range (120 V - 360 V_{DC}) in bipolar grid configuration. The results obtained in the Bipolar circuit configuration in the Low Voltage range are given higher importance considering the implementation of the RCD in Meshed LVDC Distribution Grids, where the bipolar network configuration finds itself advantageous for the many reasons as discussed in Chapter 1.

In the sub sections, initially the test circuit and method used to create a residual ground fault to sense is described. The experimental test setup with the devices used are then explained with illustration which is followed by a tabulation of the PCB parameters including the Gain Setting of the DRV 421, no. of compensation windings used and net inductance offered by the winding stack. Finally, the output voltages ($\boldsymbol{V_{out}}$) of the residual current detector (RCD) for each residual current magnitude is shown with respect to the reference voltage ($\boldsymbol{V_{ref}}$ = **1.65**$\boldsymbol{V}$) as Voltage vs. Time graphs wherein the values of output voltage $\boldsymbol{V_{out}}$, $\boldsymbol{Time}$ and their respective changes from their original values: $\boldsymbol{\Delta V}$ (Differential Voltage) and $\boldsymbol{\Delta T}$ = $\boldsymbol{T_r}$ (Rise Time) or the time taken for the output voltage of the sensor to rise to the expected magnitude with respect to the detected residual current are shown.

The output voltage rise time ($\boldsymbol{T_r}$) of the sensor is very important in determining the net reaction time of the protection system which includes the RCD and the circuit breaker, in detecting and breaking residual ground fault currents. A minor delay in the breaking time would be lethal considering possibility of high currents which need to be detected and removed within a particular duration (e.g. 10 s for $\boldsymbol{I_{RES}}$ > **200 mA**) as discussed under Section 1.2 in Chapter 1. Initially the experimental setup is discussed for test at Extra Low Voltage (ELV) level ranging from **5** - **120** $\boldsymbol{V_{DC}}$ along with the circuit, parameters and devices used. Then the results obtained at Low Voltage (LV) level **120** - **1500** $\boldsymbol{V_{DC}}$, which are of primary importance in this study, are presented in the same format. Residual Current Detection is used in accordance with

6.1. Unipolar Grid Configuration

Many factors need to be considered in testing any device at higher voltage ranges such as safety and precautionary measures to be taken due to higher probability of occurrence of large peak currents that could be achieved at smaller loads due to certain manual actions on the circuit like a pole disconnection or switching at higher voltages and other phenomenon like circulating net currents (CNC). Ensuring the ability of the source

to regulate voltage levels and installed reliable circuit protection systems to prevent damage to any component owing to temperature intolerance of the device at high currents and other safety precautions form part of the measures when testing at higher voltages. Considering these factors, the device is tested initially at lower and controllable voltage levels. This also allows flexibility in the use of different load resistances to vary the residual current levels to test the functionality of the built RCD. In this section, the test performed in the extra low voltage range (< 120 V_{DC}) is explained and the results are discussed.

6.1.1. Test in Extra Low Voltage Range

As discussed in the previous section, the designed RCD prototype is initially tested in Unipolar circuit configuration at ELV power supply range to test the functionality of the device for different residual currents. The following sub - sections will explore the test in detail.

Test Circuit and Setup

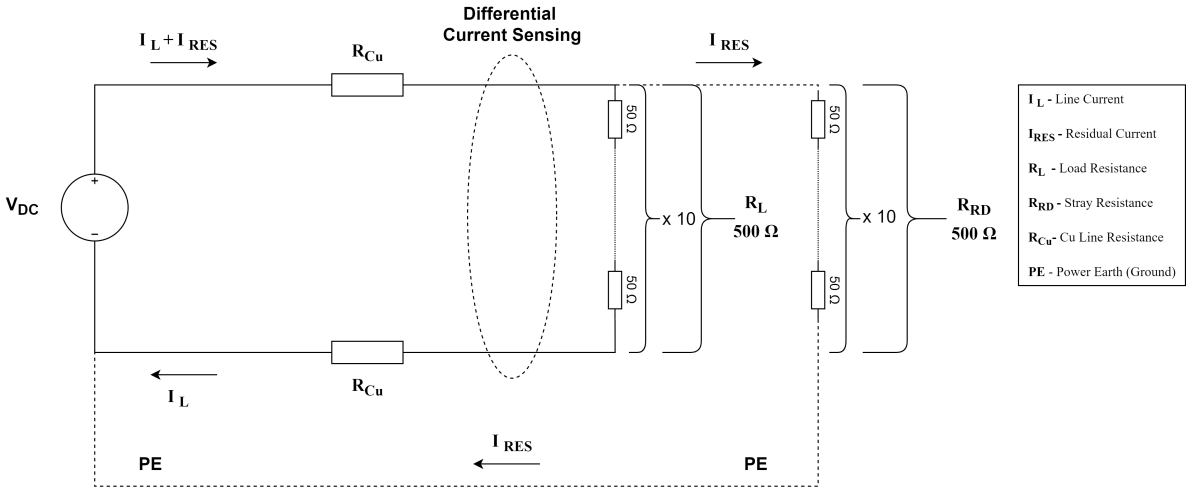

Figure 6.1: Circuit Diagram for Unipolar Test setup.

The Fig. 6.1 represents the Unipolar circuit for the testing of the RCD. A net load resistance of 500 Ω consisting of ten 50 Ω resistors is placed across the Positive (+) and Negative (-) terminals of the mains supply. To simulate a residual current, another 500 Ω resistance consisting of ten 50 Ω resistors are connected across the Positive (+) and Protective Earth (**PE**) terminals via a Multimeter to measure the residual current and bypass the sensor in order to create a residual ground fault. The **PE** is externally shorted with the Negative at the entry terminals to the PCB near the source to close the circuit path for the residual current. This enables to simulate a residual ground fault scenario for various residual current magnitudes by varying the supply voltage. The Fig. 6.2 shows the experimental test setup. The next sub section shows and discusses the results obtained from the experiment.

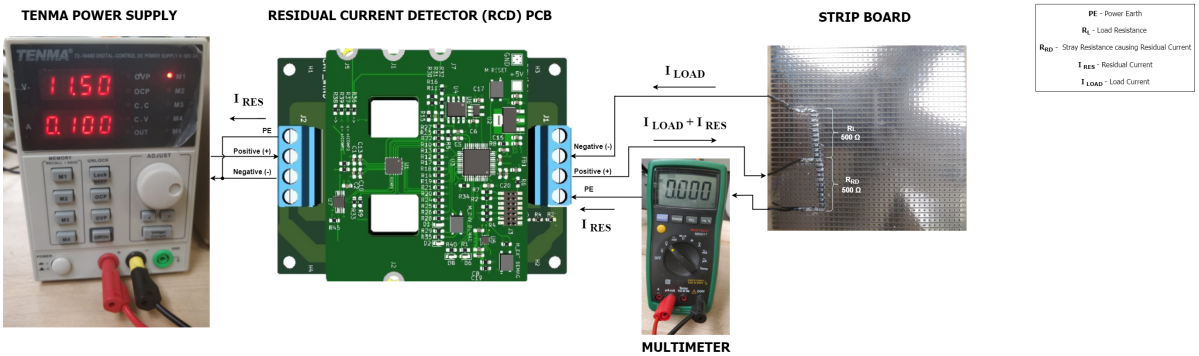

Figure 6.2: Test setup for Unipolar case.

Test Results and Analysis

The source voltage is varied from 5 - 20 V to generate equivalent residual currents for detection. The imbalance in differential current across the main line is seen as voltage difference across the shunt resistor (**R_{Shunt}**) which when multiplied by the gain of the shunt sense amplifier within the DRV421 IC appears as voltage at it's **V_{Out}** terminal. The voltage difference between the reference and output voltage levels is the detected residual current value. This voltage difference $(V_{out} - V_{ref})$ is then converted back to the residual current value using equation 3.1. In the graphs below **V1 - Output Voltage** and **V2 - Reference Voltage**. The results obtained using the discussed test set up in the previous subsection are presented below :

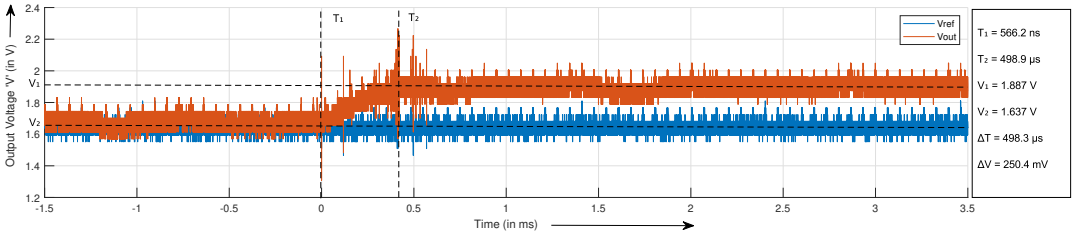

Figure 6.3: Residual Current: **8.1 mA** detected within **498.3 μs** at **5V** supply voltage.

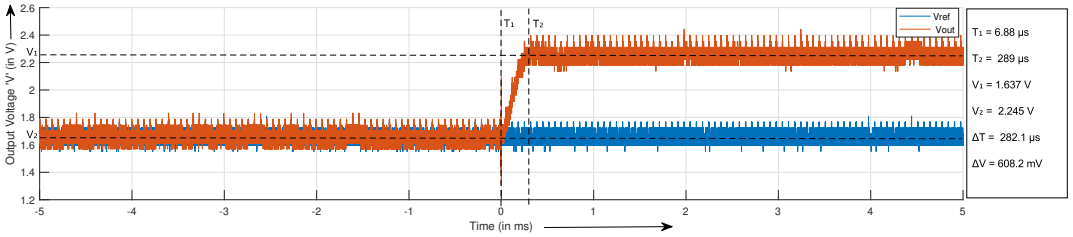

Figure 6.4: Residual Current: **20 mA** detected in **282.1 μs** at **11.5 V** supply voltage.

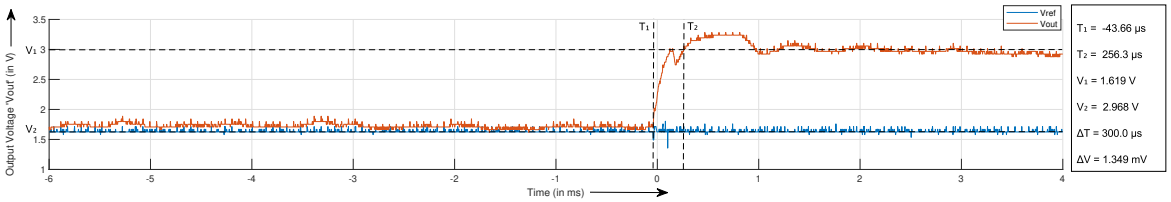

Figure 6.5: Residual Current: **20 mA** detected within **300 μs** at a Unipolar supply voltage **92V** through electronic load.

Table 6.1: Tabulated Results of RCD testing in Unipolar Grid Configuration.

S.No.	I_{res}(mA)	R_{sh} ($K\Omega$)	N_S	V_{ref} (V)	V_{out} (V)	$(V_1 - V_2)$(V)	Cal. I_{res} (mA)	Acc.(%)	T_r (μs)
1.	8.1	7.13	936	1.637	1.887	0.25	8.2	1.23	498.3
2.	20	7.13	936	1.637	2.245	0.608	19.95	-0.25	282.1
3.	20	15	936	1.619	2.968	1.349	21.04	5.2	300

It can be observed from Table 6.1 that the reaction time or rise time (T_r) of the RCD is between 300 - 498.3 μs and the accuracy in percentage calculated of the readings with Tenma Power supply and shunt resistance of 7.13 KΩ is within $\pm$ 1 % . However for the electronic load at high R_{sh} of 15 KΩ, the accuracy is 5.2 % . This indicates that extremely high shunt resistor values can lead to closed loop instability that can lead to high accuracy errors. From this the importance of selection of the right parameters for the RCD for the specified range of residual currents especially to ensure closed loop stability.

6.2. Bipolar Grid Configuration

This section deals with testing of designed RCD in bipolar grid configuration at ELV and LV mains voltage ranges. Initially the RCD is tested at ELV (5 - 16 V) using two Tenma power supplies in bipolar configuration by creating residual current faults with magnitudes ranging between 8.1 - 26.2 mA across the PE.

Then an Electronic Load is used to generate a higher voltage level of 92 volts and the designed RCD is tested by creating an external residual ground fault across the PE, similar to the extra low voltage test. The PCB is then tested in bipolar configuration across Low Voltage levels of 100 - 360 V with larger load to create a residual ground fault within 20 - 30 mA .The obtained results are then tabulated and analyzed.

6.2.1. Extra Low Voltage : Test Circuit and Setup

The test circuit and setup for the RCD in bipolar power supply configuration at ELV levels is presented in this subsection. The circuit diagram for the test is shown in Fig.6.6 . Two Tenma power supplies are used to create the bipolar configuration across parallel loads of 980 Ω each connected to the Positive to Neutral (P-N) and Neutral to Negative (N-Ne) configurations. The Residual ground fault is created by connecting a net resistance value of 1200 Ω across the Positive to PE for positive residual currents or Negative to PE for negative residual currents respectively within the range of ± 5 to 25 mA.

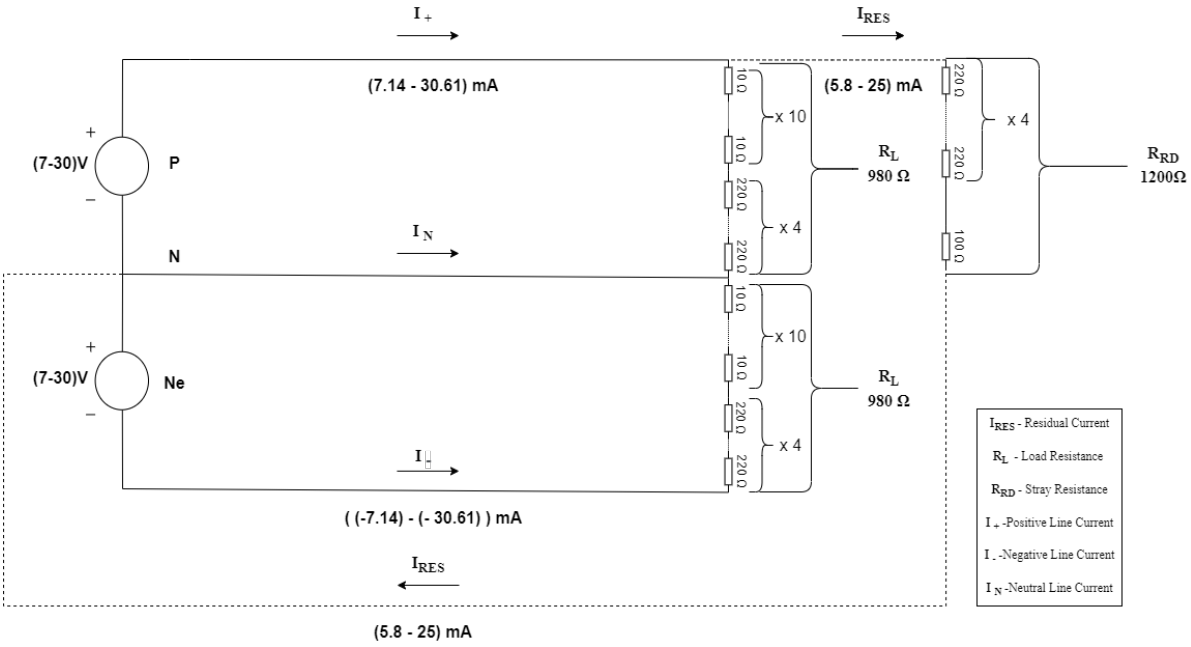

Figure 6.6: Circuit Diagram for Bipolar test setup for Extra Low Voltage Configuration.

6.2.2. Test Results and Analysis

Here below are the test results of the RCD tested in bipolar grid configuration at ELV power supply levels:

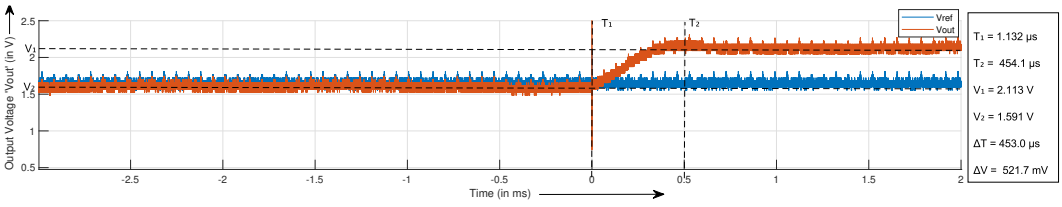

Figure 6.7: Residual Current: **20 mA** detected within **453** μ**s** at a Bipolar supply voltage: Positive '+ve' 16 V ; Negative '-ve' - 8.4 V; Neutral 'N' - 7.6 V supply voltage.

Above figure 6.7 shows the detected 20 mA residual current in 453 μs at a positive pole voltage of 16 V,

negative pole voltage of -8.4 V and neutral pole voltage of 7.6 V.

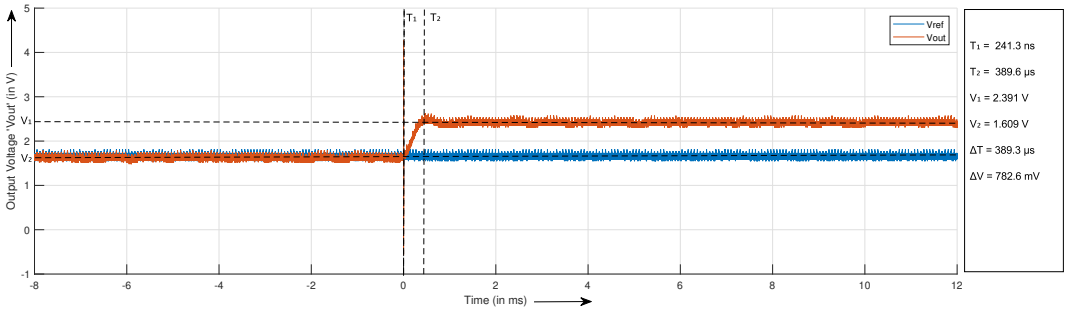

Figure 6.8: Residual Current: **30 mA** detected within **389.3** μ**s** at a Bipolar supply voltage: Positive (+ve) 20.8 V ; Negative (-ve) 16 V; Neutral (N) 4.8 V supply voltage.

Above figure 6.8 shows the detected 30 mA residual current in 389.3 μs at a positive pole voltage of 20.8 V, negative pole voltage of -16 V and neutral pole voltage of 4.8 V.

Table 6.2: Tabulated Results of RCD testing in Unipolar Grid Configuration.

S.No.	I_{res}(mA)	R_{sh} ($K\Omega$)	N_S	V_{ref} (V)	V_{out} (V)	$(V_1 - V_2)$(V)	Cal. I_{res} (mA)	Acc.(%)	T_r (μs)
1.	20	6.8	936	1.591	2.113	0.522	17.96	10.18	453
2.	30	6.8	936	1.609	2.391	0.782	26.91	10.3	389.3

From the results tabulated in Table 6.2, it can inferred that the accuracy of the RCD decreases with reduction of shunt resistance (R_{shunt}) and the reaction or rise time (T_r) of the RCD does not change. This is because the rise time (T_r) of the RCD depends on the inductance (L) which is determined by the no. of secondary turns on the compensation winding together with the effective magnetic permeability of the magnetic core. Higher the shunt resistance, better the accuracy when detecting low magnitude currents.

6.2.3. Low Voltage : Test Circuit and Setup

The test circuit and setup for the RCD in bipolar power supply configuration at Low Voltage levels is presented in this subsection. The circuit diagram for the test is shown in Fig.6.9 . A Bipolar power supply configuration for Low Voltage Levels (120 - 360 V_{DC}) is created across a DC Bipolar Power supply regulator that is controlled using impedance. Two DC motor fan loads are connected between Positive - Neutral and Neutral - Negative polarities.

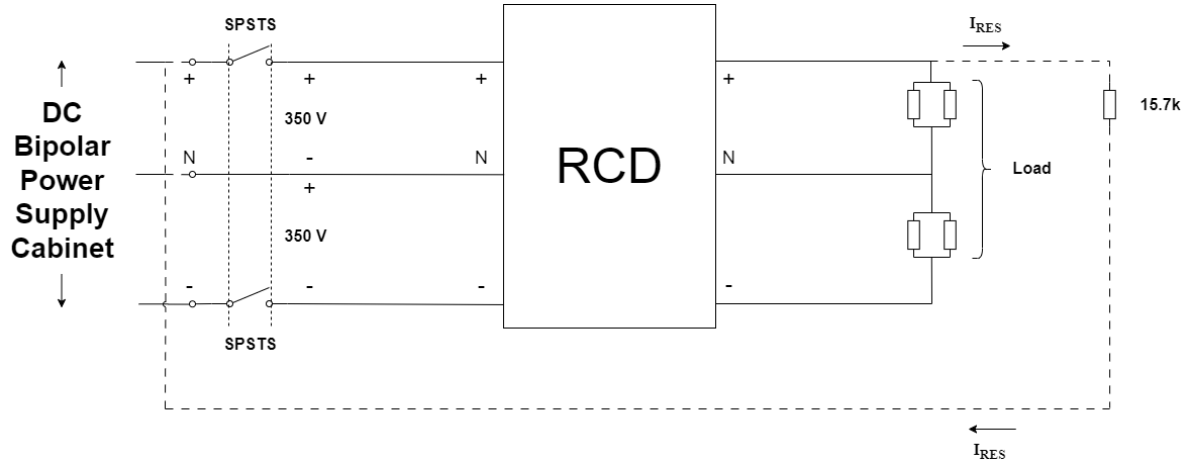

Figure 6.9: Circuit Diagram for Bipolar test setup.

6.2.4. Test Results

Results obtained from testing the PCB in bipolar configuration at Low Voltage Levels (120 - 360 V) are displayed below :

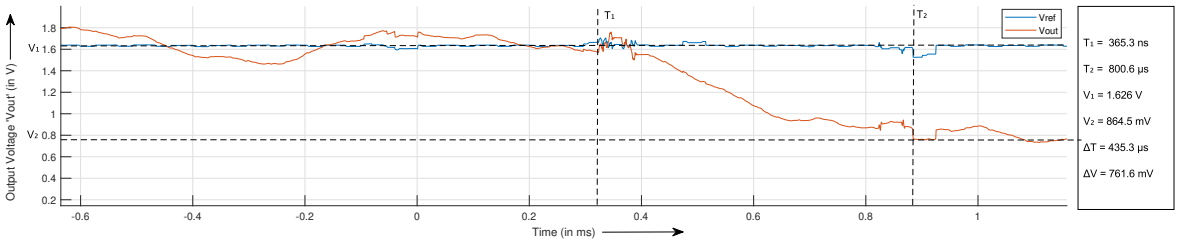

Figure 6.10: Residual Current: **-22 mA** detected within **435.3** μ**s** at a Bipolar LVDC supply of: Positive (+ve) 350 V

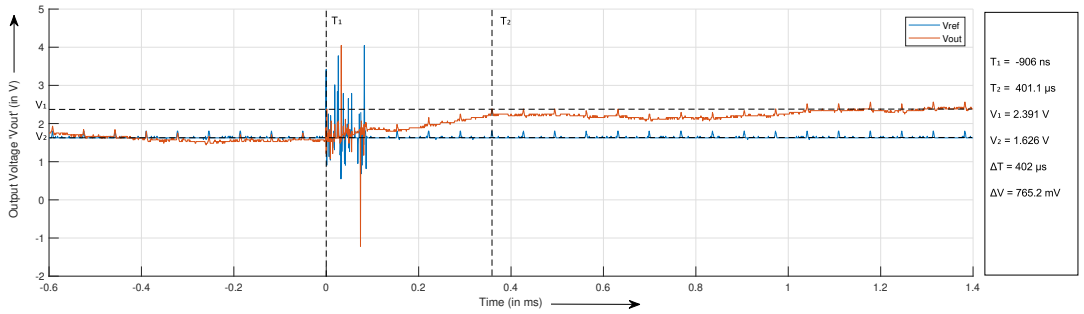

Figure 6.11: Residual Current: **19 mA** detected within **402** μ**s** at a Supply Voltage of 295 V at the Positive Polarity.

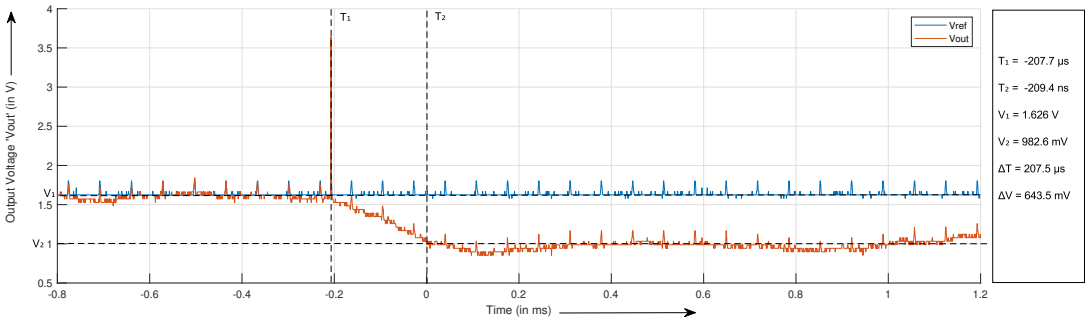

Figure 6.12: Residual Current: **-19 mA** detected within **207.5** μ**s** at a supply voltage of 298.3 V on the Positive Polarity.

Table 6.3: Tabulated Results of RCD testing in Bipolar Grid Configuration.

S.No.	I_{res}(mA)	R_{sh} ($K\Omega$)	N_S	$V_{ref}(V)$	V_{out} (V)	V_1 - V_2 (V)	I_{cal} (mA)	Acc(%)	T_r (μs)
1.	-22	7.13	936	1.626	0.8645	0.7615	24.99	13.59	435.3
2.	19	7.13	624	1.626	2.391	0.765	17.55	-7.63	402
3.	-19	7.13	936	1.626	0.9826	0.6434	21.11	11.1	207.5
4.	22	6.8	624	1.619	2.434	0.8155	18.708	14.96	2144

From the results, the rise/reaction time of the RCD output is (T_r) is found to be well within the critical time limit of 10 ms before which the sensor must trip and the breaker must act. The reaction should ideally be fast with a secondary coil of 624 turns and 139.56 mH inductance compared to that with 936 turns and 312 mH inductance. However, from observation 4 in Table 6.3 it can be seen that the reaction time has slowed

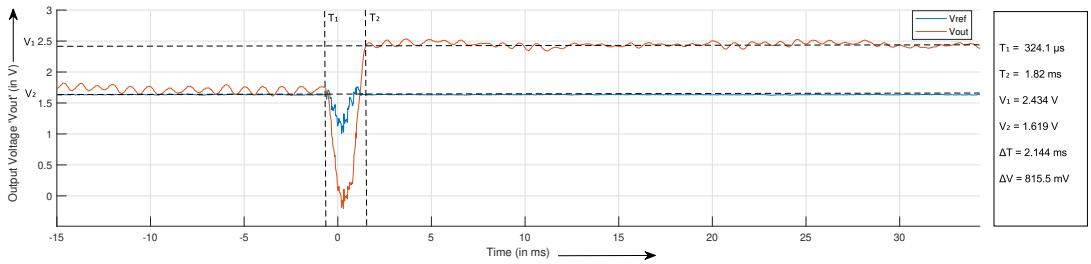

Figure 6.13: Residual Current: **22 mA** detected within **389.3 μs** at a Bipolar supply voltage**350V** supply voltage.

down considerably even with 624 secondary turn and around 140 mH. This is due to the reason the rise time also depends on the time taken to create the fault. In this thesis project, the external stray current path of the residual current to flow is designed through 15.7 kΩ is connected manually by plugging in the wire. This action of physically plugging in the wire may lead to the reaction time appearing longer or slowed down however it is not the case due to the absence of solid state switches or faster switching mechanisms to create and remove a residual ground fault in the laboratory.

6.3. Results Discussion

In the chapter the experiments conducted on the designed RCD and the obtained results were presented and discussed. The most critical parameters of rise time (T_r) and accuracy were assessed and compared with two PCBs with different secondary turns (N_s) : 936 and 624 respectively.

With both the PCB configurations, a fast rise time within 500 μs is observed. This is due to the nature of inductance itself to resist change in output voltage. The RCD with the higher inductance gives more accurate results compared to the one with lower net inductance (in mH). This is owing to the recommendation for ≥ 100 mH or 300 mH for closed loop stability of the sensor. Higher the closed loop stability the more closer the output voltage will be to the sensed residual current. Accuracy achieved by the designed sensor lie in a range between ± 10 % with few outliers within ± 15 % respectively.

The variation in output voltage accuracy with respect to the Reference Voltage (V_{ref}) can be attributed to instability of the magnetic core (loosely attached core), shift in position of air gap due to a poorly attached core, remnant magnetization of the magnetic core due to saturation, strong environmental magnetic field arising due to EMI, Earth's magnetic field, assymetric nature in compensation due to physical design errors like the PCB not properly stacked on top of the other due to extra solder on terminals in between the PCB or heating of the sensor leading to increase in errors. Further the output values are mainly affected by harmonics present in the supply to the sensor PCB or primary current in the bipolar configuration across which residual current is to be detected.

7

Conclusion and Future Scope

This thesis explored the possibility of design and development of a cost effective and reliable RCD for Bipolar LVDC Distribution Grids.

At low voltage distribution, DC distribution system is found to be more effective than AC distribution system. This is considering the integration of renewable energy sources and requirement for power electronic control among many other advantages such as reduction in power supply loss during distribution and ability to directly serve increasing number of dc loads such as electronic appliances connected to the local distribution grids. This lowers the requirement for large no. of conversion stages thereby increasing power supply efficiency. This system can therefore be effectively applied for rural electrification in developing countries where rural areas are relatively isolated from access to central or main distribution systems owing to economical constraints decided by geographical issues. The DC Distribution System is implemented in bipolar configuration for increased reliability, robustness and power supply efficiency.

Characteristics of DC residual ground faults being different than it's AC equivalent, requirements of Residual Current Detector (RCD) for Bipolar LVDC Distribution Grids are also different. The magnitude of DC residual currents are higher than AC residual currents for the same voltage level. This necessitates fast detection and isolation of the faulty section of the grid within a short duration of 10 ms as per IEC 60479-1 standard for recommended tripping times for direct currents as discussed in Chapter 2.

The RCD prototype has been designed to be implemented for Bipolar LVDC Distribution grids. The prototype uses a sensor IC from Texas Instruments named DRV 421 that operates on the principle of closed loop zero flux detection. Closed loop zero flux approach ensures non-intrusive detection with higher sensitivity and accuracy in detecting extremely low magnitude currents such as residual ground fault currents in the range of few milli amperes.

The design involves detection of fringing flux generated due to a differential current flowing across the bipolar power supply between a small air gap in a race track shaped magnetic core that is made to sit exactly on top of the sensor. A compensation current equivalent to the detected flux generated by the differential current across the main power supply during a residual ground fault, is sent by the flux-gate sensor to effectively compensate the same. This ensures a faster, accurate and linear response with a very low temperature drift.

The RCD design includes a planar compensation coil configuration. The planar compensation winding are concentrically laid on a pcb across the two shorter limbs of the nano-crystalline racetrack shaped magnetic core for effective compensation. Planar compensation was selected for the prototype due to advantages over coil wound configuration such as relative isolation from the magnetic core preventing heating of compensation coil, localised eddy currents and preventing possibility of quick saturation of the magnetic core at sudden peak currents in the main power line. A critical advantage gained from implementation of a planar compensation coil is the provision to increase or decrease the inductance provided by the magnetic core and compensation coil combination by just adding or removing compensation winding PCB. Additionally planar winding allows for development of a compact RCD that consumes less space on the DC circuit breaker PCB.

The designed and developed RCD prototype also allows it to be placed on a DC circuit breaker without

need for extra wires for detection as the Bipolar Main Line is laid as Cu tracks in the RCD PCB making the design simple and compact. The designed and developed RCD prototype is tested across different voltage levels for different residual current magnitudes between ±30 mA due to laboratory and experimental constraints.

7.1. Answers to Research Questions

In this subsection the outcome of the project obtained in the form of information gained from the process of design and development till experimental results from testing of the prototype are used to answer the proposed research questions delineated in Chapter 1.

1. **How to design a Residual Current Detector (RCD) for Bipolar LVDC Distribution Grids.**

   The proposed RCD was built around the critical and central component of the DRV 421 flux-gate detector IC. Using the IC reduced the no. of components, size and complexity of the prototype RCD. Planar compensation winding configuration was used instead of coil wound configuration thereby effectively decreasing the size of the RCD. Provision to change net inductance by adding or removing compensation winding PCB becomes a great advantage in the design. The relative isolation of the planar compensation winding from the Magnetic Core prevents magnetic saturation of the core during sudden current peaks that may occur across the main line during power electronic switching, opening or closing of poles or capacitive discharge of grounding capacitors during a voltage fluctuation scenario.

   With the Bipolar main power supply lines laid across the PCB as Cu tracks allows for detection of residual ground fault currents without need for any external wires. This design reduces the effective space occupied by the RCD if installed on a circuit breaker PCB. Therefore, requirements for highly sensitive, accurate but cost effective and compact RCD with a simple design was met by the use DRV 421 IC. The outcome of this project shows that design and development of a cost effective and reliable RCD is possible.

2. **What is the suitable technique for measuring RCD currents in DC grids.**

   Flux-gate detection technique has been used in this project owing to the requirement for high sensitivity and accuracy in the design. As discussed in Chapter 3, flux-gate technique works on the principle of detection of voltage change in the gating flux pulses that periodically saturate and de-saturate a ferromagnetic core or iron piece in this case that forms the front end sensor within the DRV 421 IC. The signal conditioning unit within the DRV 421 flux gate detector IC, integrates and amplifies the voltage difference that appears across the compensation terminals to send in a compensation current to counter the magnetic flux generated due to differential current in the main power line for zero flux detection.

   Since minute voltage differences in the gating pulses are observable, it allows for successful noiseless detection of extremely low magnitude residual currents which is not possible in a Hall Effect sensor due to presence of a higher threshold of magnetic flux required to create a hall effect. There is no such minimum magnetic flux threshold for operation of a fluxgate sensor like the DRV 421. The minimum magnetic flux threshold for polarity detection has been mentioned to be around $\pm 13\ \mu$T that equals 19.9 mA (~ 20 mA) of residual current for 652 μT/A sensitivity of the designed magnetic core obtained from COMSOL simulation of the prototype model. However this threshold is only for overcurrent/overload detection. As can be seen, the sensitivity of the flux gate sensor is very high such that very low magnetic flux produced by low magnitude residual currents are quickly detected and measured. Hall effect sensors have a minimum detection threshold in milli Teslas to initiate the hall effect operation and sensing. This aspect of high sensitivity to extremely low magnitude currents was the primary reason for selection of flux-gate detection technique for the residual current detection in this thesis project.

3. **What will be the design of the magnetic core for the proposed RCD with planar compensation winding ?**

   Race track shaped magnetic core made up of Nanocrystalline Amorphous Fe material was chosen for this thesis project. Requirement for high sensitivity to lower magnitude currents necessitated use of a magnetic material with very high initial permeability (μ_i). Nanocrystalline Amorphous Fe material available at Acal Magnetics company possessed an initial permeability of 30,000 which was found suitable for the application of residual current detection. Higher initial permeability increase the magni-

tude of effective permeability (μ_e) that is provided by the magnetic core post introduction of any air-gaps or cuts which was part of this design. Introduction of three air gaps with total length of 0.26 mm (L_g) achieves an effective permeability of 337.7 as calculated in Appendix A. This provided the minimum required sensitivity of 652 μT/A that was projected onto the front end sensor (iron piece) placed within the DRV 421 IC.

The racetrack shape, a derivative of the rectangular shape with curved edges was selected specifically to guide the magnetic flux lines generated due to differential current across the three poles during a residual ground fault, smoothly onto the DRV 421 IC. Absence of sharp corners in this design prevents concentration of magnetic lines of force at certain areas that would cause lesser flux to cross the DRV 421 and subsequent loss of accuracy in detection. The air gap is calculated to provide the maximum effective permeability (μ_e) possible. Lesser the air gap, larger the available effective magnetic permeability which in turn influences the amount of inductance (L) that can be obtained with a specific no. of turns. Higher the effective permeability, larger the inductance that can obtained from a specific no. of turns on the secondary or compensation winding.

With the turns on the compensation winding being split across four layers of the PCB, the minimum no. of turns that can be obtained on a single PCB is very high. With 13 turns around each of the shorter limbs of the magnetic core forming 26 turns on a single layer, a four layered PCB contains 104 turns in total. High inductance close to the value of 300 mH by the compensation winding and magnetic core combination is recommended by the data-sheet for the control loop stability of DRV 421. Higher inductance ensures rejection of sudden frequency changes or variations in the output due to phenomena in the main line such as a common mode frequency introduced by a power electronic converter. This stabilizes the output voltage of the DRV 421 that appears as the equivalent of the detected residual current across the bipolar supply mains.

4. **What will be the proposed reaction time of the RCD ? What will be the accuracy of the RCD ?**

   Reaction time is determined by the time taken for the output voltage of the DRV 421 sensor to rise to a particular voltage value from the reference voltage level of 1.65 V to a magnitude equivalent to the residual current detected. In simple words it is the time taken for the output voltage of the sensor to rise to a stable value post occurrence of a residual ground fault.

   As per the recommendation of IEC 60479-1 standard, the critical time taken for detection and isolation of a residual ground fault is within 10 ms beginning from a residual current magnitude of 200 mA. As discussed in Chapter 2, in DC distribution, the magnitude of a residual current on contact of a human body with nominal resistance is higher compared to AC distribution. For e.g. a body with net resistance (including contact resistance and that of the total current path across the body) of 1000 Ω at 200 V DC supply voltage across the mains is 200 mA which is enough to shock a person to death within a time span of 10 ms. Therefore for the selected nominal supply voltage level of 350 V across a Bipolar LVDC Distribution system, the reaction time should be very less. This imposes a strict requirement on the residual current detector for a very fast reaction time.

   Higher inductance obtained with the compensation winding and magnetic core combination leads to longer reaction times. For 936 turns compensation winding obtained by stacking 9 compensation winding PCB of 0.8 mm thickness each, the obtainable inductance is 312 mH using the equation 3.2. Similarly for 6 compensation winding PCB with 624 turns in total, the obtainable inductance is 139.56 mH. From the experimental results discussed in Chapter 6, it was found that the reaction time for an inductance range between 139.56 - 312 mH ranged between 200 - 600 μs. This is a favorable result considering 10 ms being the recommended time limit for detection and isolation of residual ground fault in LVDC grid.

   Further the accuracy obtained by the Residual current detector prototype is within ± 10 % with few outliers within the range of ± 15 % respectively. This shows that even-though there being some large deviations from the ideal residual current value, the accuracy are stable and lie within a particular range. This supports the choice of RCD design and proves that accurate, compact and cost-effective residual current detectors can be built. The large deviation from the actual value can be due to the following reasons :

   - Improper fixing of the Core on top of the sensor. The existence of a relative gap between the DRV 421 IC and the air gap of the magnetic core that can lead to less magnetic flux being concentrated

on the sensor and thereby more deviation from the actual value.

- A larger than recommended air gap due to the two L - Shaped pieces and single U shaped piece of the core not being fixed properly with each other. A small increase or decrease in the air gap can lead to large deviations in the sensor output due to change in the amount of magnetic flux the sensor is able to detect.
- Due to saturation of the magnetic core owing to sudden high peak currents across the main line that induce a large deviation in the output voltage from the reference value of 1.65 V prior to occurrence of residual ground fault. This could also happen due to the Demagnetization operation of the DRV 421 IC not getting triggered on time due to a fault in the programming or the Demagnetization function not being able to effectively demagnetize magnetic core.

  The primary issue can be solved by improving the code used for programming the DRV 421 IC via the STM Microcontroller. In case of the latter issue, an external demagnetization system must be set as an option in case a larger voltage than that which can be provided by the DRV 421 sensor is necessary for demagnetizing the core with high initial and effective permeability. More tests need to be conducted on the core itself to identify the characteristics of the core during operation which was not possible in this thesis project due to laboratory constraints and unavailability of testing equipment like zero flux chamber to determined the BH curve of the three piece core assembled together.
- EMI from nearby electronic devices, radio waves or influence of Earth's Magnetic flux. An appropriate shielding for the RCD, especially for the magnetic core must be designed so that it encapsulates the magnetic core and protects it from EMI. An entire research on the shielding material and techniques can be conducted to prevent EMI from influencing the output of the DRV 421.

Therefore it can be observed that the designed RCD prototype has a very fast reaction within micro seconds and has a fairly good accuracy that can be further improved. If the solutions provided for the outlined issues amounting to large deviations in the output voltage are implemented, the results of the sensor can be more accurate and stable. The precision or resolution of the sensor can also be improved with the implementation of the mentioned solutions.

7.2. Future Research

In this section we explore the scope for future research in this project or those that can be inspired from this project. As discussed in the previous section, many improvements can be made to the design of the RCD prototype to positively influence the results obtained from it. The suggestions for improvements in design and projects that can be inspired with the research performed in this thesis are given in the subsequent subsections.

7.2.1. Holding Case or Protective Shell for the Magnetic Core and Shielding

Holding Case or Protective Shell for the Magnetic Core

The Residual current detector depends heavily on the placement of the magnetic core with respect to the fluxgate sensor. Hence ensuring the rigidity and immovability of the placement of the magnetic core itself forms a major part of the RCD design. A custom case can be created to hold the magnetic core tightly in it's position making it impervious to sudden movements or displacements. This would ensure a reliable and sustained output from the sensor. A 3D printed cubical case or one custom designed to fix the core permanently in it's position can be designed and implemented.

It is also essential to prevent change in the air gap of the magnetic core. For this any material with the required air gap thickness can be placed or glued in-between the air gap of the magnetic core so that the it remains unchanged throughout the duration of service of the RCD. Equalized external and internal pressure from a custom designed shell will be able to hold the three pieces of the magnetic core stable together. If possible, a rectangular separator for making the Air-Gap with the required thickness can be incorporated into the design of the shell so that no separate material is required to be placed within to form the same.

Furthermore this shell or holding case has to be designed in such a way that the material used and the geometric shape are not disturbed by the heating and magnetic forces produced due to large differential

currents across the bipolar main line. The case or shell can be isolated or cushioned from the surface of the magnetic core using thin polyol (polypropylene) sheet attached along the inner surface of the case facing the magnetic core. Polypropylene sheet being a good heat insulator will prevent the external shell from getting too hot along with the core.

Shielding from EMI

Magnetic shielding is a must for any RCD device that is performing the highly sensitive operation of sensing extremely low magnitude currents. EMI can be a big problem hindering the accurate and robust functioning of the RCD as it would lead to huge deviations from the actual value of residual current that needs to be detected. Earth's magnetic flux that carries a value in-between 35 to 65 μT that would translate to 53.68 to 99.69 mA which would introduce a very large error in detecting extremely low magnitude currents.

To prevent occurrence of such errors due to EMI and Earth's magnetic flux, a proper shielding using a ferromagnetic material needs to be placed on top or within the holding case or shell with proper insulation between the shielding sheet and the magnetic core. For proper shielding from external magnetic disturbances, the outer shield needs to have a higher magnetic permeability than the magnetic core itself so that external magnetic lines of force are guided along the external ferromagnetic shield without being attracted to the magnetic core within the RCD. However this can create a problem for residual current detection as the magnetic flux created due to the differential current during a ground fault may be redirected to flow across the ferromagnetic shield instead of the magnetic core itself owing to reluctance provided by air gaps. Therefore the magnetic permeability of the ferromagnetic material must be selected and designed intelligently to only shield the magnetic core within the RCD from external magnetic interference.

A ferromagnetic or ferrous material of magnetic permeability lower than the Nanocrystalline magnetic core can be used and wrapped around the holding case in such a way that ensures external magnetic flux to get redirected along the external shield and differential flux generated due to residual currents are allowed to flow without any interference within the magnetic core.

The design of a protective case for the magnetic core and the shielding along with it's practical implementation in a prototype can be a good internship topic.

7.2.2. Common Mode Filtering and Effective Demagnetization system

Common Mode Filtering

Common mode frequencies along the main line induced by power electronic switching, abrupt opening and closing of poles or capacitive discharge from multiple grounding capacitors, if used, need to be filtered out for accurate and noiseless detection of residual currents. This is especially important due to the extremely low magnitude of residual currents. Although there being a gain selection option within the DRV 421 sensor to select the minimum integrator corner frequency, the DRV 421 easily allows frequencies till 3 KHz or higher. This implies that common mode rejection needs to be paramount for proper functioning of the RCD.

In regular RCD devices, toroid shaped cores are implemented in IT configuration which is a three core setup with three windings for different purposes. The primary and secondary compensation winding are wound across all the three cores for detection and compensation. A third winding is used to counter the common mode appearing across the main line to isolate the actual measurement of residual currents from the same for accurate, robust and precise detection.

Since in the designed RCD prototype only a single core is used due to it's feasibility when using DRV 421 IC. Especially for a cost effective and less space consuming device to be implemented in bipolar LVDC distribution grid systems for rural electrification, the dependence on an external filter on the main line to remove the common mode prior to detection becomes evident. A research can be conducted on the LVDC distribution architecture implemented for rural electrification or DC street lighting and implemented grounding configuration (multiple and capacitive grounding) through simulations or prototypes and based on the results an appropriate filter can be designed to filter out the common mode from the main line thus allowing only the differential current due to residual ground faults to be detected by the RCD. The design of the filter would also depend upon the area in the grid the RCD is being implemented which has to be taken into consideration.

Effective Demagnetization System

Sudden peak currents in the main Bipolar LVDC power line can saturate the magnetic core of the RCD along with the internal front end sensor or iron piece (ferromagnetic material) within the DRV 421 IC. This can introduce a constant error in the measurement before occurrence of a residual ground fault. If the error is not removed then the magnetic flux generated by residual currents will not be isolated from the permanent magnetic flux due to saturation and both will be detected together by the sensor inducing huge errors in detection. This error in the difference in magnitude of the output voltage of the DRV 421 with respect to the reference voltage (1.65 V) may appear like a larger line to line fault than a residual ground fault. This when fed to a circuit breaker or electronic relay carries the potential to trigger the protection system for larger faults than for residual currents alone leading to opening of several poles or larger portions of the DC distribution grid system which translates into a big failure of the protection system as a whole.

To prevent such mishaps from occurring, it is required to keep the magnetic core of the RCD demagnetized especially immediately after an event saturating the core or the front end sensor. An option for demagnetization is provided within the DRV 421 IC itself. This option tries to effectively demagnetize the magnetic core. Due to larger size and permeability of the magentic core often times the demagnetization option available within the DRV 421 IC is rendered ineffective. This is especially due to the limitation in supply voltage used to operate the DRV 421 IC which operates on either 3.3 V or 5 V power supply. In case the saturation in the core is larger, then the supply voltage magnitude should also be larger.

Demagnetization as discussed in Chapter 3, involves sending in square wave voltage pulses in positive and negative polarities with increasing frequency to effectively depolarize and rearrange the magnetic bi-poles within the magnetic core to their original orientations. When all the magnetic bi-poles are re-oriented, the magnetic core is de-saturated and the output voltage (V_{Out}) terminal of the DRV 421 IC reads the reference voltage. DRV 421 IC has an in - built Search Function to de-saturate the front end sensor by raising the ICOMP1 terminal to Supply Voltage (V_{DD}) and connecting the ICOMP2 to ground (GND). The compensation current sent through the compensation winding effectively demagnetizes the front end sensor. The Search Funtion is initiated by the internal programming of the DRV 421 when the demagnetization option does not de - saturate the sensor and an offset error exists even after demagnetization cycle of 100 ms. If the Search Function is unable to de - magnetize the core after 60 ms, the error pin remains pulled to active low showing that the error could not be resolved. Ideally to prevent saturation of a core on startup, the DRV 421 IC is powered up first prior to powering up the supply mains as the Search Function and Demagnetization Function are already on standby for resolving saturation.

If the internal programming of the DRV 421 becomes ineffective in de - saturating the magnetic core, then an external demagnetization option with a larger power supply needs to be provided. In this case a programmable switch is need to be used controlled by STM Microcontroller along with a larger power supply voltage for the switch that is capable to effectively demagnetize the magnetic core.

In order to determine the exact demagnetization voltage many tests need to be performed on the magnetic core to assess it's characteristics with the existence of the air gaps and the three pieces assembled together. Zero flux chambers need to be used to plot the BH curve of the custom magnetic core and the saturation characteristics. The minimum peak current magnitude that can saturate the core and the voltage that effectively demagnetizes the core needs to be determined by several tests with demagnetization pulses sent across the planar compensation windings at different voltage levels. The result with the lowest voltage difference between the output voltage and the reference voltage needs to be attained. Then the voltage can be selected for external demagnetization.

The design of an effective demagnetization system for the RCD along with designing of a filter for rejection of common mode can be a separate thesis topic altogether.

7.2.3. Novel design for Residual Current Detectors

As discussed in Chapter 2, there are various techniques for detection of residual currents that have developed over time with research and experimentation. Increase in technological advancements can bring about new techniques for detection of residual ground fault currents. Highly sensitive hall effect sensors if developed can be used instead of flux gate technique for detection of residual ground fault currents. This would ensure a less power consuming alternative to flux - gate detection.

Core-less Flux-gate sensing topologies are also under research which removes the requirement for sepa-

rate IC or components for residual current detection. Such topologies involve planar winding of bipolar main supply lines around a single cubical iron piece etched onto the PCB at the center of the winding. The differential flux detected across the iron piece is used for determining the residual ground fault current. The design despite being simple is challenged by it's high sensitivity and vulnerability to EMI and other interference in the form of EM waves which can cause heavy offset errors. Similarly other novel techniques can be developed with advent of newer technologies that are more efficient, accurate, robust and precise.

A

Magnetic Core Design

A.1. Design of Magnetic Core and Calculation of Parameters for DRV 421 IC

This section presents the numerical design of the magnetic core for the developed RCD using DRV 421 IC. The magnetic core design for DC residual current detection depends primarily upon the high initial magnetic permeability (μ_i) provided by the material. High initial permeability decides the sensitivity of the device which is determined by the Relative Permeability (μ_r) offered by the magnetic core with the no. of secondary turns and air gaps. Small currents in the range of milliamps require magnetic cores with high permeability to amplify the magnetic flux density appearing around the mains due to a current imbalance. The selected tape wound Nanocrystalline Fe - Amorphous material has an initial magnetic permeability (μ_i) around 30,000 making it suitable for the application. The Fig.A.1 shows the magnetic permeability curve of the selected Nanocrystalline material kOr 120 model with cuts.

Shape and size depending on the RCD PCB configuration form the second set of considerations. As discussed in Chapter 4 racetrack shaped core is selected considering uniform magnetic path length with curved corners. Size of the magnetic core decide the cost. Larger the magnetic core higher the cost. The smallest available thickness and girth was thus selected for the application to reduce the net cost of the magnetic core. The dimensions of the magnetic core are provided in the custom data-sheet from the company Acal Bfi in Fig. A.2.

Parameteric values considered for the calculations :

1. Initial Permeability (μ_i) = 30,000
2. Total Gap Length (L_g) = Horizontal Gap + Air Gap = 30μm*2 + 0.2 mm = 0.26 mm
3. Magnetic Path Length (L_m) = 88.8 mm
4. Open loop Current - to - field transfer of Magnetic Core $\boldsymbol{G_{core}}$ = 652 μT/A 4.19

Given below are the calculations of the parameters of the selected magnetic core :

1. **Effective Permeability** ($\boldsymbol{\mu_e}$)

$$\boldsymbol{\mu_e} = \frac{\boldsymbol{\mu_i}}{\mathbf{1} + \frac{\boldsymbol{L_g} * \boldsymbol{\mu_i}}{\boldsymbol{L_m}}} \tag{A.1}$$

$$\boldsymbol{\mu_e} = \frac{\mathbf{30000}}{\mathbf{1} + \frac{\mathbf{(0.03*2+0.2)*30000}}{\mathbf{88.8}}} \tag{A.2}$$

$$\boldsymbol{\mu_e} = \mathbf{337.694 \sim 337.7} \tag{A.3}$$

acal bfi Acal BFi kOr Magnetics products Technology Centre

Specification for Soft Magnetic Material
kOr 120 / kOr 120HF rev. 5
page 3

Data for impregnated uncut and single cut cores of kOr 120

Effective Permeability vs. Frequency

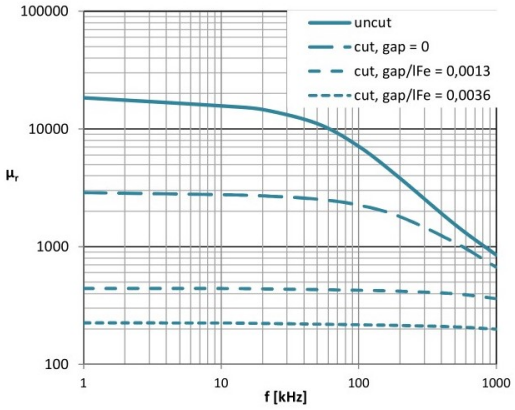

Notes:
Cores are impregnated with Epoxy.
Typical curves are shown.
gap/lFe denotes single gap width in relation to mean path length l_{Fe} for l_{Fe} = 100 - 500 mm

N = 1, U_{eff} = 100 mV

Nominal / minimum permeability for
single cut cores without additional gap:
10 kHz: 2500 / 1600
100 kHz: 1900 / 1200
Nominal permeability at 10 kHz up to 10.000 is possible with special cut quality on request.

Effective Permeability vs. Bias Field

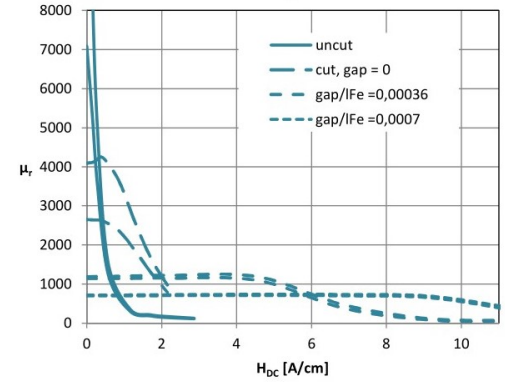

N = 1, U_{eff} = 100 mV
upper curves: 10 kHz; lower curves: 100 kHz

$$I_{DC} = H_{DC} \cdot l_{Fe}$$

Differential Permeability vs. Pulse Field

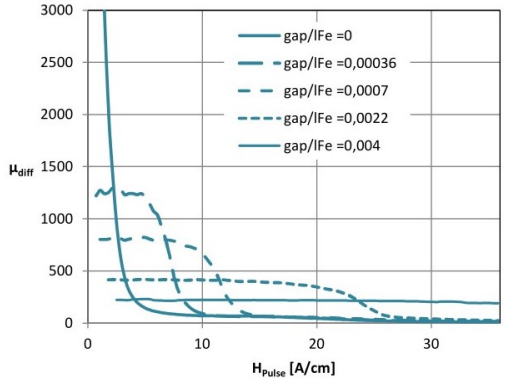

μ_{diff} monitored during pulse

Figure A.1: Material Data sheet of Nanocrystalline kOr 120 cut cores.

2. **Gain Factor (G_{MOD})**

   The Gain Factor (G_{MOD}) is calculated to determine and select the corner frequency of the integrator within the DRV 421 for obtaining a Loop gain to ensure control loop stability and get the accurate output devoid of any gain errors. It is simplified form of loop gain equation that removes dependency on the frequency only using the obtainable inductance from the magnetic core - secondary winding combination for determining the corner frequency [33][34].

$$G_{MOD} = \frac{G_{core} * N_{winding}}{L} \tag{A.4}$$

$$G_{MOD} = \frac{652 * 10^{-6} * 936*}{0.312} \tag{A.5}$$

$$G_{MOD} = 1.956 \tag{A.6}$$

   The application report by Texas Instruments on "Designing with DRV 421 : Control Loop Stability" pg 5. [35], recommends current sensors with Core Gain factors between 1 and 3 ($1 < G_{MOD} < 3$) and core inductance between 200 and 600 mH (200 mH < L < 600 mH) to select mode GSEL as : 0 1 (GSEL1 = 0 and GSEL0 = 1) which allows integrator corner frequency up to 3.8 KHz and 50 V/mT flat band gain. This is because for residual current sensors with large shunt resistors (R_{Shunt}) can lead to high transformer pole frequency (f_{tf} which decreases the overlap between the active compensation loop that functions for pure DC and transformer effect at high current frequencies in the supply mains. The GSEL (1,0) : 0 1 mode helps in counteracting this reduction in overlap as it provides a larger flat band cross - over frequency.

acal bfi European leader in advanced technology solutions
Custom Services for Magnetic Components

Acal BFi kOr

Specification for Soft Magnetic Core
Part Number: **120-RI-081913-TC-1** rev. prel.

Nominal Data:

		bare core	finished core
build width A	[mm]	7,5	7,5
window width B	[mm]	19,4	19,4
window length C	[mm]	13,2	13,2
height D	[mm]	10,0	10,0
core width E	[mm]	34,4	34,4
core length F	[mm]	28,2	28,2
weight	[g]	40,1	41
l_{Fe}	[mm]	88,8	
A_{Fe}	[mm^2]	61,5	
filling factor FF	[%]	82	
inductance A_L @ 10 kHz	[µH]		

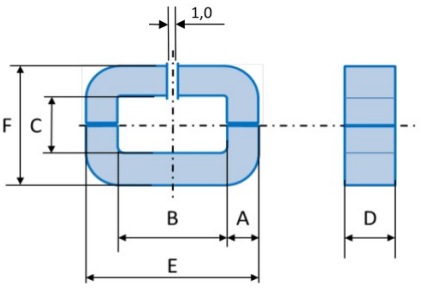

Specified Data:

		min	max	test conditions
build width A	[mm]	7,0	8,0	
window width B	[mm]	18,8		
window length C	[mm]	12,6		
height D	[mm]		10,5	
core width E	[mm]		36,0	
core length F	[mm]		30,2	

Typical and Informative Data:

material class		Fe-based amorphous	
material		**kOr 120**	*for details, see core materials information sheet*
cuts		one cut in the middle of core length C; one gap in one leg	
nominal effective permeability			
min. flux	[µWb]	66	
finishing		Epoxy impregnated	
color		-	

Recommended Usage:

max. operating temp.	[°C]	150	
max. wire thickness	[mm]	-	*no winding directly on core recommended*
max. net current	[A*turn]	-	*to avoid saturation*
remarks		all data and specifications given for room temperature. legs are not fixed and can be moved to adjust gap width	

	issued	approved
date	11. Aug 20	
name	WGU	

Figure A.2: Data-sheet of Nanocrystalline Fe - Amorphous Magnetic Core.

B

PCB Development Images :

B.1. 3D Rendered Images in KiCAD :

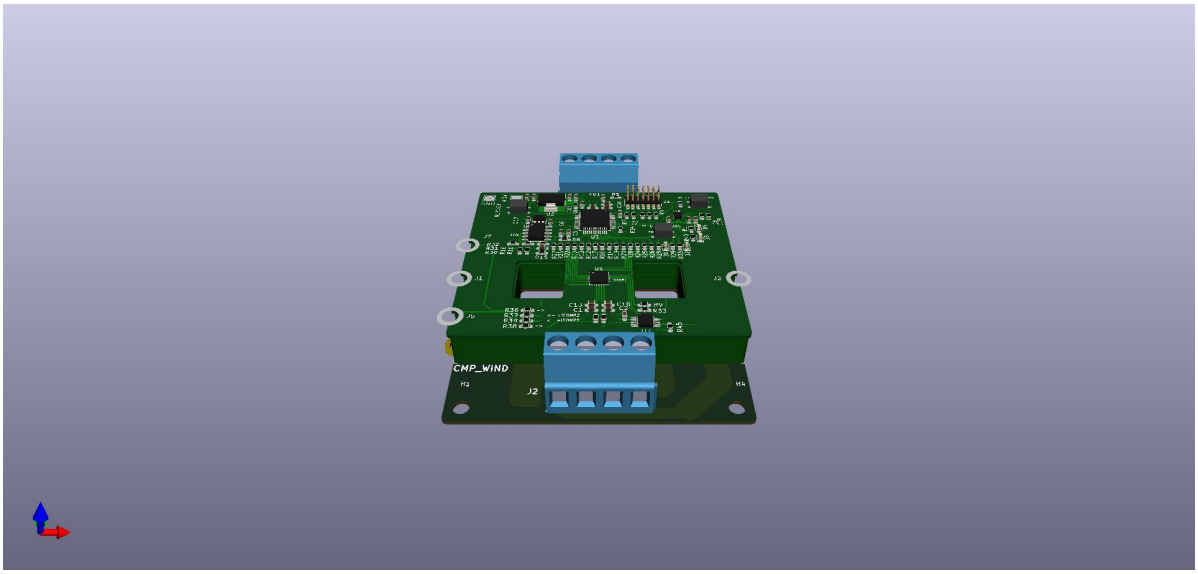

Figure B.1: A 3D image rendered on KiCad displaying the Front view of the designed PCB.

B.2. Images of the fully developed PCB :

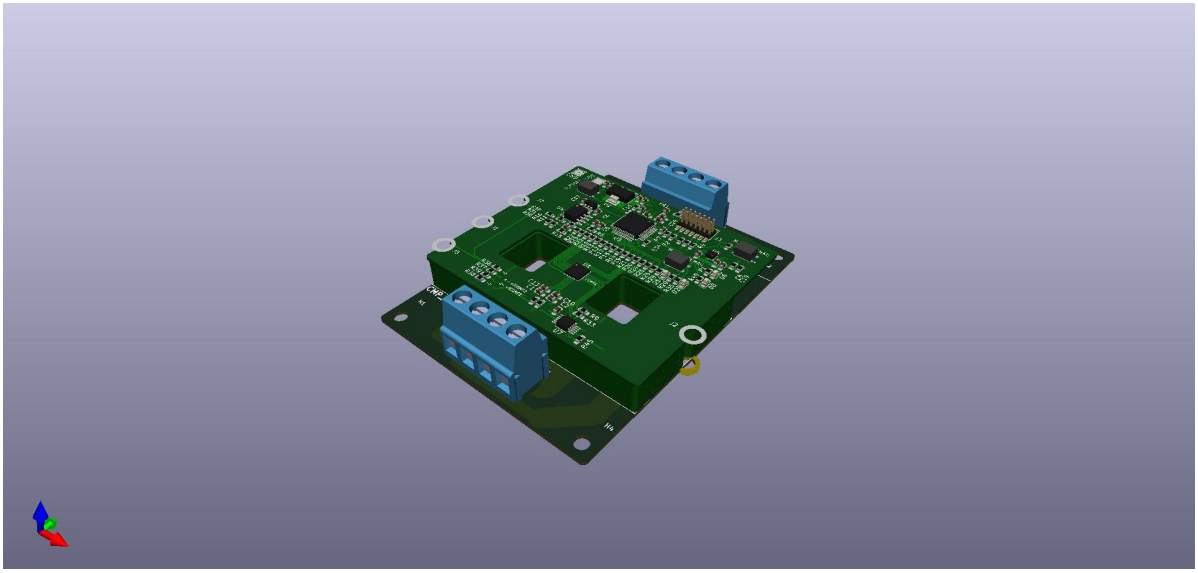

Figure B.2: A 3D image rendered on KiCad displaying the Diagonal Right view of the designed PCB.

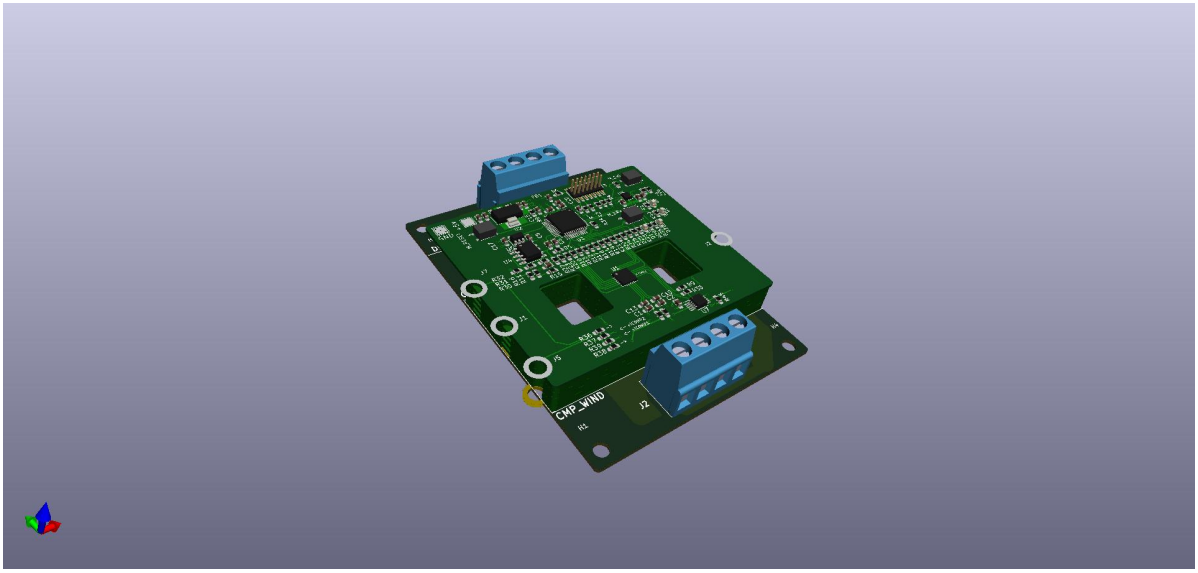

Figure B.3: A 3D image rendered on KiCad displaying the Diagonal Left view of the designed PCB.

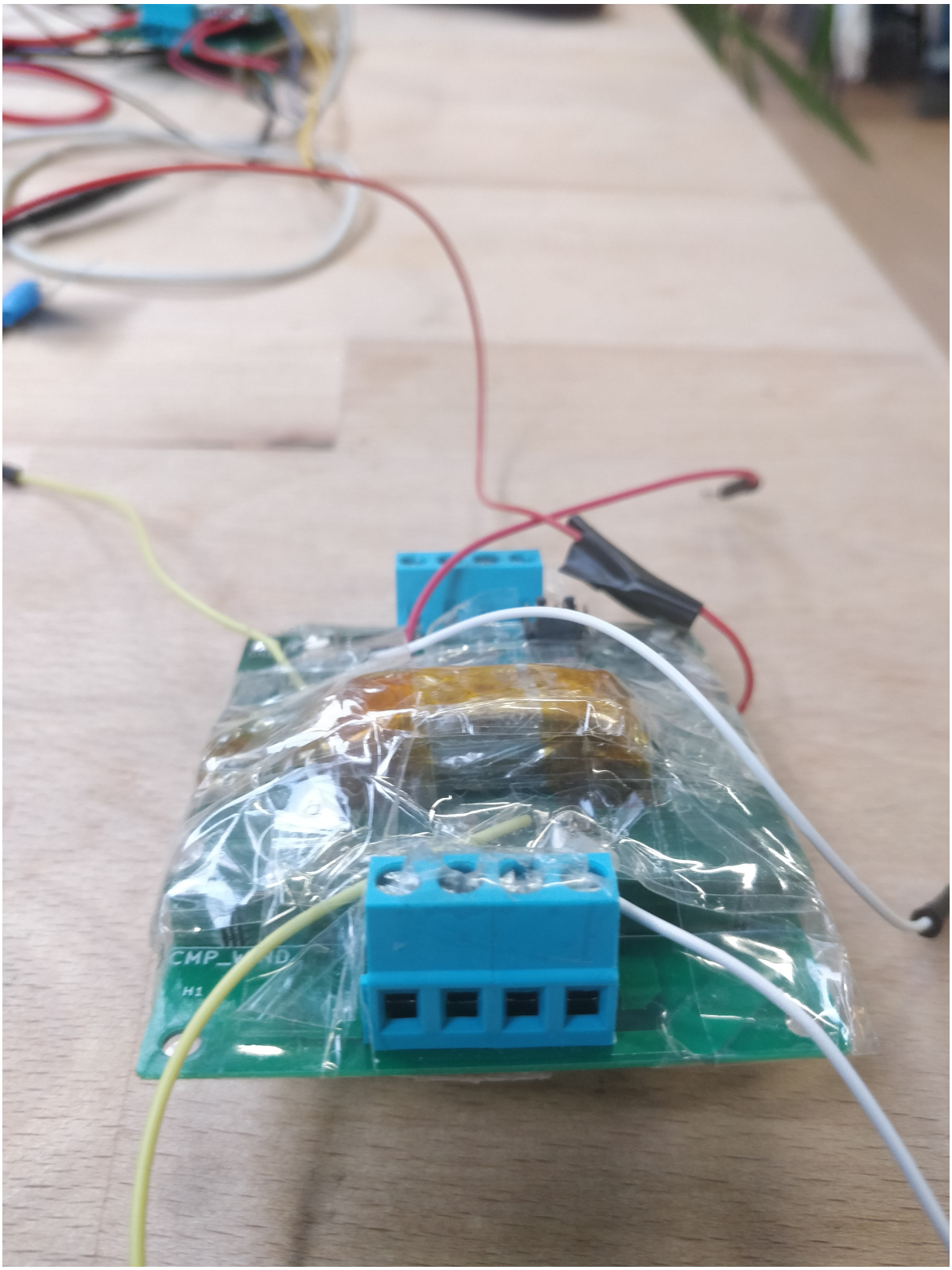

Figure B.4: Front View of RCD PCB

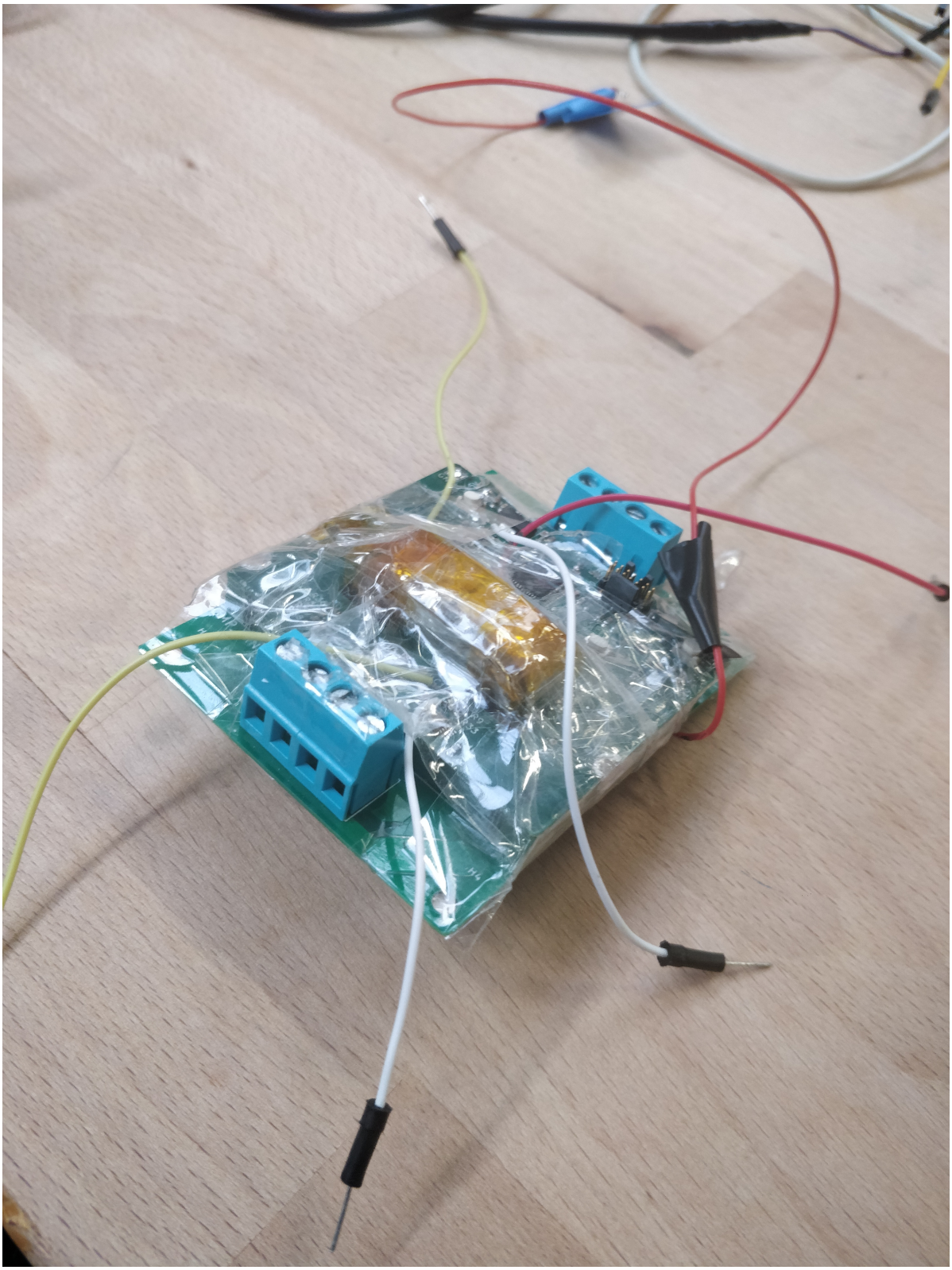

Figure B.5: Side View of RCD PCB

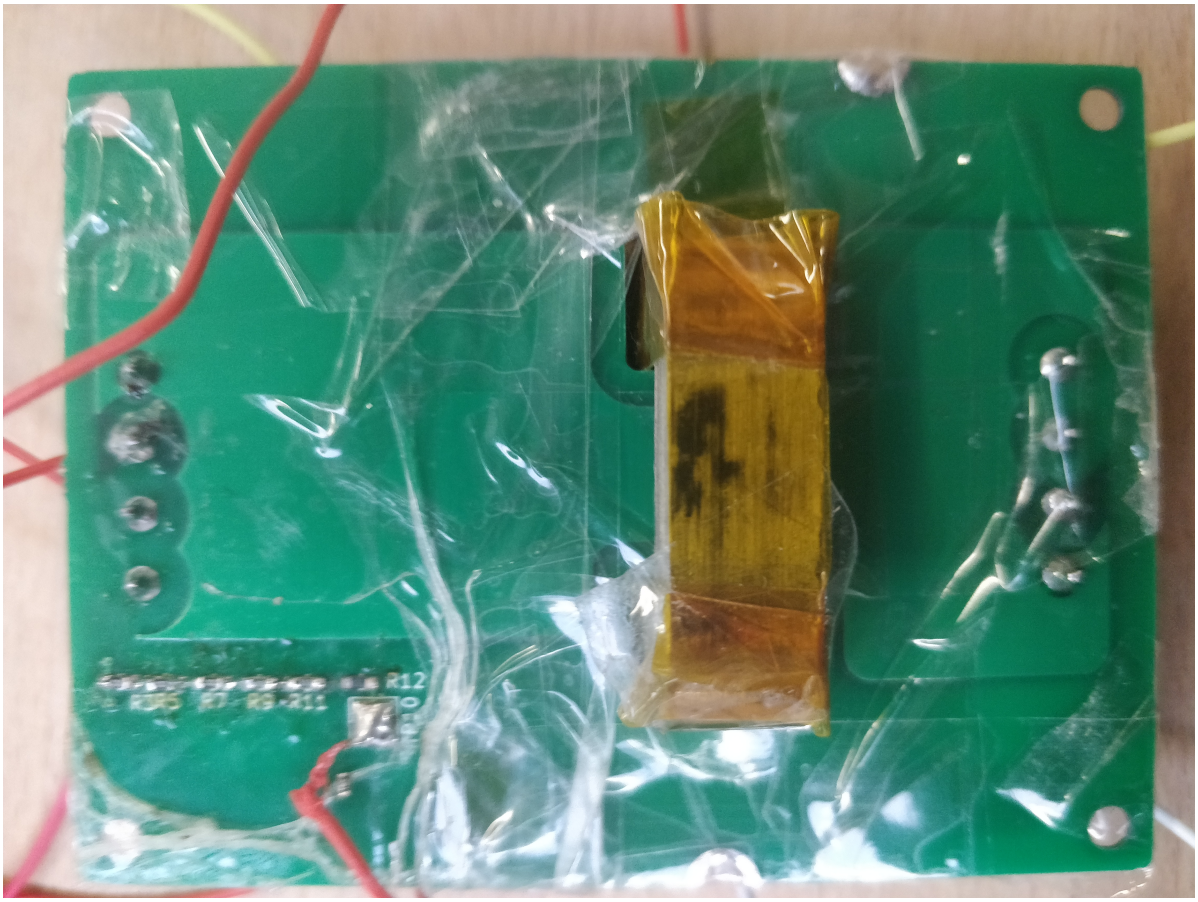

Figure B.6: Bottom view of RCD PCB.

C

Other Test Results of RCD for Bipolar LVDC Distribution Grids

C.1. Test Results - Unipolar Extra Low Voltage Configuration

In this section, results obtained other than the main test results presented in Chapter 6 between voltage levels 5 - 100 V_{dc} are presented and tabulated. The first two results are obtained by testing of the designed RCD using Tenma power supply with maximum 30 V supply voltage and residual currents of 12 and 26.2 mA while the third result is obtained from Electronic voltage source used to directly create a residual current of 20 mA with 50 V power supply.

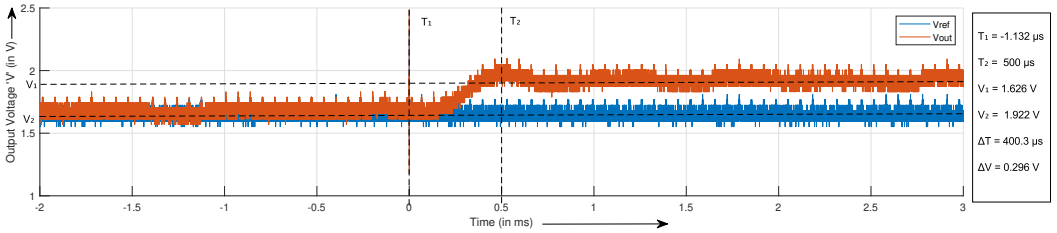

Figure C.1: Residual Current: **9 mA** detected in **501.132** μ**s** at **6 V** supply voltage.

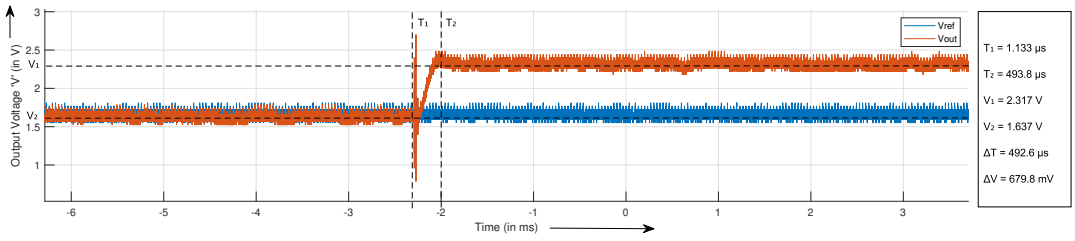

Figure C.2: Residual Current: **26.2 mA** detected in **492.6** μ**s** at **16V** supply voltage.

Table C.1: Tabulated Results of RCD testing in Unipolar Grid Configuration.

S.No.	I_{res}(mA)	R_{sh} ($K\Omega$)	N_S	V_{ref} (V)	V_{out} (V)	($V_1 - V_2$)(V)	Cal. I_{res} (mA)	Acc.(%)	T_r (μs)
1.	9	7.13	936	1.626	1.922	0.296	9.714	-19.05	400.3
2.	26.2	7.13	936	1.637	2.317	0.68	22.32	-14.81	492.6
3.	20	7.13	936	1.648	2.33	0.682	22.38	11.9	441.7

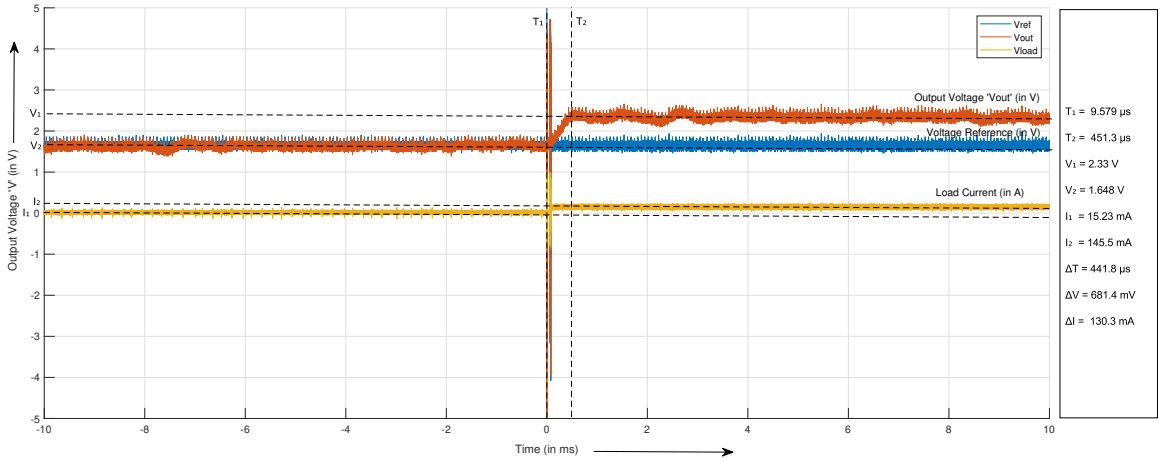

Figure C.3: Residual Current: **20 mA** detected within **441.7 μs** at a Unipolar supply voltage: Positive '+ve' 50 V supply voltage using electronic source.

The main reason for the large deviation from the true value in the above tabulated results is mainly due to the change in air gap in the magnetic core owing to absence of strong shell to hold the pieces together.

C.2. Test Results - Bipolar Low Voltage Configuration

Test results obtained other than the main results shown in Chapter 6 are presented here. The results presented here are obtained from residual current detection test conducted in between 120 - 360 V_{dc}

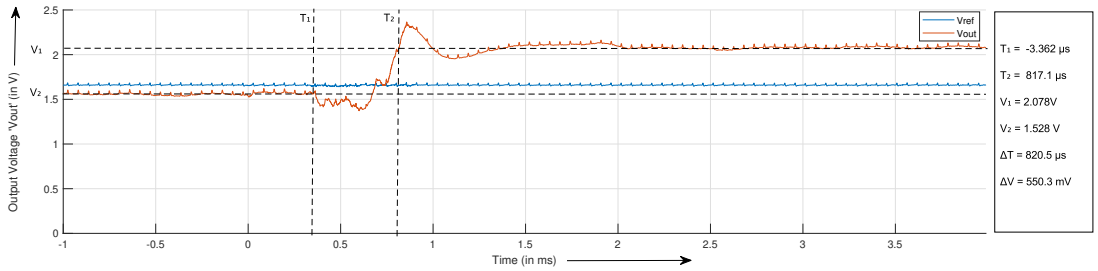

Figure C.4: Residual Current: **27.78 mA** detected within **454.9 μs** at a Unipolar supply voltage: **+350 V** supply voltage.

The above Fig C.5 shows the action of the V_{COMP}, the Comparator voltage rising to logic high due to the residual current crossing the positive threshold of 2.2 V. This test was conducted to ensure that the comparator trigger designed, reacted when the output voltage crossed 2.2 V which from the result can be confirmed to be working correctly.

Table C.2: Tabulated Results of RCD testing in Unipolar Grid Configuration.

S.No.	I_{res}(mA)	R_{sh} ($K\Omega$)	N_S	V_{ref} (V)	V_{out} (V)	($V_1 - V_2$)(V)	Cal. I_{res} (mA)	Acc.(%)	T_r (μs)
1.	27.78	6.8	936	1.528	2.078	0.55	18.893	31.87	820.5
2.	27.78	7.13	936	1.637	2.317	0.68	22.32	-14.81	492.6

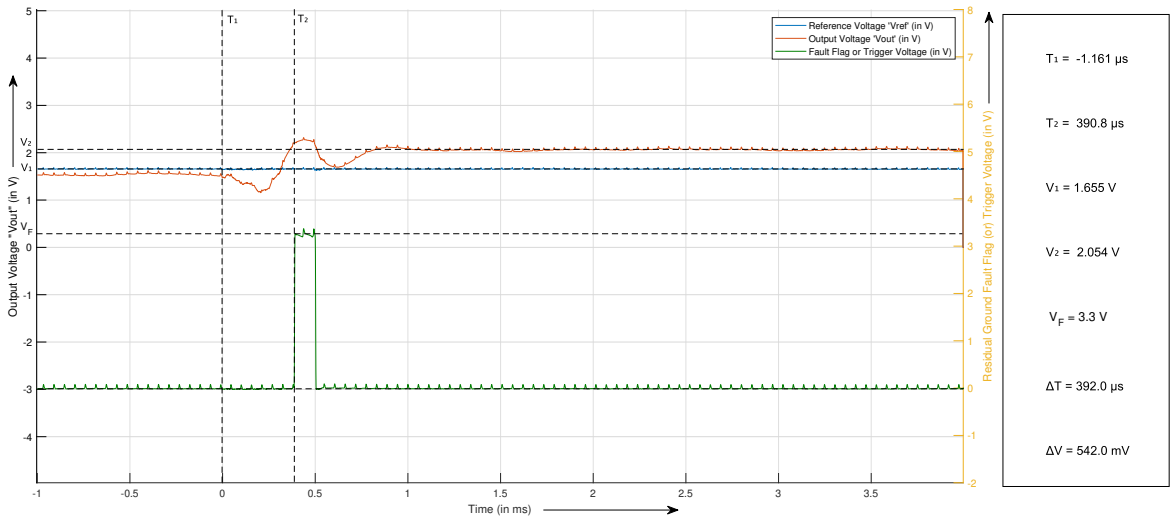

Figure C.5: Graph shows Fault Flag rising to Logic High depicting a fault condition, when $\boldsymbol{V_{out}}$ reaches or rises above 2.2 V for Residual Current: **27.78 mA** detected within **392 μs** at a supply voltage: **+350 V**.

C.3. Picosope Graphs

C.3.1. LV Bipolar Case

Graphs of detected output voltages from DRV 421 fluxgate sensor IC referring to the magnitude of residual fault current detected at Low Voltage : 120 - 360 V_{DC} in this project are presented below. In each of the output graphs in Picoscope, the **Blue** colour represent Output Voltage (V_{out}) with respect to the selected reference voltage (V_{ref}) of 1.65 V that is represented in **Red** colour respectively. The legend at the top right corner represent the actual output voltage ($V_{out} - V_{ref}$) using which the magnitude of the residual current detected can be found out via the following equation :

$$I_{RES} = \frac{(V_{out} - V_{ref})N_{sec}}{4R_{Shunt}} \tag{C.1}$$

where,

I_{RES} = Residual Ground Fault current (in mA).

V_{out} = Absolute Output Voltage of DRV 421 IC (in V).

V_{ref} = Selected Reference Voltage (in V).

N_{sec} = No. of turns on the Secondary (Compensation) Winding.

R_{Shunt} = Shunt Resistor (in Ω) used for limiting the compensation current around the compensation winding and across which the Output voltage is obtained and later amplified by a gain factor of 4 by the Shunt Sense amplifier built into the DRV 421 IC that gives the V_{out} with respect to the selected reference voltage V_{ref}.

The Fig.C.6 shows the output voltage V_{out} obtained from the DRV 421 IC with respect the reference voltage (V_{ref}).

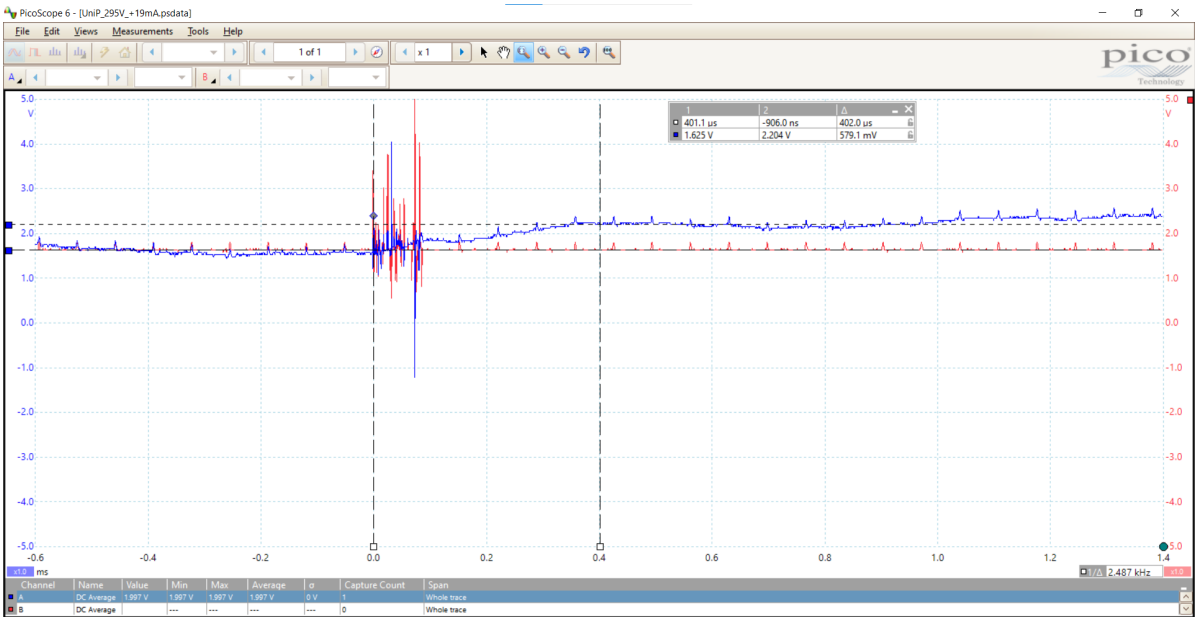

Figure C.6: Residual Current: **19 mA** detected within **402 μs** at a Bipolar supply voltage at Positive polarity of : **+295 V**.

Bibliography

[1] P. Juroszek, P. Racca, S. Link, J. Farhumand, and B. Kleinhenz, *Overview on the review articles published during the past 30 years relating to the potential climate change effects on plant pathogens and crop disease risks,* British Society for Plant Pathology **69**, 179 (2019).

[2] X. Chen, L. Wang, Z. Niu, M. Zhang, and J. Li, *The effects of projected climate change and extreme climate on maize and rice in the yangtze river basin, china. agricultural and forest meteorology,* British Society for Plant Pathology **282**, 107867 (2020).

[3] K. Verichev, M. Zamorano, and M. Carpio, *Effects of climate change on variations in climatic zones and heating energy consumption of residential buildings in the southern chile,* Science Direct Energy and Buildings **215**, 109874 (2020).

[4] V. Koubi, *"climate change, the economy, and conflict",* Current climate change reports 3 **4**, 200 (2017).

[5] I. E. A. (I.E.A), *The role of ccus in low-carbon power systems, iea, paris,* (2020).

[6] I. E. A. (I.E.A), *Global energy review, iea, paris,* (2021).

[7] B. S. R. of World Energy, *"Primary Energy Consumption By Source, World",* (2021).

[8] U.N, *Transforming our world: The 2030 agenda for sustainable development.* (2016).

[9] W. B. Group and E. S. M. A. Program, *"Renewable energy Policies and Regulations, Regulatory Indicators for Sustainable Energy (RISE)",* (2020).

[10] F. Daniel, D. Keles, T. Kaschub, and W. Fichtner, *Impacts of selfgeneration and selfconsumption on german household electricity prices,* Journal of Business Economics **89**, 869 (2019).

[11] WEC, *PRICING ENERGY IN DEVELOPING COUNTRIES*, Tech. Rep. June (World Energy Council, 2001).

[12] L. Abdallah and T. El-Shennawy, *Reducing carbon dioxide emissions from electricity sector using smart electric grid applications,* Hindawi Journal of Engineering , 1 (2013).

[13] I. Worighi, A. Maach, O. Hegazy, and J. V. Mierlo, *Integrating renewable energy sources in smart grid system : Architecture, virtualization and analysis,* Sustainable Energy, Grids and Networks **1** (2019), 10.1016/j.segan.2019.100226.

[14] IEC, *European Academies Science Advisory Council*, Tech. Rep. (International Electrotechnical Commission, 2018).

[15] L. Mackay, T. Hailu, G. Mouli, L. Ramirez-Elizondo, J. Ferreira, and P. Bauer, *From dc nano-and microgrids towards the universal dc distribution system- a plea to think further into the future,* IEEE Power and Energy Society General Meeting , 1 (2015).

[16] L. Mackay, T. Hailu, L. Ramirez-Elizondo, and P. Bauer, *Towards a dc distribution system-opportunities and challenges,* IEEE First International Conference on DC Microgrids (ICDCM) **69**, 215 (2015).

[17] G. B. Solar, *"solar panels for rural communities",* (2021).

[18] AFSTOR, *"afstor solar home and cooking system",* (2021).

[19] W. Bank, *"world rural population",* (2021).

[20] W. Bank, *"rural population - sub saharan africa",* (2021).

[21] W. F. Council, *"solar home systems",* (2021).

[22] N. Jones and P. Warren, *Innovation and distribution of solar home systems in bangladesh,* Climate and Development **13**, 386 (2021).

[23] D. Opportunities, *"usb-c based fast charging station for modular solar home systems for rural electrification",* (2021).

[24] S. Mukherjee, A. Kumar, and D. Maksimovi, *Efficiency-optimized current-source resonant converter for usb-c power delivery,* in *2021 IEEE Applied Power Electronics Conference and Exposition (APEC)* (2021) pp. 500–505.

[25] I. E. Agency, *"net renewable capacity additions by technology (pv)",* (2022).

[26] IEC, *Effects of current on human beings and livestock - Part 1: General aspects*, Standard (International Electrotechnical Commission, Geneva, CH, 2018).

[27] E. Vandeventer, *Residual Current Protection of a Meshed DC Distribution Grid with Multiple Grounding Points*, Master's thesis, Delft University of Technology (2016).

[28] BEAMA, *"the rcd handbook - guide to the selection and application of residual current devices (rcds)",* (2019).

[29] IEC, *Residual direct current detecting device (RDC-DD) to be used for mode 3 charging of electric vehicles*, Standard (International Electrotechnical Commission, Geneva, CH, 2018).

[30] IEC, *Type F and type B residual current operated circuit-breakers with and without integral overcurrent protection for household and similar uses*, Standard (International Electrotechnical Commission, Geneva, CH, 2009).

[31] N. C. for Environmental Information, *"geomagnetism - geomagnetic elements, earth's magnetic field intensity",* (2023).

[32] N. Lucius, J.-F. Rey, M. Paupert, and S. Tian, *Why to Choose Type B Earth Leakage Protection for Safe and Efficient People Protection*, Tech. Rep. (Schneider Electric, Rueil-Malmaison, France, 2018).

[33] *Datasheet : DRV421 Integrated Magnetic Fluxgate Sensor for Closed-Loop Current Sensing*, Texas Instruments (2016), rev. 2.

[34] *Designing with the DRV421: Closed Loop Current Sensor Specifications*, Texas Instruments (2015), rev. 1.

[35] *Designing With the DRV421: Control Loop Stability*, Texas Instruments (2015), rev. 1.